UNIVERSITÀ DEGLI STUDI DI SIENA

DIPARTIMENTO DI BIOTECNOLOGIE, CHIMICA E FARMACIA

DOTTORATO DI RICERCA IN

CHEMICAL AND PHARMACEUTICAL SCIENCES

CICLO XXXVI

Coordinatore del corso: Prof. Maurizio Taddei
Settore scientifico-disciplinare: CHIM/02

IN VITRO SELF-ASSEMBLING PROTEIN NANOPARTICLES FOR THE DESIGN OF NEXT GENERATION CARBOHYDRATE-BASED VACCINES

DOTTORANDA

Marta Dolce

Firmato digitalmente da
MARTA DOLCE
04/06/2024 23:21:53 +0200
powered by cheFirma!

TUTOR

Prof. Alessandro Donati

GSK TUTOR

Dott. Filippo Carboni

Dott.ssa Maria Scarselli

ANNO ACCADEMICO 2022/2023

Abstract

Self-assembling protein nanoparticles (NPs) can be exploited as carrier for antigen delivery to increase vaccine immunogenicity by promoting a robust adaptive immune response and long-lasting protective immunity.

The aim of my PhD is to explore key parameters of protein nanoparticles as carriers for saccharide-based vaccines.

First, to explore the impact of NP size and shape, oligosaccharides from *N. meningitidis* type W capsular polysaccharide were conjugated to ring-shape or nanotubes of *P. aeruginosa* Hemolysin-corregulated protein 1 (Hcp1) and to spheric *H.Pylori* Ferritin. The corresponding glyco-NPs were compared in animal studies.

The rod shape glyconanoparticles resulted less immunogenic than spheric glyconanoparticles, probably due to a different internalization efficiency. Furthermore, the increase in size for nanotubes did not improve MenW-specific immune response.

Further, the potential combination of NP and adjuvant platforms was investigated by exploiting the ability of Qβ VLPs to entrap genetic material that acts as an adjuvant of the immune response to surface-exposed antigens. By using *in vitro* processes Qβ VLPs entrapped RNA was removed and specific, homogenous ssDNA based adjuvant – TLR 9 agonist CpG – was successfully introduced inside the Qβ cage or linked to its external surface.

Qβ VLPs were subsequently conjugated with bacterial capsular polysaccharides. When entrapped in the glyco-NPs, the CpG adjuvant triggered an immune response after a single dose of vaccine that was equivalent to two doses of the corresponding CRM_{197} conjugate. This effect was entirely absent when the adjuvant was attached to the Qβ surface or simply co-formulated.

In conclusion, protein nanoparticles that meet defined characteristics in terms of size and shape combined with adjuvants platforms can pave the way for the development of a new generation of super-potent multicomponent glycoconjugates vaccines.

TABLE OF CONTENT

Chapter 1
Introduction

Part of this chapter has been published: Sorieul, C.; Dolce, M.; Romano, R. M.; Codée, J.; Adamo, R.; Glycoconjugate vaccines against antimicrobial resistant pathogens. Expert Rev Vaccines, 2023. 22(1): p. 1055-1078.

I.1 A brief history of vaccination

I.1.1 The father of vaccination

The development of vaccines has been one of the most significant achievements in the field of medicine during the 20th century. According to the World Health Organization, vaccination saves 2-3 millions of lives each year by preventing deaths and illnesses caused by infectious diseases [1]. The story of vaccination begins with Edward Jenner, who is regarded as the "father of vaccination." In 1796, Jenner demonstrated that infection with cowpox could provide immunity and protect against smallpox. He inoculated an 8-year-old boy named James Phipps with matter collected from a cowpox sore, and two months later, Phipps was challenged with human smallpox to test his resistance. Phipps was not infected becoming the first vaccinated person against smallpox [2, 3]. The term "vaccine," derived from the Latin word for cow, vacca, was later coined. Jenner predicted that vaccination could eventually lead to the eradication of smallpox, and in 1980, the World Health Assembly declared the world free of naturally occurring smallpox [4].

I.1.2 Live-attenuated and inactivated vaccines

A century after Jenner's groundbreaking studies, Louis Pasteur advanced vaccine development by proposing their applicability to all virulent diseases. Pasteur pioneered the creation of the first attenuated vaccines, wherein pathogens were exposed to oxygen or heat to weaken their virulence. This method was employed in developing notable vaccines such as the rabies and anthrax vaccines. Subsequently, the technique progressed to cultivating pathogens in vitro or unconventional hosts, resulting in attenuated strains. For instance, the serial cultivation of bovine tuberculosis bacteria in artificial media produced a strain that conferred protection against human tuberculosis. Likewise, Theiler and Smith attenuated the yellow fever virus through serial passage in chicken embryo tissues [2]. In 1923, Glenny and Hopkins utilized formalin treatment to reduce the toxicity of diphtheria toxin [5]. Ramon later built upon this discovery, demonstrating the possibility of neutralizing toxicity while retaining the ability to induce toxin-neutralizing antibodies [6]. Chemical inactivation was extended to viruses in the 20th century, with the influenza vaccine marking the first successful inactivated virus vaccine [7]. Influenza vaccine was the first successful inactivated virus vaccine and experience with that vaccine served Salk well in his successful effort to develop an inactivated polio vaccine in 1955 soon replaced by live-attenuated oral vaccine developed by Albert Sabin in 1963. The administration of Sabin's oral vaccine was simpler and, notably, did not carry the risk of triggering paralysis like the reactivation of the Salk's inactivated polio virus [3].

In 1994, the World Health Organization (WHO) announced the eradication of naturally occurring poliovirus from the Western Hemisphere [8].

I.2 Current state of modern vaccines

I.2.1 Carbohydrate-based vaccines

During the same period, there was an exploration of the significance of surface polysaccharides in bacterial virulence and the protective role of antibodies against polysaccharides [9]. This inquiry aimed to address inherent risks and instability associated with live attenuated and inactivated vaccines.

The initial tetravalent anti-pneumococcal polysaccharide vaccines became available in 1945 [10]. However, their development faced obstacles with the advent of antibiotics, leading physicians to believe that the challenges associated with bacterial diseases were resolved. It was only later, with the emergence of antibiotic-resistant strains, that research on antibacterial polysaccharide vaccines resumed. Their efficacy was demonstrated in large clinical trials, resulting in the licensing of the first anti-meningococcal and anti-pneumococcal polysaccharide vaccines in the seventies [11-14].
While polysaccharide vaccines partially addressed bacterial diseases caused by encapsulated microorganisms, they proved to be scarcely immunogenic in children below 2 years of age [11, 12, 15]. This prompted the development of glycoconjugate vaccines, revisiting the idea proposed by Avery and Goebel in 1931 that covalent coupling of bacterial carbohydrates with a protein antigen enhances the immunogenicity of carbohydrates. The initial protein-polysaccharide conjugate vaccines were formulated against *Haemophilus influenzae type b* (Hib) [16-19], and they were licensed between 1987 and 1990.

Research on glycoconjugate vaccines expanded to target various pathogens, leading to the development and licensing of glycoconjugate vaccines against Neisseria meningitidis, Streptococcus pneumoniae, and Salmonella Typhi (Vi) [20-24]. A comprehensive discussion and list of currently licensed glycoconjugate vaccines are provided respectively in section I.3 and Table 1.

I.2.2 VLP-based vaccines

The advancement of gene engineering techniques has played a crucial role in shaping vaccinology. This influence is evident in the cloning of genes responsible for viral vector structures and their expression in host cells, leading to the emergence of virus-like particle (VLP) technology [25]. In the early 1980s, this breakthrough facilitated the development of a novel vaccine against Hepatitis B (HBV), utilizing recombinant yeast cells carrying the HBV S antigen coding sequence (HBSAg) for large-scale production [26, 27]. This innovative approach replaced the traditional vaccine derived from the blood serum of HBV-infected patients [26, 28-30]. As a result, the successful production of recombinant viral structural proteins became a pivotal factor in inaugurating the VLP era in vaccinology with four types of prophylactic VLP-based vaccines that have been licensed for human use. Notable examples include a cervical cancer vaccine variant based on the major structural protein L1 VLP of the human papillomavirus (HPV) [31], produced through various expression systems, and a Hepatitis E vaccine constructed from a single, truncated capsid protein of HEV, generated in *E. coli* cells [25, 32].

I.2.3 Reverse vaccinology

In the early 21st century, the field of vaccinology underwent a transformative shift due to significant progress in bioinformatics. The ability to determine the complete sequence of a bacterial genome led to the idea to utilize genomic information to discover novel antigens that had eluded traditional vaccinology methods. This innovative reverse vaccinology approach required the in-silico analysis of microbial genome sequences [33]. It was initially employed to identify protein antigens as potential candidates for the first vaccine against serogroup B meningococcus (MenB) [34]. This approach was crucial as there were no existing polysaccharide-conjugate vaccines for MenB, due to the poor immunogenicity of MenB polysaccharide, which posed a risk of potential autoimmune reactions.

I.2.4 mRNA vaccines

Nucleic acid vaccines have gained significant attention particularly by the recent development of mRNA vaccines targeting SARS-CoV-2, the causative agent of COVID-19. This is especially notable in rapidly producing vaccines to promptly combat infectious diseases. Although mRNA was initially identified as a means to transfer genes *in vivo* in the early 1990s, the exploration of mRNA vaccines occurred much later, primarily due to the inherent instability of mRNA when compared to DNA [35]. mRNA stability and its efficacy in translating target proteins can be enhanced through various measures, such as introducing regulatory elements in the 5′ untranslated region (UTR) and the 3′ UTR [36], incorporating a Poly(A) tail [37], optimizing sequences and/or codons [38], and utilizing modified nucleosides to reduce innate immune responses [39-41].

Methods to encapsulate RNA have been explored to augment the stability and immunogenicity of RNA vaccines. This approach has been employed with exosome-encapsulated RNA [42], as well as cationic LNPs (lipid nanoparticles). When fully optimized, RNA vaccines may confer an immunogenic advantage over DNA vaccines, attributed to the activation of multiple cellular pathways involved in innate immunity responses to foreign RNA, including toll-like receptors (TLRs) and RIG-I-like receptors [43-45].

Despite multiple advancements in the field of vaccinology, emerging obstacles to provide worldwide protection must be tackled. Perhaps, by combining acquired knowledge, accumulated expertise and cutting-edge technologies, we might successfully fulfill this requirement.

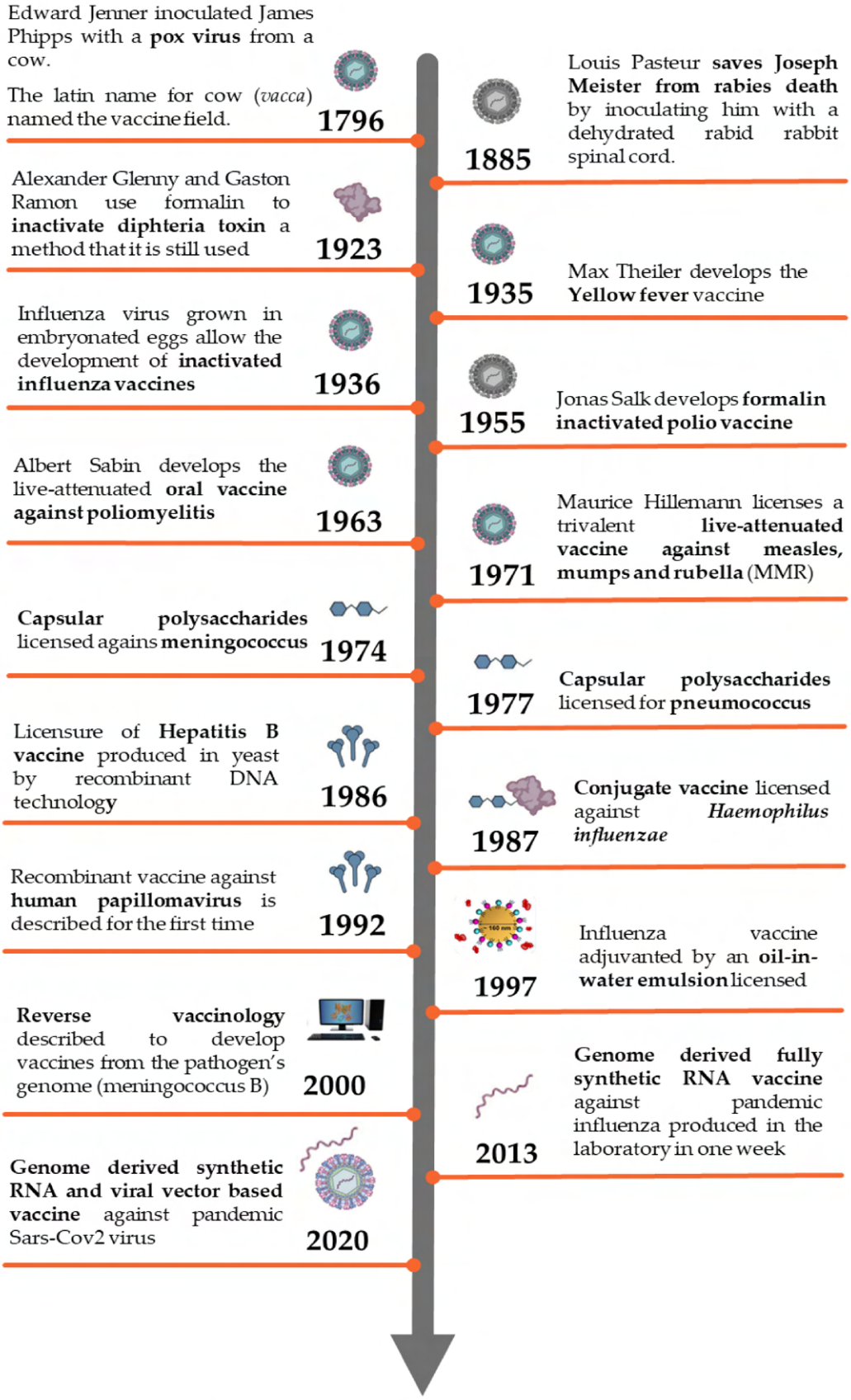

Figure 1. Timeline of vaccines. Image adapted from Rappuoli, R; "Timeline: vaccines"; Cell (2020) [46] and created with BioRender.com

I.3 Glycoconjugate vaccines

I.3.1 From polysaccharide to glycoconjugate vaccines

Most bacteria are coated with a PS network, termed glycocalyx, which includes i) lipid-linked structures, such as lipopolysaccharides (LPS) for Gram-negative and teichoic acids (TA) for Gram-positive species; ii) surface peptidoglycans for Gram-positive species; and iii) capsular polysaccharides (CPS) for Gram-positive and -negative encapsulated bacteria. These surface PS contribute to biofilm formation and fuel virulence by increasing host attachment and supporting immune evasion [47, 48].

Plain PS-based vaccines have shown limited clinical efficacy due to their T cell (or thymus)-independent (TI) antigenic character [47, 49]. PS are built up with highly repetitive epitopes, and can activate specific B cells in a polyvalent fashion by crosslinking membrane-bound pentameric immunoglobulin M (IgM) B cell receptor (BCR) clusters [49]. However, they typically induce B cells differentiation into plasma cells, without formation of memory B cells (MBC) [47, 50-53], resulting in secretion of low-affinity IgM, and to a lesser extent IgG antibodies (mainly IgG2) [52, 54]. The mechanism of B cell activation, based on the crosslinking of multiple BCR, explains why the immunogenicity of these vaccines is size-dependent, with only high molecular weight (MW) antigens being able to induce an effective immune response [47]. PS antigens thus activate the immune system without involving major histocompatibility complex class 2 (MHCII) molecules, and consequently without T cell help [52, 54].

Adult individuals who have acquired PS-specific MBC prior to vaccination, likely through exposure to relevant pathogens [49, 55] or to cross-reacting PS from commensal bacteria or ingested food, can produce PS specific antibodies after vaccination [55, 56]. However, most of these antibodies are IgM and IgG2, which are poor complement activators and therefore less effective [47, 52, 54]. Additionally, repeated immunization does not lead to increased antibody titers, but can rather trigger hyporesponsiveness [57-59].

PS-based vaccines are not effective in immunologically naïve populations, such as children younger than 2 years, because of the lack of pre-existing MBC and the immaturity of their splenic marginal zone (MZ), which is the primary site for B cell stimulation [52, 54, 60]. In the elderly, limited production of naïve B cells in the splenic MZ prevents induction of a robust antibody production towards PS vaccines [52, 54, 61].

Of note, not all PS are TI antigens: zwitterionic polysaccharides (ZPS) such as *S. aureus* CPS type 5 and 8, *S. pneumoniae* Sp1 and *B. fragilis* PSA are well-studied examples of such ZPS [52].

Eliciting a T cell-dependent (TD) immune response against PS can be accomplished by coupling carbohydrates to a carrier protein to generate a glycoconjugate vaccine, which contains both B and T cell epitopes (Figure 1). Glycoconjugate vaccines induce a PS-specific adaptive immune response, a normal B cell affinity maturation in germinal centers, IgM to IgG class-switch recombination, B and T cell memory, and significantly higher protection compared to plain PS vaccines [55, 62].

Glycoconjugates are proposed to bind to carbohydrate-specific B cells through BCR or pattern recognition receptors and, upon internalization, the protein component is digested by proteases in the endosomal compartment, forming peptides which interact with MHCII molecules. The resulting complex is then transported to the B cell surface and presented to T cells. Activation of T cells induces B cell maturation, resulting in IgM to IgG class-switching and production of high-affinity carbohydrate-specific antibodies. The generated antigen-specific memory B and T cells can

be activated upon exposure to pathogens and consequently provide efficient protection [52, 62]. Critical events for mounting an appropriate humoral response, particularly T and B cell interactions in the germinal center, are outside the scope of this review but have been detailed elsewhere [55].

More recently, it has been shown that glycan-peptide fragments can be loaded onto MHCII molecules via the peptide and displayed at the B cell surface resulting in the generation of so-called Tcarb cells (carbohydrate-recognizing CD4+ T helper cells) [63-65]. Carbohydrate-specific T cell-mediated humoral responses have been found for a variety of glycoconjugates (*S. pneumoniae* type 3 CPS, *S. Typhi* Vi, *S. agalactiae* type Ib and *H. influenzae* type b), although it has not been seen for others, such as meningococcal group C CPS conjugate [66] which suggests coexistence of different processing mechanisms depending on the type of PS [67]. Tcarb activation may be an important element of the anti-carbohydrate immune response and should be taken into account in the design of new glycoconjugates.

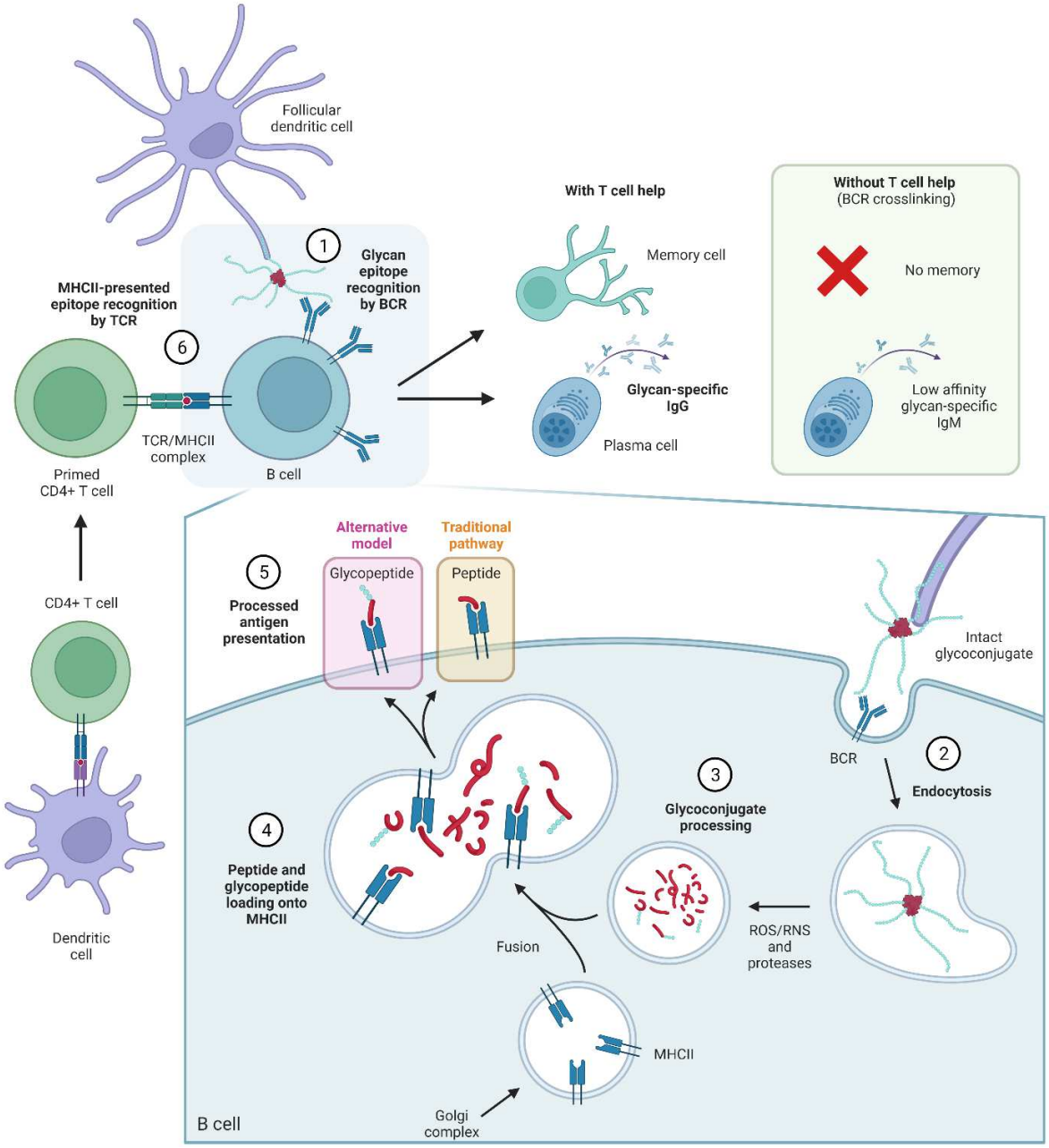

Figure 2. **Immunological pathways for processing glycoconjugates**. **1)** Glycoconjugates vaccines are taken up by antigen-presenting cells (APC) and presented to B cells, which recognize glycan epitopes through the B cell receptor (BCR). **2)** Upon BCR recognition, glycoconjugates are engulfed into the B cell via endocytosis. **3)** In the cell, glycoconjugates are exposed to acidic conditions and further degraded to fragments by enzymes and reactive oxygen/nitrogen (ROS/RNS) species. **4)** The resulting peptides and glycopeptides are loaded onto peptide-binding MHCII complexes, responsible for trafficking and exposing antigens to the cell surface. **5)** As MHCII molecules can only bind peptides (and ZPS), only processed peptides were thought to be displayed at the surface for T cell recognition, however, studies have shown that T cells can also recognize carbohydrates, suggesting glycopeptides can also bind MHCII. **6)** Primed T helper cells can recognize the presented antigen through their T cell receptor (TCR), and can, upon co-stimulation, initiate B cell maturation and production of memory cells and glycan-specific antibodies. In the absence of peptides, B cells cannot recruit T cell help and do not mount an efficient immune response. Image created with Biorender.com.

I.3.2 Glycoconjugate vaccines: 30 years of success

Glycoconjugate vaccines, developed over the past 30 years, are highly effective and safe tools for preventing life-threatening bacterial infections like meningitis and pneumonia. The introduction of the first conjugate vaccine against *Haemophilus influenzae* type b (Hib) between 1987 and 1990 [16, 19] marked a significant improvement in vaccine efficacy. This development addressed the limitations of earlier licensed Hib vaccines based on capsular polysaccharide, leading to a drastic reduction in reported cases, especially in infants under one year of age [15, 68-70].

The success of Hib glycoconjugate vaccines extends to other vaccines targeting *Neisseria meningitidis* and *Streptococcus pneumoniae*. Meningococcal groups A, B, C, W and Y are the most common causes of invasive disease as meningitis and/or septicaemia. Meningococcal vaccines have notably reduced the incidence of meningococcal disease, particularly among children under five years old [23, 71]. The UK's national immunization program since 1999 has played a crucial role in these declines across all age groups [72].

Invasive pneumococcal disease (IPD), caused by prevalent *Streptococcus pneumoniae* serotypes 14, 9V, 1, 8, 23F, 4, 3, 6B, 19F, 7F, was a major health concern before routine pneumococcal conjugate vaccination [73]. The introduction of PCV7 in 2006, followed by PCV13 in 2010 [74], resulted in substantial reductions in IPD due to targeted serotypes [75]. High vaccine coverage and both direct and indirect protection contributed to the success of the immunization programs, demonstrating the significant impact of glycoconjugate vaccines in preventing bacterial infections.

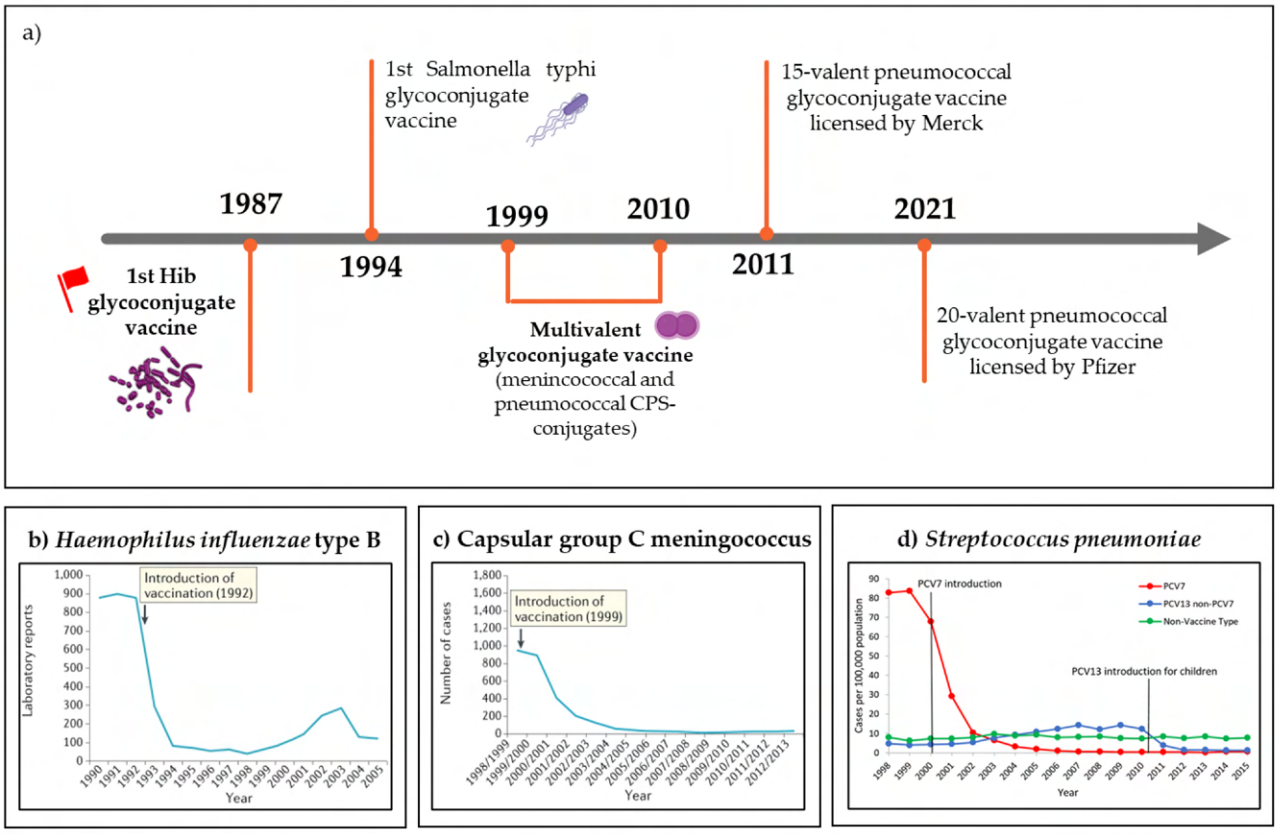

Figure 3. Timeline and impact of glycoconjugate vaccines. a) timeline of glycoconjugate vaccines (created with BioRender.com) and the impact of vaccination against b) *Haemophilus influenzae* type b [4], c) capsular group C meningococcus [4] and d) *Streptococcus pneumoniae* (materials developed by CDC) [4, 75].

Pathogens	**Type of Conjugate**	**Manufacturer**
***Haemophilus influenzae* type b**	PRP-TT PRP-OMPC PRP-CRM_{197} PRP-CRM_{197}	Sanofi-Pasteur Merck Nuron Biotech GSK
***Neisseria meningitidis* serogroups A, C, W and Y**	MenA-TT	Serum Institute India
	MenC-CRM_{197}	Nuron Biotech; GSK
	MenC-TT	Baxter
	MenACWY-DT	Sanofi-Pasteur
	MenACWY-TT	Pfizer
	MenACWY-CRM_{197}	GSK
***Haemophilus influenzae* type b** ***Neisseria meningitidis* group C and Y**	MenC/Hib-TT	GSK
	MenCY/Hib-TT	GSK
Streptococcus pneumoniae	7-valent-CRM_{197} (4, 6B, 9V, 14, 18C, 19F, 23F)	Pfizer
	13-valent-CRM_{197} (1, 3, 4, 5, 6A, 6B, 7F, 9V, 14, 18C, 19A, 19F, 23F)	
	20-valent-CRM_{197} (1, 3, 4, 5, 6A, 6B, 7F, 8, 9V, 10A, 11A, 12F, 14, 15B, 18C, 19A, 19F, 22F, 23F, 33F)	
	10 valent-DT/TT/ProteinD (1, 4, 5, 6B, 7F, 9V, 14, 18C, 19F, 23F)	GSK
	15-valent-CRM_{197} (1, 3, 4, 5, 6A, 6B, 7F, 9V, 14, 18C, 19A, 19F, 22F, 23F, 33F)	Merck
Salmonella Typhi (Vi)	Vi polysaccharide-TT	Biomed Barath Biotech

Table 1. Glycoconjugate vaccines currently licensed in US/EU/WHO [76]

I.4 Glycoconjugate vaccines production

I.4.1 Glycan antigen production

Licensed glycoconjugate vaccines are commonly produced by chemical conjugation of extracted bacterial PS to a carrier protein. PS are generally purified from bacteria and covalently linked randomly along the saccharide chain to a carrier with the formation of high MW, cross-linked and heterogeneous structures (Figure 4a) [77, 78]. The production of well-defined and uniform PS populations with a lower MW is sometimes preferred for consistency, as the elicited immune response can then better be correlated with the oligosaccharide's chemical structure [78, 79]. Recently, alternative approaches have been developed to produce oligosaccharides through organic synthesis or chemoenzymatic approaches (Figure 2a) [77, 78].

Specifically, organic synthesis has the advantages of producing well-defined and highly pure structures, which are more easily characterizable and devoid of any potential bacterial contaminants [78, 79]. Fully synthetic antigens have reached the clinic, notably with a synthetic *H. influenzae* type b (Hib) vaccine in Cuba [80], a PNAG conjugate that completed Phase I (NCT02853617), and more recently a vaccine against shigellosis that progressed to Phase II [81]. Novel synthetic transformations and deepened insight into glycosylation reaction mechanisms, combined with swifter synthetic protocols, based on one-pot reactions and automated synthesis, are allowing complex bacterial glycans to be more readily available [82]. Achievements in the production of synthetic glycans from PS expressed by AMR pathogens have recently been reviewed [78]. Despite the cost reduction provided by these modern methodologies, the manufacturing of complex multivalent vaccines remains a challenge.

Enzyme-catalyzed oligosaccharide assembly is an environment-friendly alternative to the chemical synthesis of bacterial carbohydrates. which could be attractive for industrialization [79]. Development of enzyme-based approaches has been shown feasible, particularly for meningococcal CPS synthesis [83]. Oligomers with a defined length could be obtained through solid-supported enzyme catalysis with simplified manufacturing and purification [84, 85]. The enzymatic approach, however, is limited by the availability of glycosyl donors, due to the variability of bacterial monosaccharides and the potential presence of rare sugars which would need *ad hoc* synthetic protocols for their preparation. No example of chemoenzymatic glycoconjugate vaccine has so far reached the clinical stage.

I.4.2 Protein carrier

As discussed above, protein carrier plays a crucial role by providing T cell epitopes to confer a T-dependent character to T-independent antigens, such as capsular polysaccharides (PS). The five carrier proteins in licensed conjugate vaccines are diphtheria toxoid (DT), tetanus toxoid (TT), CRM_{197}, Haemophilus protein D (PD), and the outer membrane protein complex of serogroup B meningococcus (OMPC) [86].

DT, TT, and CRM_{197} are detoxified bacterial toxins, chosen for their safety record from decades of tetanus and diphtheria vaccination. OMPC has been utilized in Hib and first-generation pneumococcal conjugate vaccines [87, 88]. PD, a 40 kDa protein from non-typeable H. influenzae, serves as a carrier in multivalent pneumococcal conjugate vaccines [89, 90]. CRM_{197} is a 58 kDa nontoxic mutant of diphtheria toxin with a single Glycine to Glutamic amino acid substitution at position 52 [91, 92], extensively used in licensed Hib, multivalent meningococcal, pneumococcal conjugate vaccines, and other developmental vaccines [93, 94]. Additionally, other carriers like the recombinant non-toxic form of Pseudomonas aeruginosa exotoxin A (rEPA) have been tested in preclinical and clinical studies, demonstrating versatility in carrying antigens for various vaccines, including Shigella [95], Staphylococcus aureus [96], and Salmonella Typhi Vi antigen [97, 98].

Exploring novel carrier proteins is fundamental considering that anti-carbohydrate immune response decreased due to pre-exposure or co-exposure to carriers, and the potential dual role of a carrier serving as both a carrier and protective antigen. Emerging multivalent carrier systems, including nanoparticles and OMV/GMMA, are being investigated for their ability to present multiple copies of carbohydrate antigens and for their inherent adjuvant properties [99] discussed in detail in sections I.6 and I.7.

I.4.3 Approaches for glycoconjugation

For long PS, conjugation to the carrier protein is carried out randomly along the carbohydrate chain, taking advantage of the abundant lysine residues and the high reactivity of activated saccharide residues. Because there is no or little control in the regiochemistry of this conjugation chemistry, the random approach results in cross-linked glycoproteins with variable saccharide loading and antigen positioning (Figure 5a) [79]. In contrast, conjugation of oligosaccharides to the protein can take place directly through the reducing end of the sugar or via a spacer, to reduce steric hindrance, with the formation of more defined and easy to characterize radial structures (Figure 5a) [77]. More selective approaches are required for proteins that serve a dual role as antigen and glycan carrier. Two main strategies for site-selective protein engineering are applied for glycoconjugation: the incorporation of unnatural amino acids (uAA) and the *in vivo* bioconjugation referred to as protein-glycan coupling technology (PGCT) (Figure 5b) [100].

Recent examples of glycoconjugates relying on uAA include the development of a malarial vaccine, in which a glycosylphosphatidylinositol antigen was incorporated at the C-terminal p-azidomethyl phenylalanine of a Malaria protein Pfs25, that was expressed *E. coli* [101]. A conjugate obtained through a similar approach, based on the polyrhamnose backbone of the universally conserved cell wall carbohydrate from Group A *Streptococcus* (GAS) and the toxin antigen streptolysin O, generated in mice functional antibodies against both virulence factors and provided protection against systemic GAS challenges [102]. A 24-valent pneumococcal vaccine where PS were site-selectively coupled to engineered CRM_{197}, bearing multiple uAA for conjugation away from the most relevant T cell epitopes, induced opsonophagocytic antibodies in rabbit, raising IgG levels

comparable to PCV13 for the same serotypes [103]. The vaccine completed Phase II clinical studies, while a 31-valent vaccine is under preclinical development.

PGCT is a single-step *in vivo* bioconjugation of the saccharide antigen and the carrier protein, which are both expressed in *E. coli*, thus avoiding the need for separate expression and purification of each component [104]. The technology is based on the N-linked glycosylation system from *Campylobacter jejuni* that can be functionally expressed in *E. coli* [105]. More specifically, PglB, the oligosaccharyltransferase enzyme, couples the PS synthesized on a undecaprenol pyrophosphate lipid anchor within the cytoplasm to the acceptor carrier protein having the acceptor sequon (D/E–X–N–X–S/T) to generate the bioconjugate [77]. Generally, up to 4-5 consensus sequences are inserted within the protein, although full occupancy can be difficult to achieve. PGCT is not limited to the use of PglB, and new enzymes are continuously being discovered to further extend bioconjugation toolbox [106, 107].

A variety of bioconjugate vaccines based on O-antigens (*A. baumannii*, *B. pseudomallei*, *E. coli*, *F. tularensis*, *K. pneumoniae, S. dysenteriae* and *S. flexneri*) and CPS (*S. aureus*, *S. pneumoniae*) have been generated and found immunogenic in animal preclinical models [106, 108-110]. Some of these bioconjugates are currently undergoing clinical evaluation: a *Shigella* 2a vaccine[111] was shown to induce anti-lipooligosaccharide antibodies associated with a reduction of disease in a Phase II study[112]; a 9-valent vaccine against extraintestinal pathogenic *E. coli* (ExPEC9V) to prevent invasive infection in older adults with a history of UTI has advanced to Phase III (NCT04899336) [113] while a *S. pneumoniae* (NCT03303976) and a 4-valent *K. pneumoniae* vaccine have entered Phase I studies (NCT04959344) [77]. The limited amount of saccharides that can be incorporated using site-selective technologies might pose some challenges for less immunogenic PS, and clinical studies will be relevant to inform on this.

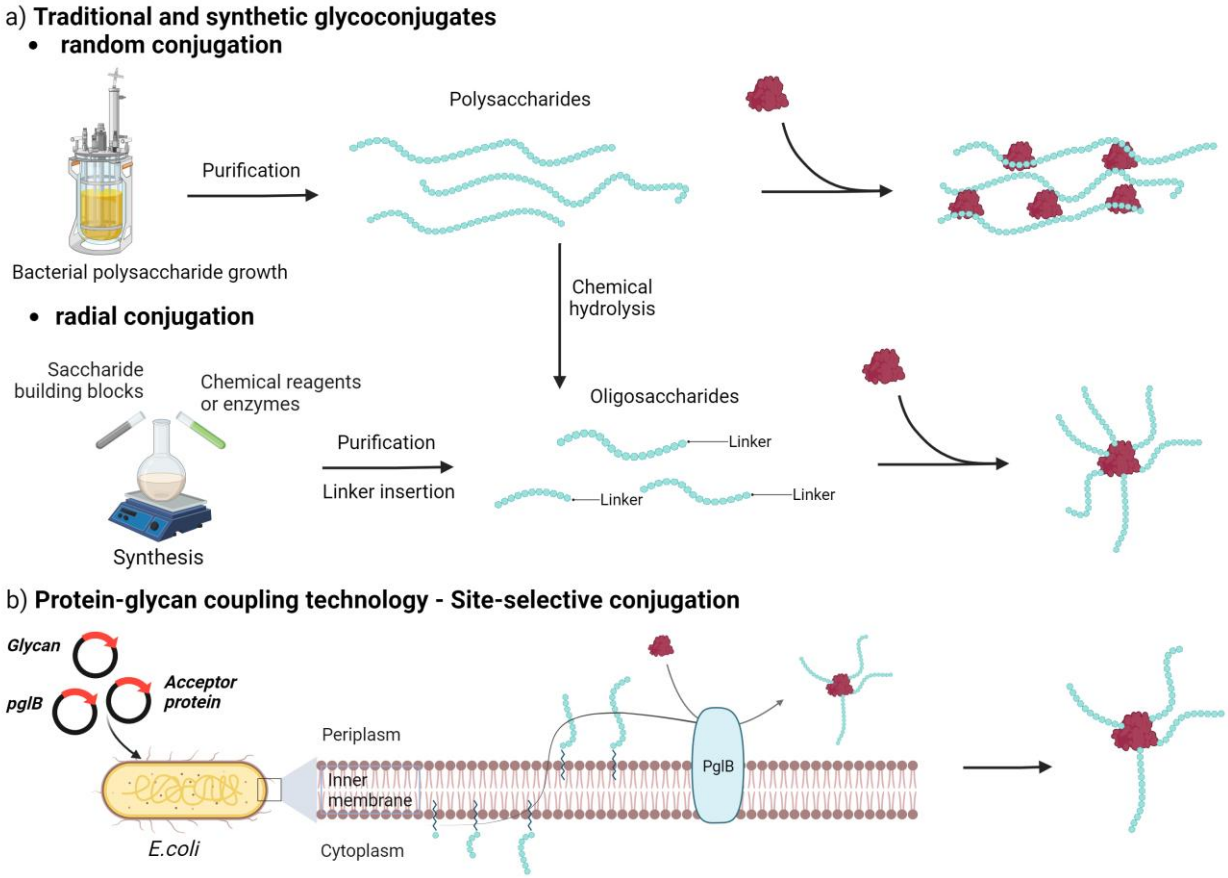

Figure 5. Simplified pathways for production of glycoconjugate vaccines. Oligosaccharides can be obtained from isolated PS through hydrolysis or oxidation. Various conjugation chemistries can be employed, resulting in site-selective or random conjugation on the carrier and/or the saccharide. Site-selectivity can be achieved on reactive groups or at the reducing end of the carbohydrate through reductive amination, while uAA engineering or N-terminal linkage can reach selectivity on carrier proteins. Classical random conjugation strategies usually involve Lysine or Cysteine residues (e.g. N-hydroxysuccinimide (NHS) esters or thiol-maleimide reactions) for the protein, and hydroxyl groups for the saccharide (e.g. 1-cyano-4-dimethylaminopyridine (CDAP) activation and conjugation). Images created with Biorender.com.

I.5 Weakness of glycoconjugate vaccines

Licensed glycoconjugate vaccines have had a huge impact on global mortality and morbidity by decreasing and controlling historical burden of humankind overcoming the incomplete protection induced by polysaccharide-based vaccines.

Whereas conjugate vaccines have shown significant efficacy, certain high-risk groups, such as the elderly or immunocompromised individuals, continue to face challenges with poor immunogenicity [114]. Moreover, most glycoconjugate vaccines necessitate multiple booster doses to confer complete protection and are slow to induce protective antibody titers [115]. Another complication arises from the mutable global distribution of serotypes and serotype replacement events for pneumococcal and meningococcal infections, necessitating ongoing surveillance of vaccine serotype coverage [116-119] and the addition of new serogroups to existing vaccine formulations that led to the very recently approved (2021) 15-valent [120] and a 20-valent [121] pneumococcal conjugate vaccines. Additionally, the utilization of alternative protein carriers to enhance vaccine immunogenicity is advised, particularly in multivalent formulations, overcoming preexisting immunity to protein responsible of "carrier epitope suppression" associated to reduced immunogenicity [122-124]; for this reason, new carrier protein and alternative platform as virus-like particles, vesicles and multivalent display platforms for the delivery of saccharide antigen are under development in clinical and pre-clinical stage (see section I.6).

A lot of progress has been done on techniques for the development of glycoconjugates understanding the correlation between glycoconjugate features with induction of a higher immune response testing diverse saccharides in length, composition on distinct carrier proteins using different glycoconjugation approaches [65, 125-128]. Whereas there is an increasing interest in understanding the behavior of conjugates vaccines in different populations, a field poorly explored because of the complexity of immune system differently activated depending on age and healthy status.

The immune response undergoes changes throughout life, progressing from neonatal and infant stages through adulthood, including pregnancy, and ultimately experiencing a decline in old age. At birth, a child is protected by maternal antibodies possessing an immature innate and adaptive immune system, which gradually matures and develops memory through vaccinations and natural infections (Fig. 6) [129]. However, in old age, the immune system weakens and becomes hyporesponsive, resembling the state of an immunocompromised [130]. These changes result in varied responses to vaccines based on the life stage and overall health condition.

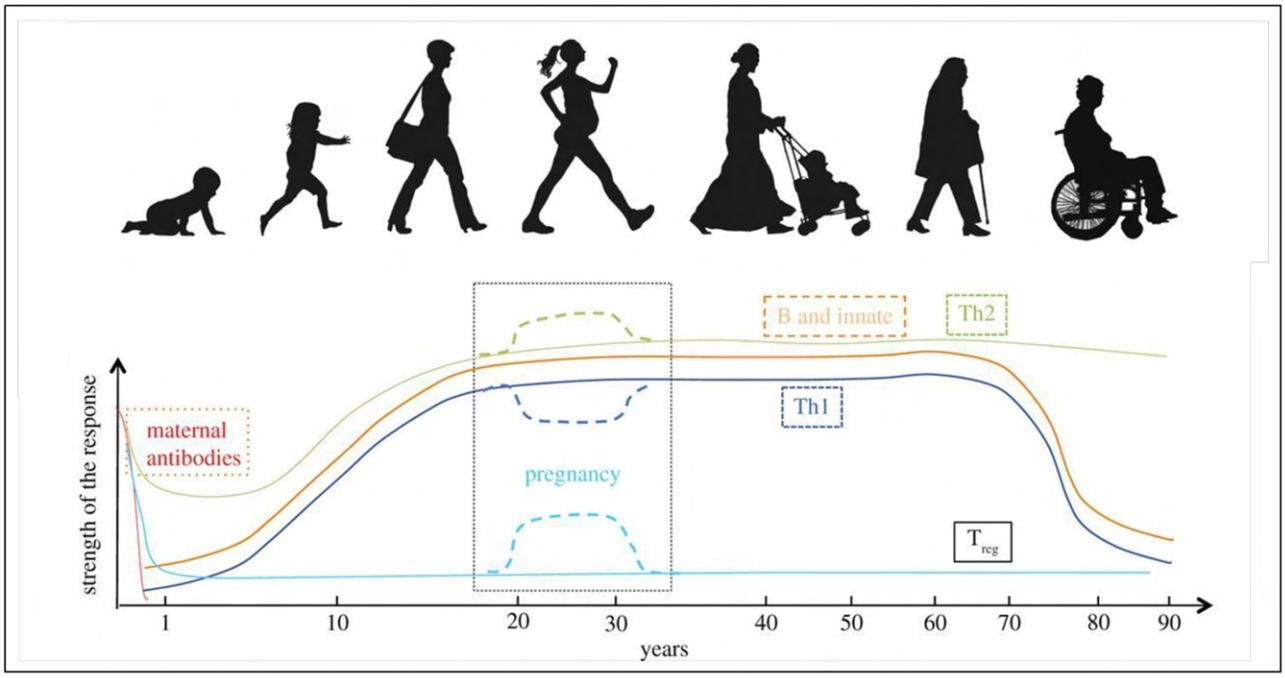

Figure 6. Schematic graph of the different arms of the immune response over the lifetime of an individual [129].

In adults with a fully developed immune system, glycoconjugate vaccinations prompt efficient responses, generating protective antibody levels even after the initial dose. Although these antibody levels decrease over time, they persist at higher levels compared to those in non-vaccinated individuals. Administering a booster dose three or more years later significantly elevates antibody levels, indicating that a single dose can stimulate memory B cells capable of responding swiftly to a booster immunization (Fig. 7) [55].

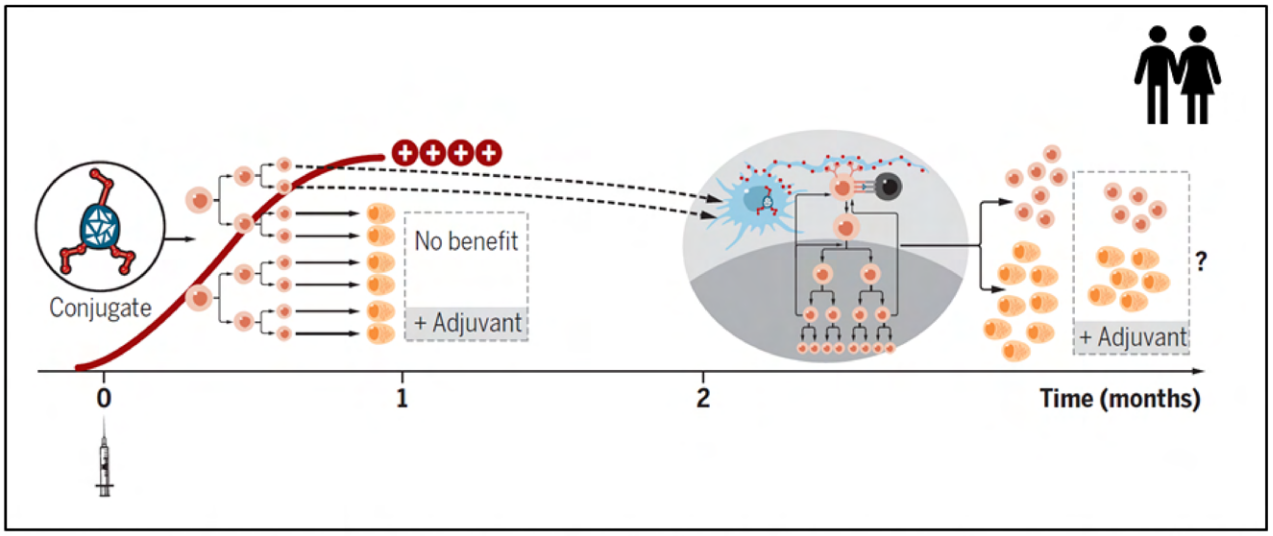

Figure 7. Immune response to glycoconjugate vaccine in adults [55]. Conjugate vaccines induced in adolescents and adults a T-cell independent extrafollicular proliferation of pre-existing low affinity memory B-cells, which produce a rapid immune response; Affinity maturation in the GC also occurs, leading to a stronger response to a booster dose.

Immunocompromised individuals, the elderly, and infants exhibit limited responsiveness to vaccinations compared to healthy adults. This is primarily attributed to the immaturity of the

immune system in infants, immune senescence in the elderly [131], and compromised immune mechanisms in immunocompromised individuals. Present vaccination schedules address these challenges by incorporating multiple booster immunizations or the utilization of potent adjuvants to elicit a robust immune response.

Infants, in particular, necessitate a minimum of 2-3 doses of the glycoconjugate vaccine administered at intervals of 30-60 days to reach protective antibody levels. Unlike in adults, a single dose is inadequate to activate the immune response in infants, and the efficacy may be enhanced through the use of adjuvants (Fig. 8) [55, 132].

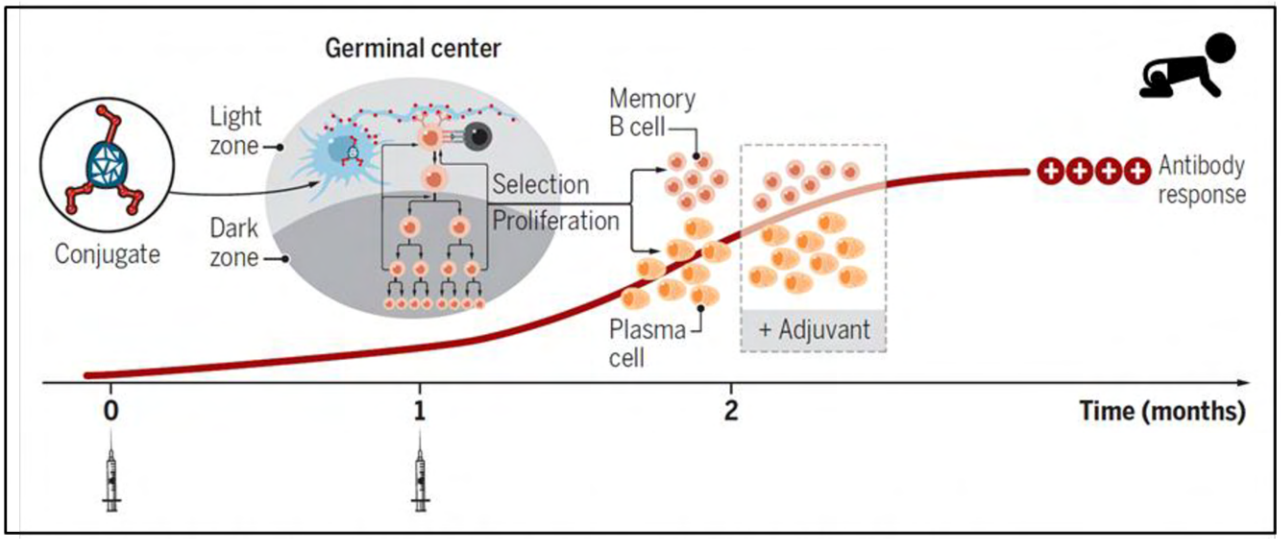

Figure 8. Immune response to glycoconjugates vaccines in infants [55]
Conjugate vaccines contain B and T cell epitopes and can induce normal affinity maturation of B cells in Germinal Center (GC) after at least two immunizations. The use of adjuvant can potentiate the GC reaction.

A study conducted in US about vaccination coverage among children under 2 years old revealed that only 25% receive all the six recommended vaccinations [133, 134], indicating that too many children did not complete the six recommended vaccinations underlining the importance of renewed efforts toward the designing of single dose vaccines. Importantly, if a proper programme of maternal immunization is implemented, it will be possible to relax the aggressive immunization schedules of today, providing protection for the foetus and the infant during early life [135]. Despite these benefits, low vaccine confidence remains a significant barrier to vaccine uptake among pregnant women worldwide and a small number of vaccines are recommended for routine use during pregnancy [136].

For example, Group B Streptococcus (GBS) disease affects newborns and is caused by the bacterium *Streptococcus agalactiae* that can be present in the reproductive tracts of some women without causing symptoms [137]. During childbirth, an infant can be exposed to GBS, leading to infection [138]. Newborns with GBS infection may exhibit severe symptoms including pneumonia, meningitis, and sepsis [139]. Prevention strategies involve administering antibiotics during labor to reduce the risk of transmission to the newborn [140]. Maternal vaccination represents and alternative strategy to antibiotics to prevent GBS colonization in pregnant women, thus reducing the risk of transmission to newborns during childbirth [141-144]. Ideally, the vaccine should be administered during the third trimester of pregnancy eliciting a strong immune response to optimize the

transplacental transport of maternal antibodies to the foetus. The development of such vaccine remains an unaddressed medical need primarily because of the very short administration window requiring a single-dose vaccine. Actually, GBS PS conjugated to CRM_{197} or Tetanus Toxoid (TT) were tested in clinical trial resulting safe and high immunogenic in women primed by GBS colonization [145-149], while in unprimed women multiple injections within 1 years are necessary to achieve protective titers [145, 150, 151].

The elderly population represents a growing demographic group with evolving medical needs (Fig. 9). The aging immune system renders them more susceptible to infections and responsible of a diminished vaccine response. 13-valent pneumococcal conjugate vaccine efficacy declined from 65% to 40% in adults aged 75 years old compared to 10 years younger adults [152]. In many instances, the effectiveness of vaccines is augmented by adjuvants specifically tailored to stimulate the aging immune system, enhancing its responsiveness to vaccination. Certain licensed adjuvants, such as MF59 and AS01, have demonstrated efficacy in improving the immune responses after vaccination among the elderly, thereby reducing hospitalization rates [153-155]. Exploring the incorporation of such adjuvants into the formulation of glycoconjugate vaccines holds promise for effectively stimulating the aging immune system.

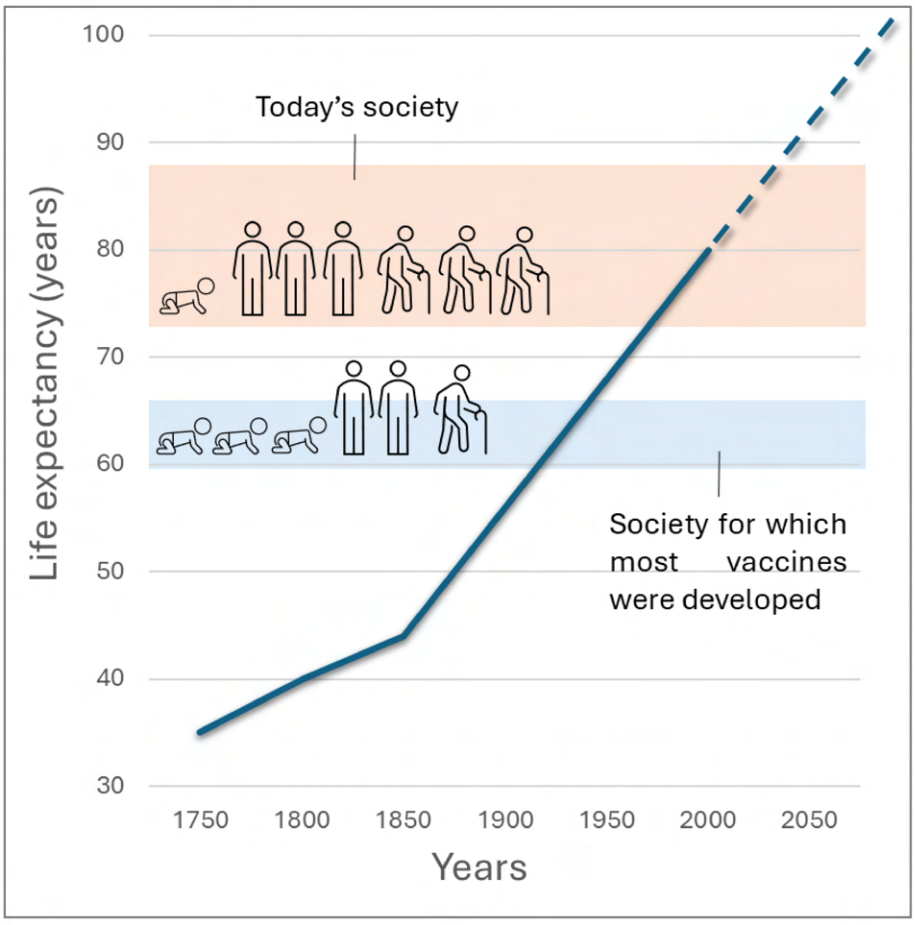

Figure 9. Increase of life expectancy (Image adapted from Rappuoli *et al.*, 2011 [156]). The society for which the majority of vaccines were originally developed had an average life expectancy of 60–65 years, with a notable demographic composition including a significant proportion of children and young individuals. This demographic landscape contrasts with today's society, marked by a predominant presence of elderly individuals and an extended life expectancy superior to 80 years.

Vaccinations are crucial also for immunocompromised individual as HIV-infected adults due to compromised host defences. In addition to immunologic reasons, HIV-infected persons are at higher risk due to frequent contact with the medical environment. Despite the elevated risk and the availability of vaccines, there are reported low coverage rates among HIV patients. Concerns about vaccine safety and uncertainties about efficacy contribute to these challenges. The optimal timing of

vaccination among HIV-infected adults in regard to HIV stage and receipt of antiretroviral therapy remain important questions [157, 158].

It is evident that there is a need to develop a more potent glycoconjugates vaccine to protect high-risk populations. This would enable them to quickly achieve protective antibody levels ideally after one dose, reducing schedule injections, thereby protecting them promptly during the critical and vulnerable stages of life.

Decreasing the number of vaccine doses could provide notable value for the society. Ideally single-administration vaccines could provide: i) the improvement of worldwide coverage of vaccination, ii) the cost decrease associated with multi-dose regimens, iii) ameliorate patient adherence. But all the efforts attempted to produce potent one-single dose glycoconjugate vaccine have been unsuccessful so far. However today, advancements in technology and a deeper understanding of the immunological mechanisms have contributed to the progress in a better vaccines design. For instance, the delivery of appropriate immune stimuli provided by an adjuvant and the development of improved antigen delivery and presentation to the immune system in novel platform can elicit robust immune responses.

I.6 New generation of glycoconjugate vaccines in clinical trial

I.6.1 Glyco-OMV/Glyco-GMMA

Gram-negative bacteria generate low amounts of outer membrane vesicles (OMV) through a blebbing process, which can be stimulated through strain engineering to destabilize the membrane and effectively produce generalized modules for membrane antigens (GMMA) (Figure 3b). GMMA faithfully resemble the bacterial outer membrane and possess self-adjuvating properties through the display of several pathogen-associated molecular patterns, which are conserved small molecular motifs in bacteria that are recognized by pattern recognition receptors on mammalian cells. For example, GMMA expose surface O-polysaccharide (OPS) chains in their natural environment and conformation, thus promoting uptake by immune cells and inducing strong immune responses. GMMA in which the lipid A portion of its LPS has been modified to modulate endotoxicity have, therefore, been proposed as vaccine candidates [159, 160]. The safety of *S. sonnei* GMMA was demonstrated in a Phase I study [79, 161, 162]. A number of PS from different pathogens (*N. meningitidis* serogroup A, *H. influenzae* type b, GAS and *S. Typhi* Vi) have been successfully conjugated to GMMA and shown to be immunogenic in animal models [163-165]. The chemical linkage was directed either to proteins or to the LPS expressed on the vesicle surface [164, 166, 167].

Alternatively, strategies to engineer *E. coli* to express heterologous PS on GMMA and OMV have been developed [168]. Glyco-OMV have been generated by exploiting the PS biosynthesis on the native undecaprenyl pyrophosphate carrier in the cytoplasmic side of the inner membrane and subsequent translocation to the periplasm side through the endogenous flippase Wzx, to enable the final transfer on the lipid A by the endogenous O-antigen ligase WaaL [168]. Glycans can also be assembled from the terminal sugars of the truncated lipid A-core expressed on the cytoplasmic side of the inner membrane and then flipped to the periplasm by the Lpt protein complex for final transfer onto the outer membrane of the vesicles [169]. Glyco-OMV expressing OPS from various pathogenic bacteria, including the highly virulent *F. tularensis* ssp. *tularensis* type A strain Schu S4 (generating Ft-glycOMV) have been produced through this approach [170]. The glycol-OMV induced antibodies protecting mice from a lethal challenge with *F. tularensis* after passive transfer and elicited a protective IgA-mediated mucosal immune response when subcutaneously administered. Glyco-OMV decorated with pneumococcal CPS were also generated and induced serum IgG opsonophagocytic titers comparable to the corresponding chemical conjugates in PCV13 [171]. Finally, the hypervesiculating JC8031 strain of *E. coli* was engineered for expression of *S. aureus* PNAG, both in acetylated and deacetylated form (dPNAG) [172]. After mice immunization, the dPNAG-OMV-elicited antibody mediated *in vitro* killing of PNAG-positive *S. aureus* and *F. tularensis holarctica* and protected mice from challenges with the two bacterial species.

I.6.2 MAPS Technology

MAPS enables the creation of a macromolecular complex by integrating glycan and protein antigens to reproduce the antigenic and immunologic strengths of whole-cell vaccines (Figure 11c). In the MAPS, differently from classic conjugate vaccines, the PS and protein are not covalently linked, but affinity binding is exploited to generate multivalent immune complexes, thus mimicking chemical and physical features of a whole-cell constructs for B and T cell activation [173, 174]. The MAPS complex is obtained by mixing a target protein antigen, genetically fused to an avidin moiety (termed rhavi), and a biotinylated PS [173]. The immunogenicity of the formed macromolecular construct depends on the size of the PS scaffold, as the protein becomes exposed along its chain. As the MAPS approach allows for the combination of a variety of protein and carbohydrate components, it appears advantageous in the design of vaccines against challenging pathogens, such as *S. aureus*, a bacterium known to have complex host-pathogen interactions [173, 175]. Depending on the size of the glycan-protein complex, the MAPS also allows to achieve Th1/Th17-biased immune responses [173].

MAPS technology appears also to streamline the manufacturing process and this feature has been exploited for the development of 24-valent pneumococcal vaccine that was successful in Phase II clinical studies [176] A multivalent vaccine to fight invasive *Klebsiella* and *Pseudomonas* infections is also in progress (Patent no. US11612647B2) [177].

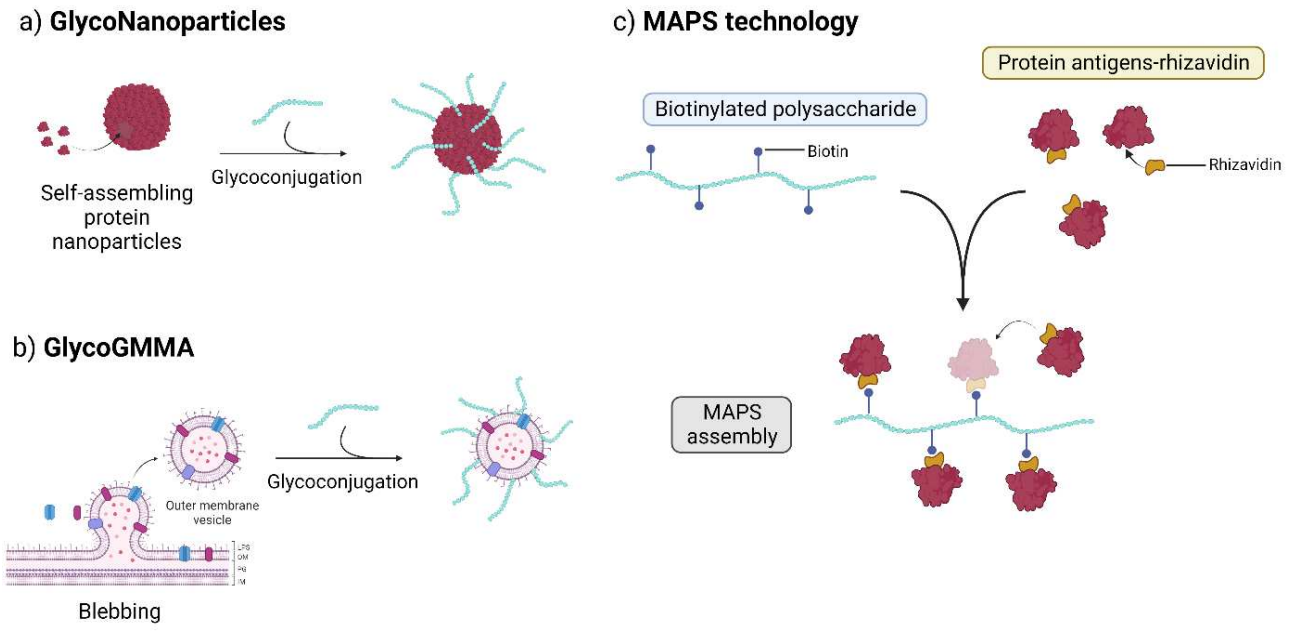

Figure 11. Innovative glycoconjugate technologies. Images created with BioRender.com.

I.7 Self-assembling protein nanoparticles: an emerging platform for vaccines development

Glyconanoparticles can display antigens with high density in a high order-structure arrangement, as naturally presented by a pathogen, enabling multiple binding events between the nanoparticle (NP) and the host cell BCR. The resulting high avidity can induce a more potent immune response than the single soluble recombinant antigens [99] (Fig. 12).

In addition, particles in the 50–200 nm size range can be actively transported by migratory cells, such as dendritic cells or macrophages, to lymph nodes which are the primary location of B cell maturation [178]. NP carriers could thus enhance antigen uptake by APC and BCR cross-linking as compared to classic protein carriers [179].

Self-assembling protein NP are protein oligomers assembling in three-dimensional structures which recently attracted interest in the field of vaccine development because of their unique properties, such as biocompatibility, enhanced stability and molecular specificity, leading to efficient delivery and antigen display at their surface [180, 181]. Virus-like particle (VLP)-based vaccines deriving from self-assembling viral structural proteins are already used in commercial vaccines (Figure 11a) [182]. Examples of VLP-based licensed vaccines include the hepatitis B virus (HBV) vaccine Recombivax HB™ [183], the human papillomavirus (HPV) vaccines, Gardasil™ (Merck) and Cervarix™ (GSK), and the hepatitis E virus vaccine Hecolin™ [184].

Recently, VLP have been tested as carrier for carbohydrates. An efficacious pneumococcal glycoconjugate vaccine based on Qβ VLP has been recently shown feasible [185]. VLP from the HBV core antigen have been exploited as carrier for the meningococcal group C CPS, generating a strong immune response in mice [186]. A conjugate vaccine developed by linking purified O-antigen from *V. cholerae* O1 to Qβ VLP using squarate chemistry generated in mice prominent and long-lasting anti O-antigen IgG antibodies that recognized native LPS from *V. cholerae* [187]. Qβ VLPs have been also used to develop a single-dose vaccine candidate for maternal vaccination against Group B *Streptococcus* (GBS).

New self-assembling NP scaffolds computationally designed with precisely control of morphology and characteristics are emerging as tools to assemble different immunological components (i.e. antigens and adjuvants) in order to amplify their immune responses [180, 181, 188, 189]. In silico designed Nano-B5 nanoparticles have been successfully bioconjugated to the O-polysaccharides of *Klebsiella pneumoniae* and *Shigella flexneri* with promising prophylactic effects in mice proving to be a potential technology for the development of AMR vaccines [190, 191].

Vaccine candidates designed through this approach and exposing glycoprotein antigens from respiratory syncytial virus (RSV), influenza and SARS-CoV-2 have been advanced in clinical trials [181, 192-195].

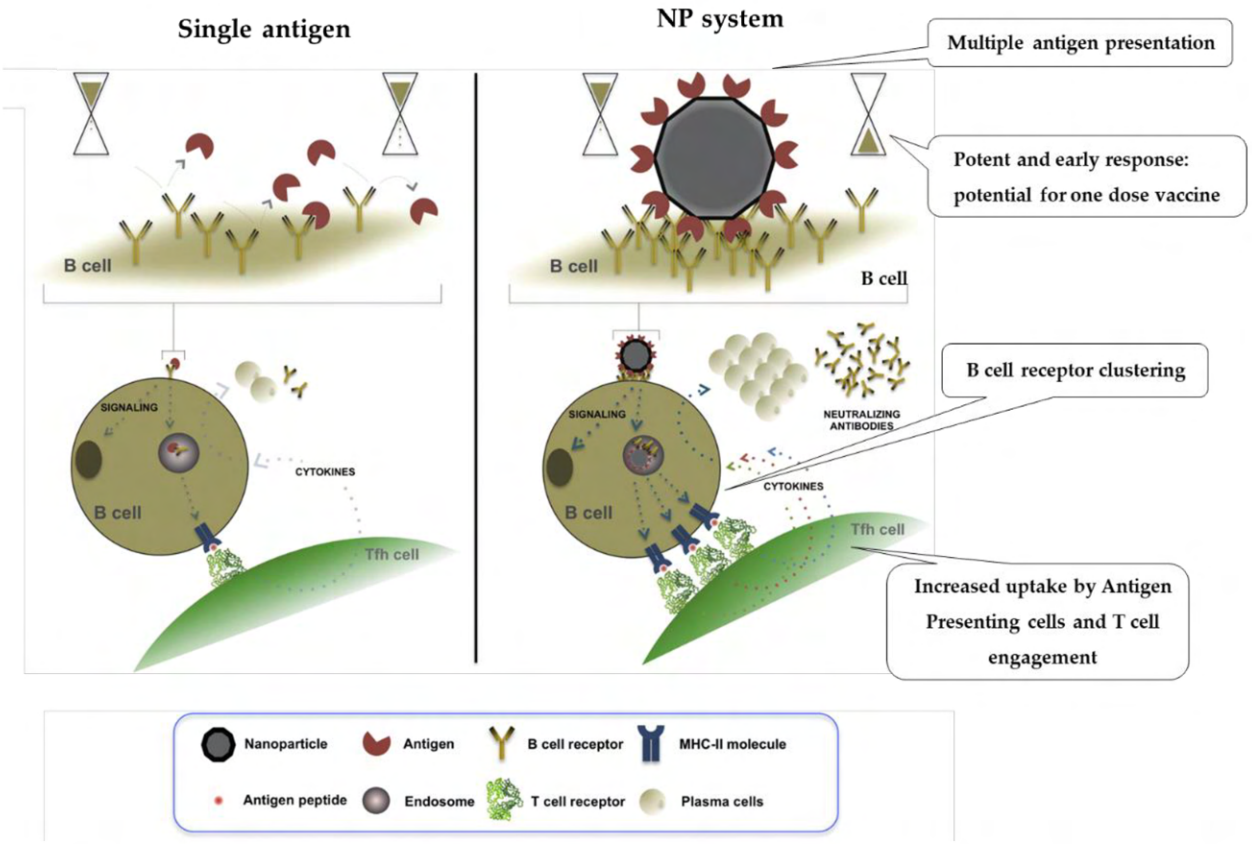

Figure 12. Comparison between nanoparticle system and single antigen in inducing an immune response [99]. The presentation of multiples copies of antigen in a highly ordered structure on a self-assembling nanoparticle generates a potent and early response enabling the clustering of BCRs for multiple and simultaneous engagement with the antigen epitopes, opposed to single antigen that provides brief interactions with the BCRs. Thus, translates into B-cell intracellular signaling, increased uptakes and processing of the antigen to present it via MHC complex to the T follicular helper cells (Tfh) evoking the cytokines secretion and maturation of B cells into plasma cells that can produce antigen-specific neutralizing Abs.

I.8 Adjuvants

The term "adjuvant" originates from the Latin words "adiuvare" (meaning “to aid”). In the context of vaccines, adjuvants are components able to enhance and shape antigen-specific immune responses. The goals of adjuvants added to a vaccine system include: i) boosting vaccine efficacy in the general population and hyporesponsive groups (such as infants, immunocompromised individuals, and the elderly) [61, 196, 197]; ii) broadening the antibody response mediated via expansion of B cell diversity [153, 198-200]; iii) reducing the required antigen dosage and the number of immunizations required for a protective immune response [201, 202]; iv) enhancing the magnitude and functionality of the antibody response [203], facilitating a quicker immune response with ultimate goal of single-dose vaccine [204, 205]. More recently, the new generation of adjuvants evolves in v) eliciting effective T cell responses incorporating agonists for Toll-like receptors (TLRs) [206].

Discovered in the 1990s, Toll-like receptors (TLRs) are a subset of pattern recognition receptors (PRRs) that serve as the initial defence against pathogens by recognizing molecular signatures on pathogen. TLRs are crucial in activating innate immune responses. Human TLRs, such as TLR3 (which recognizes double-stranded RNA), TLR4 (bacterial lipopolysaccharides), TLR5 (bacterial flagellin), TLR7 and 8 (single-stranded RNA), and TLR9 (single-stranded DNA composed of CpG motifs), each recognize specific ligands or agonists, contributing to the overall immune defence [207-209].

Until now few adjuvants have been licensed in human vaccines and are discussed below.

I.8.1 Alum

Aluminium salt-based adjuvants (alum) received approval for use in human vaccines over 90 years ago and were the only type of adjuvants used for 70 years [210]. These adjuvants, comprising aluminium hydroxide and aluminium phosphate, have played a pivotal role in enhancing immune responses against inactivated pathogens [211] and currently included in vaccines against diphtheria, tetanus, pertussis, hepatitis A and B, *Japanese encephalitis*, human papillomavirus (HPV), Meningococcus B and glycoconjugates [47, 212-214].

The introduction of aluminium hydroxide as the first vaccine adjuvant, followed by aluminium phosphate, marked significant milestones, and these forms continue to be the primary types of alum utilized in human vaccines [215]. Aluminium salt-based adjuvant are the only adjuvant authorized in conjugate vaccines such *as Haemophilus influenzae* type B and pneumococcal vaccines targeting children due to their outstanding safety [47, 216].

Alum's adjuvanticity is complex and cannot be simplified to depot-effect initially suggested by Alexander Glenny and colleagues in 1926 [217-219]. Several consistent themes have emerged, revealing that alum influences antigen uptake, triggers danger signals, recruits diverse immune cell types, and elicits Th2 responses [220, 221]. While there is ongoing debate about the signals responsible for innate stimulation by aluminium salts, it is anticipated that future research will uncover additional details and identify distinct mechanisms.

I.8.2 AS04

Aluminium salts have been employed as a platform for incorporating of Toll-like receptor (TLR) agonists as adjuvant system AS04. Specifically, AS04 is part of the registered human papillomavirus (HPV) and hepatitis B virus (HBV) vaccines and consists of aluminium salt formulated with 3-Odesacyl- 4-monophosphoryl lipid A (MPLA), a detoxified variant of lipopolysaccharide (LPS) derived from *Salmonella minnesota.* MPLA interacts with toll-like receptor 4 (TLR4) when adsorbed on aluminium salts [222-224]

The first day following the injection, an enhanced activation of monocytes and dendritic cells is observed which subsequently evolves into activation of antigen-specific T and B cells, induction of strong and persistent antibody and cellular responses [224]. The cytokine responses induced by MPL at the injection site is prolonged by aluminium salts. HBV (Cervarix™) and HPV (FENDrix™), both vaccines developed by GlaxoSmithKline [222] are adjuvanted with AS04 and induce high levels of antibodies compared to when adjuvanted with aluminium salts, revealing the added value of the TLR4 agonist MPL in humans [225, 226].

FENDrix™ contains HBV surface antigen (HBsAg) was created to improve the efficacy of HBV alum-based vaccine (Engerix-B™) in immunocompromised populations [227].

Cervarix™ contains HPV-type 16 and 18 major capsid protein, L1, as antigen with AS04 as the adjuvant [222]. This higher immunogenicity results in women between 10-55 years old into long-lasting antibodies that last more than 9 years after primary immunization preventing the formation of pre-cancerous cervical lesions [228, 229]. Some data suggest that this vaccine can be prevent also other HPV strains not covered by the vaccine [230]. This could be attributed to the generation of cross-functional antibodies or cell-mediated mechanisms triggered by AS04, similar to what observed for oil-in-water adjuvants in influenza vaccines.

I.8.3 MF59 and AS03

Emulsions have been employed as vaccine adjuvants since long, but we had to wait until the final years of the last century to have them approved for human use.

MF59 is an oil in water emulsion that consists of squalene oil while AS03 is an oil in water emulsion-based adjuvant (<200 nm) composed of two biodegradable oils, squalene and D,L-α-tocopherol and polysorbate 80 surfactant [231, 232]. Thus, AS03 differs from MF59 by the presence of D,L-α-tocopherol responsible to activate human monocytes and macrophages [231, 233].

MF59 doesn't activate Toll-like receptors but relies on the MyD88 pathway for its adjuvant effects, suggesting an independent TLR signalling pathway [234].

MF59, was licensed as adjuvant for influenza vaccines targeting individuals aged 65 and older under the name FLUAD™ by Novartis Vaccines and Diagnostics Inc., MA, USA. Originally licensed in Italy, it is currently available in 30 countries [235]. During the H1N1 pandemic, MF59 received approval for use in individuals as young as 6 months because of its excellent safety profile [236], providing immune response to heterologous strain, high protection in children aged 6 months to 5 years [237]. MF59-adjuvanted influenza vaccine provides antigen dose sparing, greater antibody responses, long lasting immune response in children and adolescents [200, 238-240]. MF59-adjuvanted vaccines notably decreased hospitalization rates for elderly individuals with pneumonia, acute coronary or cerebrovascular syndrome during peak virus circulation [241]. In a recent extensive randomized study involving approximately 170,000 individuals, MF59-adjuvanted

flu vaccines exhibited a remarkable reduction in hospitalization due to influenza and pneumonia among elderly (>65) [242]. Moreover, the MF59-adjuvanted influenza vaccine showed sero-protection in HIV-infected patients [243, 244] and patients affect of chronic kidney disease and under hemodialysis [245], suggesting significant MF59 adjuvant effects in immunocompromised patients.

AS03 was approved as an adjuvant for monovalent influenza vaccines, including H1N1 vaccines (Pandemrix™ and Arepanrix™) and H5N1 vaccines (Q-Pan H5N1 and Prepandrix™, or Pandemic Influenza Vaccine) developed by GlaxoSmithKline Biologicals [246]. The use of AS03-adjuvanted H5N1 vaccines was also evaluated in elderly populations, revealing higher seroprotection rates in individuals immunized with adjuvanted vaccines compared to nonadjuvanted ones [242, 247, 248]. Similar studies conducted on the H1N1 vaccines demonstrated their high efficacy in both adults and children [236, 249].

I.8.4 AS01

AS01 is a liposome-based adjuvant composed of two immunostimulants: MPLA and QS-21. QS-21 is a triterpene glycoside purified from *Quillaja saponaria* Molina, known to enhance antibody responses and to promote specific T-cell responses [250][62].

AS01 has now been evaluated in several candidate vaccines and shown to consistently the production of antigen-specific antibodies and CD4+ T-cell responses regardless of the antigen used, and age or specific immune conditions of the subject (reviewed in [251]).

AS01 is present as adjuvant in licensed vaccines against malaria (RTS, S/AS01 or Mosquirix™) and herpes zoster (HZ/su or SHINGRIX™) [252-254],

In Phase III clinical trials, three doses of RTS,S/AS01 reduced infection and increased CD4+ T-cell responses in infants (6–12 weeks old) and toddlers (5–17 months) from seven sub-Saharan African countries [255].

Herpes Zoster vaccine was developed as a result to protect and prevent varicella-zoster virus (VZV) infections in adults (<50 years), facing the efficacy reduction age-dependent of Zostavax™ (live-attenuated vaccine) [256]. Moreover, it was able to prevent shingles for up to 4 years post-vaccination in clinical trials [257].

A synergistic effect of MPL and QS-21, mediated by IL-12 and IL-18 and macrophages, triggers cells resident in the draining LN (mainly NK cells) to rapidly produce of IFN-γ essential for the optimal DC activation and subsequently the Th1-type functional immunity [257-259].

I.8.5 CpG Oligonucleotides

When a pathogen, such as bacteria, invades the body, it releases its DNA into the surrounding tissue triggering innate immune system inducing pro-inflammatory and T helper 1(Th1) -type cytokines playing a fundamental role in mounting the immune responses against bacterial infection. The bacterial DNA serves as a pathogen-associated molecular pattern (PAMP) and interacts with Toll-like receptor 9 (TLR-9) expressed by the cells. TLR-9 is located in the late endosomal and lysosomal compartments of the endoplasmic reticulum (ER) [209, 260-262].
The bacterial DNA contains unmethylated CpG motifs, which characterized prokaryotic DNA. On the contrary, it is uncommon in eukaryotic DNA where mammalian DNA frequently contains methylated CpG motifs [263, 264]. TLR-9 recognizes these unmethylated CpG motifs and induces an immune response to limit the proliferation and spread of the pathogen [265-267].
Synthetic oligodeoxynucleotides (ODNs) containing CpG motifs can effectively mimic bacterial DNA and trigger a similar immune response in target cells. In fact, once internalized by cells, CpG ODNs reach the late endosomal compartment and interact with TLR-9 to initiate signaling absent in TLR-9 knockout mice [268, 269].

Until now, three classes of CpG ODN have been identified, each characterized by a different structure and immunological function.
CpG ODNs Class A contains a unique CpG motif and palindromic sequences that permits the formation of a stem-loop structure (hairpin). The bonds of central nucleotides are phosphodiester (PO) while the ends are present poly G motifs with phosphorothioate (PS) bonds. CpG A tends to aggregate and form multimers due to the interaction between their poly-G tails which complicates product for clinical use. Nevertheless, it was successfully packaged into virus-like particles (VLP) and used as adjuvants in several preclinical and clinical studies [270-273]. CpG A stimulates pDC to mature and produce IFNα improving the function of professional antigen-presenting cells (APCs) and cytotoxic T lymphocyte response; but have no effect on B cells [274, 275]
CpG ODNs Class B expresses 1–5 CpG motifs with a phosphorothioate (PS) backbone. The PS increases stability to nucleases digestion considerably extending half-life *in vivo* from 30–60 min to 5–10 min [276]. CpG class B stimulates pDC to differentiate and produce TNFα while promotes B cell proliferation IgM production and IgG2a switching [274, 277, 278]. CpG class B has been the most extensively tested in clinical trials as describe below.
CpG ODN Class C is similar to class B-type because of PS backbone but resemble to Class A-type too because it contains palindromic CpG motifs that can form hairpin structure. This class triggers both B cells and pDC to produce respectively IL-6 and IFNα causing immunological activity in common with both CpG class A and B [279, 280].

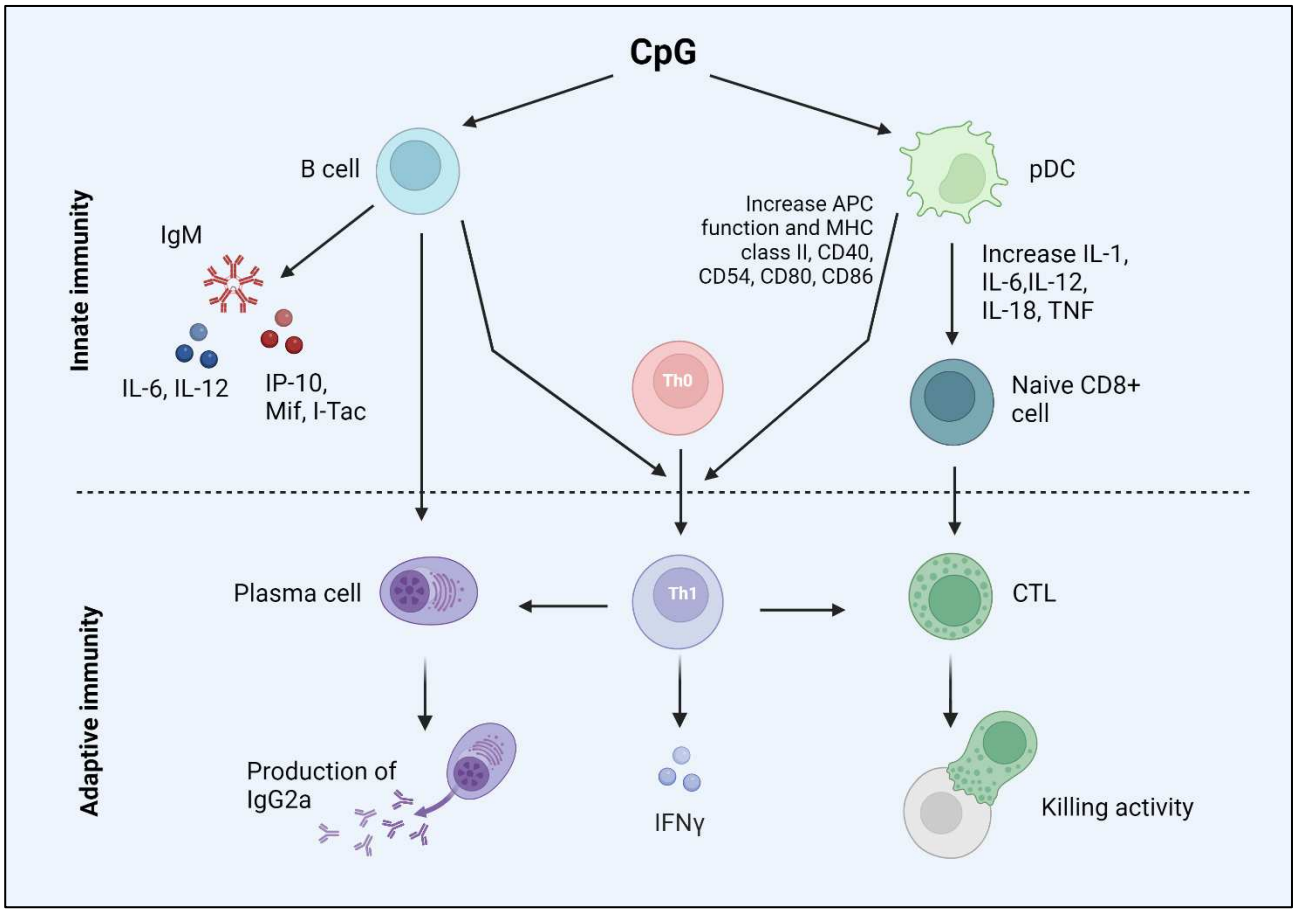

Figure 13. Mechanism by which CpG oligodeoxynucleotides activate innate and adaptive immune responses. (Image adapted from Bode *et al.* [281] and created with BioRender.com). CpG ODN directly activates pDCs and B cells leading to production of proinflammatory and Th1 cytokines and immunoglobulin. This innate immune response serves to develop antigen-specific adaptive immunity. Through enhancing the function of professional APCs, CpG ODN facilitates the generation of both humoral and cellular adaptive immune responses against co-administered vaccine antigens.

CpG ODN class B has been studying more than 100 clinical trials as adjuvants involved infectious agents, allergens, and cancer. For what concern CpG B adjuvant property in prophylactic vaccine, human clinical trials have evaluated in vaccines against HBV, *B. anthracis, Plasmodium spp., influenza virus,* and *S. pneumonia.*

CpG class B is licensed as adjuvant in only one vaccine, HBV vaccine under the name of HEPLISAV-B ™. Only two doses of adjuvanted-CpG HBV vaccine elicited faster (3 vs. 7 months), three- to ten-fold higher anti-HBsAg antibody titers and protective immunity in more subjects (95% vs. 81%) than 3 doses of alum-adjuvanted HBV vaccine (Engerix-B™) in healthy volunteers [282-285] but also in aged adults (60-70 years old) with type-2 diabetes mellitus [286]. Since CpG adjuvanted HBV vaccine was safe and effective, its activity HIV -patients was studied. The anti-HBsAg Ab response of patients immunized twice with the CpG adjuvanted vaccine was eightfold higher than patients immunized with alum-based HBV vaccine, achieving protective titers 4 weeks earlier that persist in 80% of the group over 5 years compared to 40% of non-CpG group [287-290]. In the same target population, the addition of a CpG to pneumococcal vaccine (Prevnar) significantly enhanced the proportion of vaccine responders [287].

An improved immune response was also observed by testing two-doses of CpG in Malaria or Anthrax vaccine compared to three-doses of corresponding not-CpG adjuvanted vaccine in healthy adults [291-295] and a more robust immune response in subject over the age of 65 [296].

Moreover, a dose sparing effect of CpG was observed when formulated with the human influenza vaccine (Fluviral™) and evaluated in a randomized, blinded, Phase Ib trial [297]. Those who received a 1/10th dose of the vaccine along with CpG showed a four- to seven-fold increase in IFNγ-producing PBMCs compared to recipients of a low-dose vaccine alone; nearly comparable to the level observed with a full dose of the vaccine without an adjuvant. But the inclusion of CpG did not improve hemagglutin inhibition (HI) Ab titers or total serum IgG levels.

In conclusion, the effect of CpG in vaccines demonstrate to induce a high and rapid immune response, dose sparing and promoting a long-lasting immunity even in hyporesponsiveness population to vaccination.

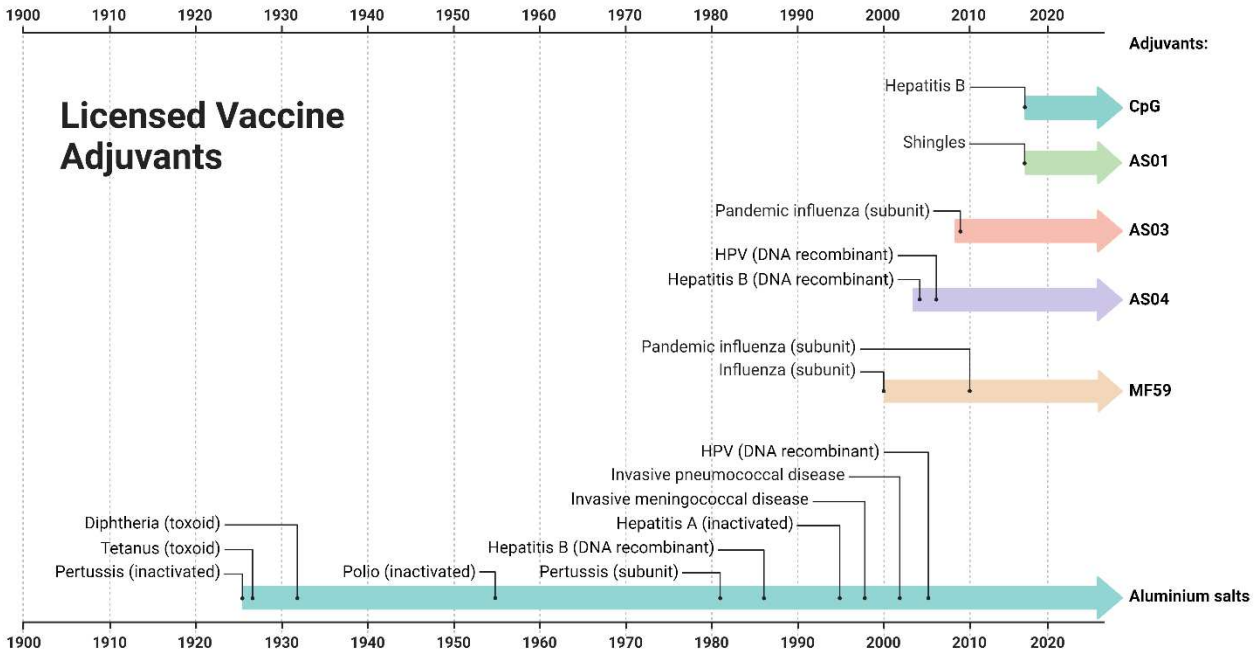

Figure 14. Timeline of Licensed Adjuvants from 1900 to 2020 used in human vaccines (Adapted from "Timeline of Adjuvant Used in Human Vaccines", by BioRender.com).

Chapter 2
Impact of protein nanoparticle shape on the immunogenicity of antimicrobial glycoconjugate vaccines

Content of Chapter 2 has been published: Dolce, M.; Proietti, D.; Principato, S.; Giusti, F.; Adamo, G.M.; Favaron, S.; Ferri, E.; Margarit, I.; Romano, M.R.; Scarselli, M.; Carboni, F. Impact of Protein Nanoparticle Shape on the Immunogenicity of Antimicrobial Glycoconjugate Vaccines. *Int. J. Mol. Sci.* **2024**, *25*, 3736.

2.1 Introduction

Vaccines are one of the most important achievements in preventive medicine because they ensure protection against a broad range of infections by stimulating humoral and cellular immune responses. Carbohydrates, found abundantly on the surface of many pathogens, are attractive candidates for vaccine development due to their interaction with both innate and adaptive immunity [298-300]. Many licensed vaccines use bacterial cell-surface antigens conjugated to subunit proteins to trigger antigen-specific protective antibodies and long-lasting immune responses by eliciting T-cell responses and memory B cell activation [301-303]. However, glycoconjugate vaccines often require adjuvants and booster injections to maintain protective antibody levels due to their low immunogenicity [55].

The field of glycoconjugate vaccines is continually advancing, improving our understanding of key carbohydrate characteristics that can influence the immunogenicity of glycoconjugates. This includes research on new and innovative techniques for creating saccharide antigens, such as synthetic or chemo-enzymatic methods, which have already yielded promising results [304, 305]. Concurrently, there is a growing interest in identifying new carrier proteins that could potentially amplify vaccine efficacy. This is achieved by displaying multiple copies of an antigen, thereby mimicking its natural presentation by the pathogen. A multivalent presentation can be achieved using protein nanoparticles that offer the possibility to chemically or genetically incorporate antigens exposed to their surface, mimicking pathogen dimensions [99, 306-308]. The elicitation of a more efficient immune response relies on the increase in cross-linking between B-cell receptors and antigens presented with consequently augmented B- and T-cell stimulation and activation [309, 310]. Moreover, protein nanoparticles have desirable traits such as biodegradability and biocompatibility, and have demonstrated efficient delivery of antigens to the lymphatic system due to their high uptake by dendritic cells [311].

Protein nanoparticle-based vaccines have already demonstrated their immunological value [25, 312] with the first approved vaccine being the Hepatitis B virus (HBV) vaccine. HBsAg, which constitutes the envelope of HBV, self-assembled into 22 nm virus-like particles (VLPs) [27] and resulted in 1000 times more immunogenicity than not-assembled HBsAg [313]. The same strategy was also used for the development of Human Papillomavirus (HPV) and Human Hepatitis E virus (HEV) vaccines [31, 32, 314].

In addition to their use as antigens, protein nanoparticles can also serve as carriers, addressing key challenges in vaccine design. They can carry various biomolecules, including polysaccharides [315, 316], viral [192, 317-319] and bacterial [320-323] protein antigens, peptides [324-326] and glycopeptides [327], nucleic acids [272] and small molecules [328, 329] making them versatile platforms for vaccine development. Protein-based nanocarriers have displayed great potential for coronavirus vaccine research [330-332], indicating their relevance in addressing current global health challenges.

Despite the licensing of various VLP-based vaccines and continuous progress in conjugation techniques for bacterial saccharide antigens, few glycoconjugated nanoparticles are currently under development in the pre-clinical stage. Carrier protein nanoparticles have been employed to promote a strong T-cell and long-lasting anti-glycan immune response against *N. meningitidis*, *K. pneumoniae*, and *V. cholerae* [186, 187, 191], to induce nanomolar affinity of antibodies towards pneumococcal saccharide antigens [185, 191] or to develop a single-dose vaccine addressing the medical need for a maternal vaccine against Group B *Streptococcus* (GBS) [316]. Additionally, in recent years, Nano-B5

nanoparticles based on the bacterial pentameric AB-5 toxin and designed through computational methods have been successfully bioconjugated to the O-polysaccharides of *Klebsiella pneumoniae* and *Shigella flexneri* with promising prophylactic effects in mice, proving to be a potential technology for the development of AMR vaccines [190].

Despite these few examples, no glycoconjugated nanoparticle vaccine candidates have advanced to the clinic. Still, limited knowledge is available on the optimal nanoparticle characteristics for glyconanoparticle vaccine candidates. In particular, the ideal size and shape to improve the delivery of saccharide antigen and enhance the immune response have not been investigated. The correlation between nanomaterial characteristics and their immune response has been primarily concentrated on gold and polymers, with minimal attention to protein nanoparticles, especially for glycoconjugate vaccine development [312, 333].

In the present study, we investigated how the size and shape of protein nanoparticles could influence the elicitation of an IgG response against bacterial saccharide antigens exposed to their surface. For this purpose, we used self-assembling proteins, manipulated in vitro, to get the desired shape and size, conjugated them to *Neisseria meningitidis* type W saccharide antigens, and tested their immune response in a murine model.

2.2 Results

2.2.1 Production of glycoconjugated protein nanoparticles

For our purposes, we looked for bacterial proteins from the literature that could: (i) cover the most represented particle shapes; (ii) be modulated in terms of size by varying their production methods; and (iii) present surface-exposed lysines as preferential sites for glycoconjugation.
We selected the Hemolysin-coregulated protein (Hcp1) from *Pseudomonas aeruginosa* to generate nanorings and nanotubes, and *Helicobacter pylori* ferritin to produce nanospheres.

Previous research by Ballister *et al.* reported that Hcp1 can spontaneously assemble into homohexameric rings with an outer diameter of 9.0 nm and a height of 4.4 nm [334, 335]. Moreover, the double mutant Gly-90/His and Arg-157/His (Hcp1cc) can stabilize through the formation of disulfide-bonded nanotubes up to approximately 100 nm in height [334].

After *E. coli* production and purification, Hcp1cc immediately originated a heterogeneous population of nanotubes with an average height of 20 nm, resulting from 4 to 5 assembled rings and reaching a maximum of 40 nm from 8 to 9 rings (Figure 1b). Longer nanotubes were generated by incubating Hcp1cc with the reducing agent dithiothreitol (DTT) to break disulfide bonds, followed by protein concentration and extensive dialysis. After 5 days of dialysis, nanotubes up to 60–80 nm in height, composed of 14–18 assembled rings, were observed by negative-stain Transmission Electron Microscopy (TEM) (Figure 1c). In summary, as shown in Figure 2 and Table 1, we produced ferritin nanospheres and Hcp1cc nanorings of comparable dimension (9–10 nm in diameter) and two populations of Hcp1cc nanotubes, one with a maximum height of 40 nm and a second one of 60 nm.

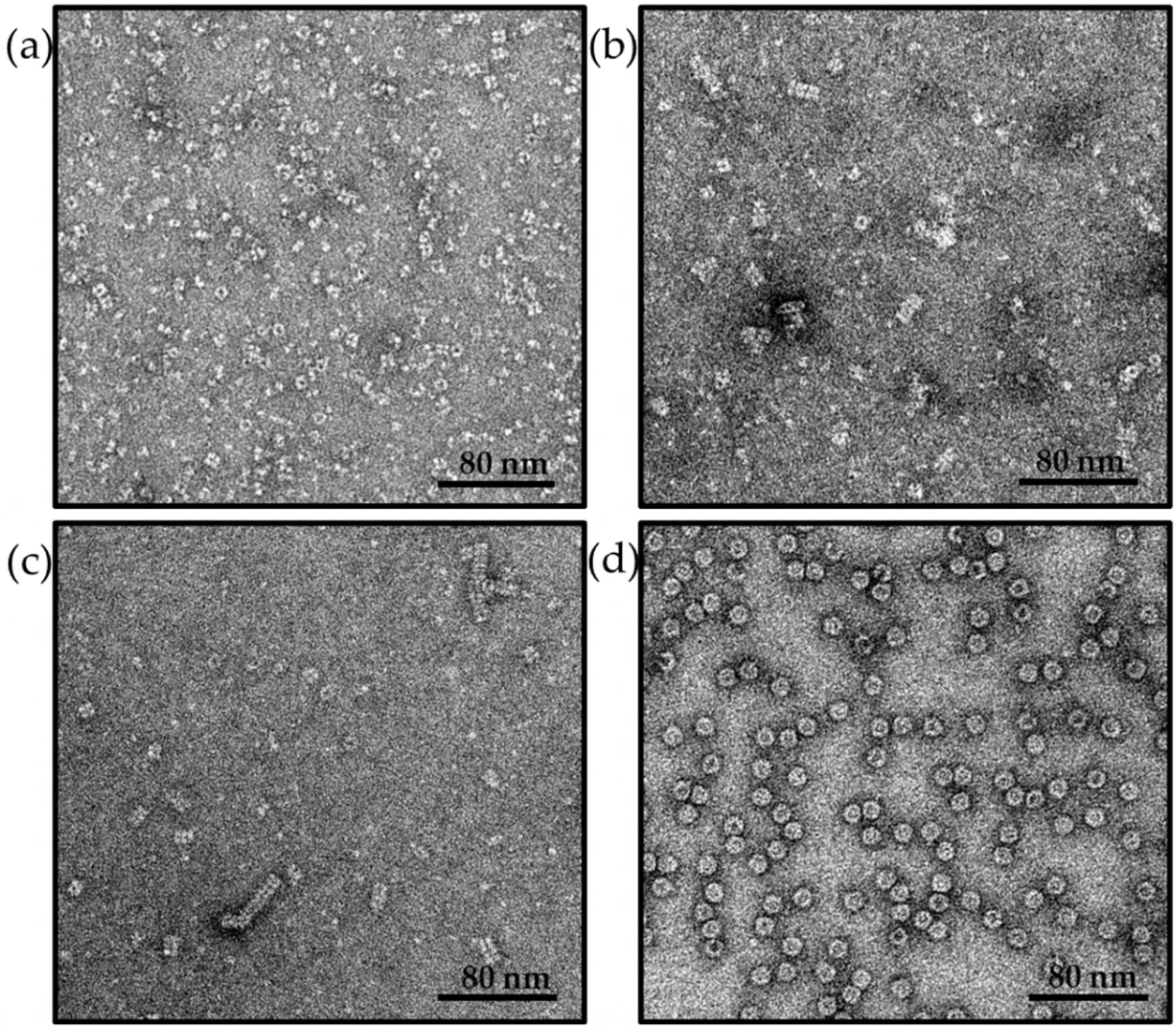

Figure 1. Transmission Electron Microscopy (TEM) of nanoparticles at different sizes and shapes after *E.coli* expression and purification. (**a**) Hcp1cc nanorings produced when Hcp1cc nanotubes are incubated in presence of reducing agent DTT; (**b**) Hcp1cc nanotubes; (**c**) Hcp1cc long nanotubes produced after oligomerization process; (**d**) *H. Pylori* ferritin.

Table 1. Summary of protein-based nanoparticles used in this study.

	Mw Monomer (kD)	**Number of Subunit**	**Mw Nanoparticle (kD)**	**Dimension (nm)**
Hcp1cc Nanoring	18.3	6 monomers (ring)	109.8	Diameter: 9 Height: 4.4
Hcp1cc Nanotube	18.3	up to 8–9 rings	Up to 878–988	Diameter: 9 Height: up to 40
Hcp1cc Long Nanotube	18.3	up to 14–18 rings	Up to 1537–1976	Diameter: 9 Height: up to 60–80
Ferritin	19.3	24 monomers	463	Diameter: 10

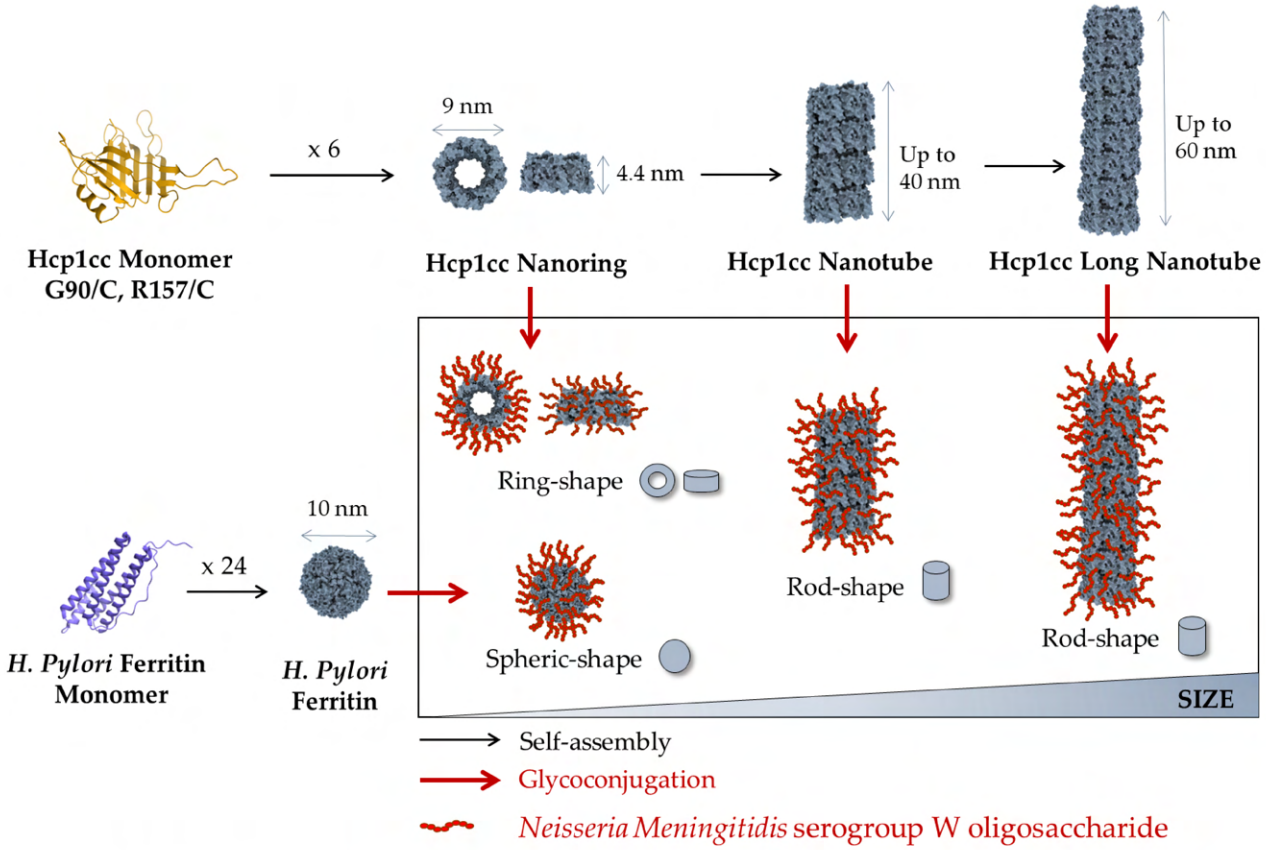

Figure 2. Workflow to produce glycoconjugate nanoparticles and their correlation in terms of sizes and shapes.

We selected oligosaccharides (OS) derived from *Neisseria meningitidis* type W (MenW) capsular polysaccharide as a model antigen to be chemically conjugated to self-assembling nanoparticles, applying the same conjugation strategy used for the commercial glycoconjugate vaccine MenACWY-CRM$_{197}$ (MENVEO™), which represents our reference [336, 337].

The Hcp1cc nanotubes were incubated overnight in the presence of the activated MenW OS, and the resulting rod-shaped glycoconjugates were purified from unreacted oligosaccharides.

To obtain glycoconjugated nanorings, Hcp1cc nanotubes were incubated with DTT (Figure 1a). The resulting Hcp1cc hexamers were then incubated with the activated MenW OS, maintaining reducing conditions. The resulting glycoconjugated nanorings were purified from unreacted oligosaccharide, and DTT. Despite the removal of the reducing agent, nanoring association into nanotubes was prevented by the presence of the conjugated saccharides that shielded the formation of disulfide bonds.

Finally, *Helicobacter pylori* ferritin was selected due to its well-known capability of self-assembling into spherical nanoparticles of 10 nm diameter, exploring an additional shape with dimensions comparable to Hcp1 nanorings. Ferritin NPs were produced in *E. coli* and purified via Size Exclusion Chromatography (SEC), while their correct assembly was assessed via TEM analysis (Figure 1d). As for the other nanoparticles, ferritin was conjugated to MenW OS.

2.2.2 Advanced characterization of glycoconjugated nanoparticles

The glycoconjugated nanospheres, nanorings, and nanotubes were widely characterized thanks to a panel of analytical techniques that allowed us to highlight their different features. In

particular, glycoconjugation was assessed via Sodium Dodecyl Sulphate-Polyacrylamide Gel Electrophoresis (SDS-PAGE) and Size Exclusion High-Performance Liquid Chromatography (SE-HPLC). The nanoparticle integrity, once glycoconjugated, was confirmed by negative-stain Transmission Electron Microscopy (TEM) analysis. Saccharide and protein contents were quantified, respectively, via high-performance anion-exchange chromatography with pulsed amperometric detection (HPAEC-PAD) and Micro Bicinchoninic Acid (mBCA), a colorimetric assay. Finally, the asymmetric flow field flow fractionation (AF4) technique was mainly utilized to assess sample heterogeneity and to cross-check the saccharide/protein molar ratio using an orthogonal tool.

Hcp1cc nanostructures, both rings and tubes, were reduced to the monomeric form due to the break of disulfide bonds in the presence of DTT and detected as a single band at 18 kDa in SDS-PAGE experiments (see lines 1B and 3B in Figure 3). Instead, in non-reducing conditions, nanotubes were described by multiple bands (4–5 bands) representing the number of rings composing the nanoparticle (line 3A in Figure 3). In the presence of SDS, rings dissociated while the disulfide bonds among the monomers that compose the height remained intact, providing information about the number of rings. After the oligomerization process, a major number of bands could be detected with increased intensity, especially for bands at high MWs because longer structures became more represented (see line 5 in Figure 3).

After glycoconjugation, SDS-PAGE experiments showed a high MW smear (see lines 2A, 4A, and 6A in Figure 3), confirming successful conjugation.

Initial SE-HPLC experiments produced Hcp1cc profiles difficult to interpret, probably due to the high MW dimensions and a possible interaction with the stationary phase of the column, which was eliminated by adding 0.1% sodium dodecyl sulfate to the elution buffer. An increase in size was observed moving from nanorings to longer nanotubes, with an increase in the heterogeneity of the sample and the shift of the peak towards shorter retention times corresponding to the increase in MW (black profiles in SE-HPLC in Figure 3). After glycoconjugation, an additional shift of peaks at lower retention times in SE-HPLC confirmed the conjugation (red profiles in SE-HPLC in Figure 3).

TEM analysis confirmed the integrity of Hcp1cc particles, showing that glycoconjugation did not impact the structure assembly once formed (Figure 4b, c). Moreover, the MenW-nanoring sample did not show nanotube structures by TEM but a ring shape with a homogeneous diameter size of 9 nm, confirming the inhibition of ring–ring association caused by the presence of the oligosaccharides (Figure 4a).

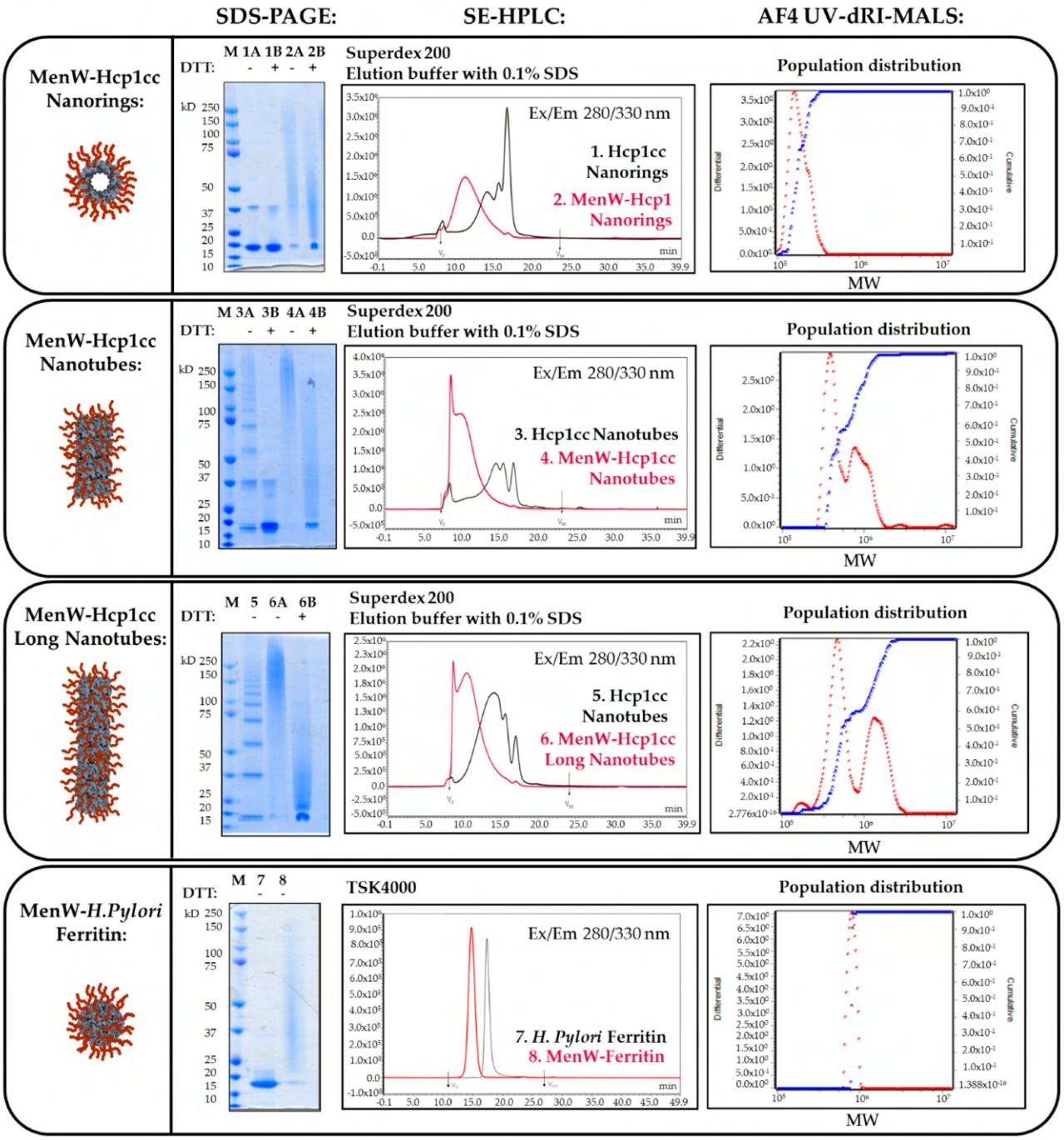

Figure 3. A comprehensive panel of analytical characterization data for glycoconjugate nanoparticles. By order of appearance: SDS-PAGE of nanoparticles and corresponding glycoconjugates in presence and absence of reducing agent DTT; SE-HPLC profiles of nanoparticles and corresponding glycoconjugates; population distribution analysis of glycoconjugates analyzed via AF4 in differential (red line) and cumulative (blue line) distribution.

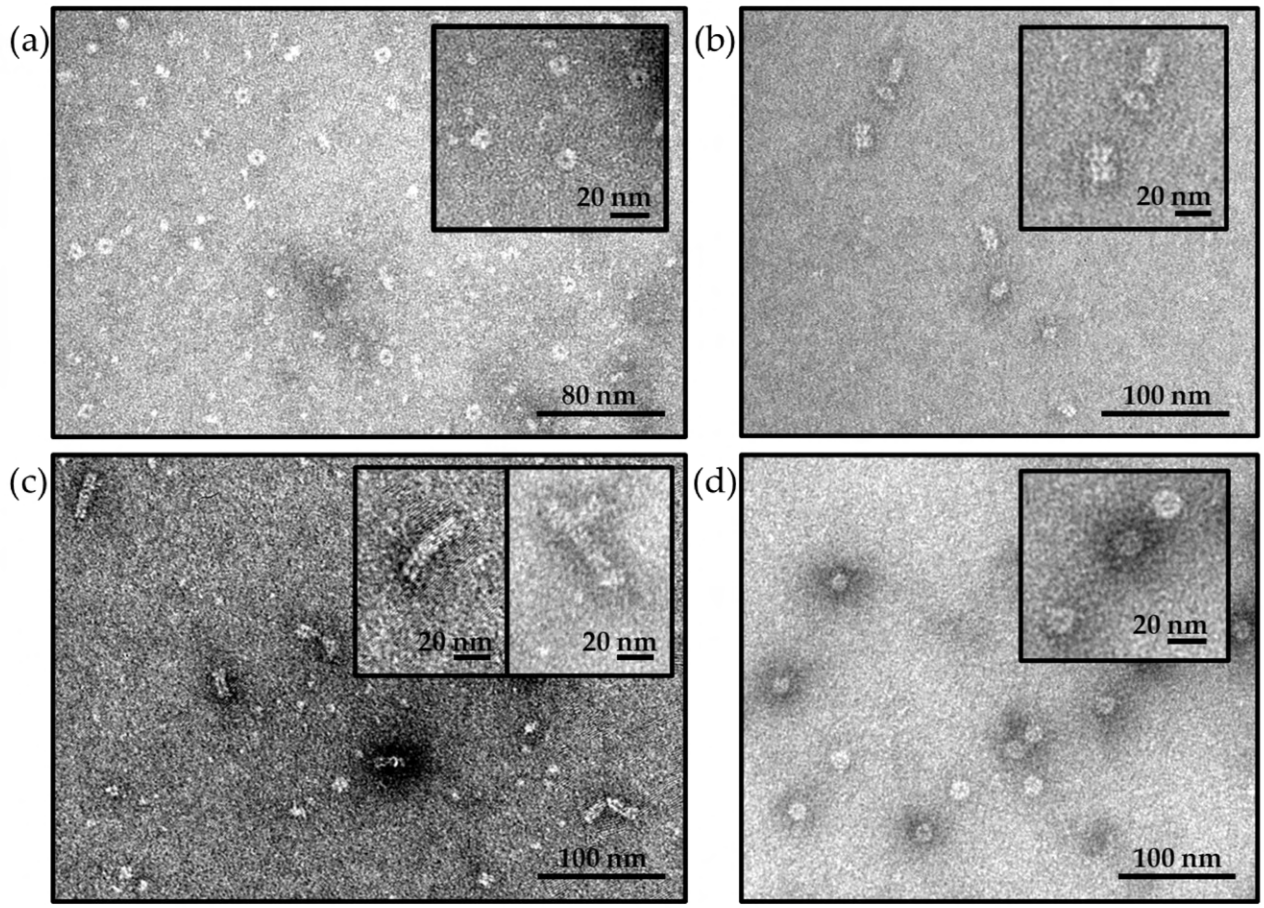

Figure 4. Transmission Electron Microscopy (TEM) of glycoconjugated nanoparticles. The integrity of glycoconjugated nanoparticles and their different sizes and shapes were assessed for (**a**) MenW-Hcp1cc nanorings characterized by only ring structures with a diameter of 9 nm; (**b**) MenW-Hcp1cc nanotubes characterized by nanotubes with a height of 20–40 nm; (**c**) MenW-Hcp1cc long nanotubes characterized by heterogeneous population of rod-shaped nanoparticles at highest order structures up to 60 nm of height; (**d**) MenW-Ferritin characterized by spheric-shaped nanoparticles with a diameter of 10 nm.

A high glycosylation degree was also confirmed by calculating the saccharide/protein ratio (Table 2; Section 4.13). Nanorings were conjugated with an average of 2 MenW chains per monomer, obtaining an average of 12 antigen copies per ring. MenW-Hcp1cc nanotubes resulted in even more glycosylation, displaying an average of 18–24 chains of MenW OS per ring repeated up to 14 times for the longest nanotubes.

Table 2. Saccharide/Protein Ratio.

Glycoconjugate Nanoparticles	**HPAEC-PAD/BCA Colorimetric Assay Saccharide/Protein Ratio**		**AF4 Protein Conjugates Tools Saccharide/Protein Ratio**
	w/*w*	**mol/mol**	**mol/mol**
MenW-Hcp1cc Nanorings	0.9	2.0	2.2
MenW-Hcp1cc Nanotubes	1.3	3.1	4.1
MenW-Hcp1cc Long Nanotubes	1.8	4.2	4.6

MenW-*H. Pylori* Ferritin Spheric Nanoparticle	0.8	1.9	1.8
MenW-CRM_{197}	0.7	5	Not done

In *H. Pylori* ferritin glycoconjugates, all 24 monomers that compose the spheric nanoparticle were derivatized with the MenW OS. In fact, analyzing the glycoconjugates via SDS-PAGE, the ferritin monomer at 19 kDa was poorly detected and turned into a high MW smear (see line 2A in Figure 3). Moreover, the efficiency of the conjugation was also demonstrated by the SE-HPLC profile, which showed a single peak with a lower retention time compared to the starting nanoparticles and the absence of detectable unconjugated protein (see SE-HPLC profile in Figure 3). The high degree of glycoconjugation did not appear to impact the nanoparticle structure, which remained spherical with a peculiar diameter of 10 nm as observed in TEM analysis (Figure 4d). From saccharide quantification, almost 2 chains of MenW OS were conjugated to each monomer of ferritin nanoparticle, obtaining an average of 45 copies of antigen exposed per particle (Table 2).

The reference MenW-CRM_{197} was also prepared and characterized. Differently from the multiple copies that were displayed on the nanoparticles under investigation, a final glycosylation degree (*w*/*w*) of 0.7 was determined, which resulted in an average of 5 chains of MenW oligosaccharides exposed to the protein.

To overcome the limitations of traditional chromatography, AF4 analysis was set up. This technique separates large aggregates and particles (e.g., LNPs, VLPs, and polymers) based on their size [338, 339]. This separation is obtained by the difference in mobility in the flow field induced by the liquid flow over an inert membrane and across the channel. The presence of different detectors in line, such as multi-angle light scattering (MALS), UV-Vis absorbance at 280 nm, and differential refractive index (dRI), allows the determination of population distribution in terms of molar mass and saccharide content using a protein conjugation tool.

Analyzing MenW-Hcp1cc nanoparticles, an increase in MW was observed along with an increase in the oligomerization state of the Hcp1cc protein. In particular, one single main population of MenW-nanotubes was detected, while two main distinct populations at higher MW were detected for MenW-Hcp1cc nanotubes that further increased after the oligomerization process as expected. The presence of a single and defined population on MenW-Ferritin was also confirmed by AF4 analysis, where a sharp and single peak is described by HPLC analysis (Figure 3).

The saccharide/protein molar ratio can be calculated using AF4 analysis by integrating UV and RI signals to calculate the protein and saccharide contributions in terms of MW composing the glycoconjugate. The ratio calculated for each glycoconjugate was consistent with the ones calculated using the results obtained by the HPAEC-PAD and mBCA assays (Table 2).

2.2.3 Evaluation of saccharide immune responses elicited by glycoconjugated nanoparticles in murin model

Groups of 10 CD-1 mice were immunized with three doses of MenW-Hcp1cc or MenW-Ferritin glycoconjugates (1 μg of MenW/dose), administered three weeks apart, in comparison with the benchmark MenW-CRM$_{197}$ [340, 341]. Each antigen was adjuvanted with AS01, a liposome-based adjuvant that contains two immunostimulants, a TLR4 ligand, 3-*O*-desacyl-4'-monophosphoryl lipid A (MPL), and a saponin, QS-21.

Two weeks after the third dose, sera were collected to measure IgG titers by ELISA assay, using MenW capsular polysaccharide as a coating reagent. After three doses, MenW-Ferritin elicited a statistically significant higher immune response (p values < 0.0001) compared to both MenW-Hcp1cc nanorings and nanotube conjugates, in which some mice with no or very low IgG titers were detected (Figure 5a).

Sera of immunized mice were also tested for functional activity in the serum bactericidal assay using human serum as a source of complement (hSBA), assessing the protective response to meningococcal vaccination. Despite the variability in the response of individual mice, MenW-Ferritin was able to elicit a higher bactericidal activity compared to MenW-Hcp1cc nanorings (statistically significant, p value < 0.033) and to the benchmark vaccine (Figure 5b). Thus, MenW-Ferritin performed best among the tested vaccine candidates.

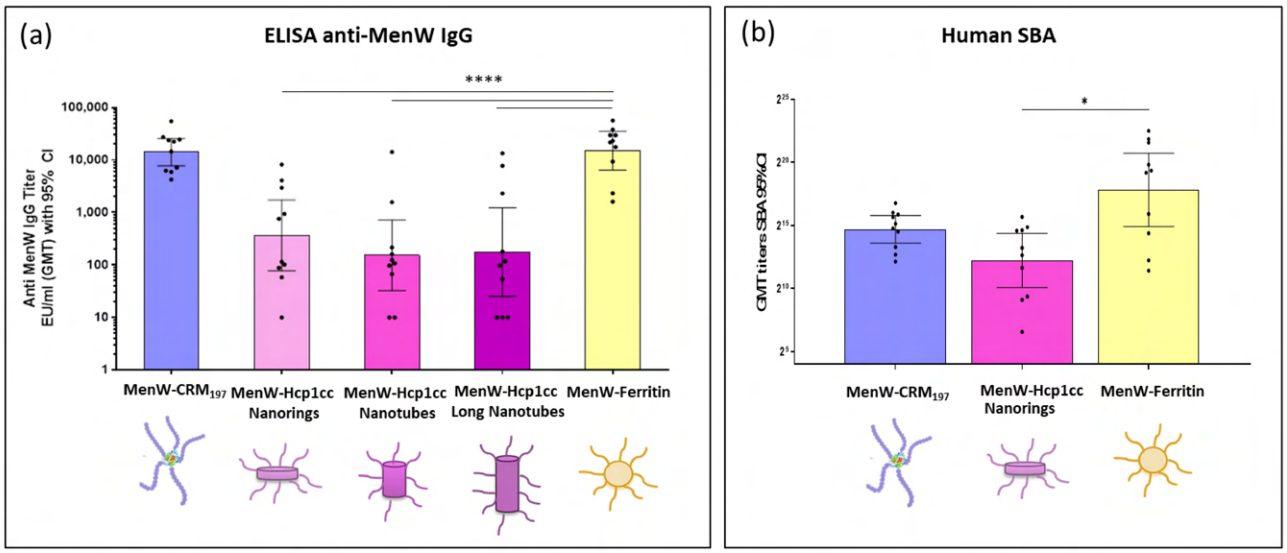

Figure 5. Anti-MenW IgG and Human SBA titers in mice immunized with MenW-nanoparticles or MenW-CRM$_{197}$. (**a**) Immune response in 10 mice per group receiving three AS01-adjuvanted doses of MenW-nanopartilces compared to MenW-CRM$_{197}$ as benchmark vaccine. The y-axis indicates the geometric mean IgG titer (RLU/mL), individual mice are indicated by the dots, and the 95% Confidence Interval is indicated by the whiskers. For non-responder sera were assigned GMT titers for half of the LLOQ (10 RU/mL). Mann Whitney test was used to compare benchmark titers with the other immunizations; **** p-value < 0.0001 (**b**) Human SBA titers from single mice sera immunized with MenW-CRM$_{197}$, MenW-Hcp1 nanorings, and MenW-Ferritin are reported and compared using Prism. Kruskal-Wallis test; * p-value < 0.033. Geometric mean titers and the 95% Confidence Interval is indicated by the whiskers.

2.3 Discussion

Despite the fact that nanoparticles have been widely examined in the field of vaccines, their role as carriers in glycoconjugate vaccine development has not been equally explored. This lack limits our understanding of the key characteristics that a glycoconjugated nanoparticle should have to induce an effective and potent immune response. Our study aimed to investigate how attributes such as size and shape of the NPs influence the immune response to saccharide antigens exposed to their surface. The ultimate goal is to guide the future design and selection of the best nanoparticles for the development of promising glycoconjugate candidates against the bacterial target.

In the present work, we identified from the literature the self-assembling Hcp1cc protein, which spontaneously arranges into ring-shaped hexamers with a diameter of 9 nm [334, 335]. These nanoparticles can oligomerize into nanotubes with a height of 40 nm that can be extended up to 80 nm via in vitro manipulation. This property allowed us to study the effects of different geometry and the impact of carrier size on antigen immunogenicity. In addition, we selected a second self-assembling protein, *H. Pylori* ferritin [318, 342-345], which forms spherical nanoparticles with comparable diameter to examine the impact of shapes while maintaining similar sizes.

All selected nanoparticles were successfully chemically conjugated to activated MenW oligosaccharides thanks to the presence of multiple lysines on their surface, achieving a high glycosylation degree. Several parameters of the nanoparticles before and after conjugation were controlled using a panel of complementary techniques, including AF4, a gold standard worldwide for nanoparticle characterization [338, 339, 346-349].

Finally, glycoconjugated nanoparticles were administered in three AS01-adjuvanted doses in mice using MenW-CRM_{197} as a benchmark vaccine. MenW-Ferritin was the most immunogenic among the tested MenW-Nanoparticles, stimulating a strong antibody response *in vivo* against the MenW oligosaccharide. Interestingly, the increase in nanotube size between 10 and 100 nm did not affect the immune response. Most importantly, MenW conjugation to spherical ferritin nanoparticles resulted in the highest bactericidal activity in a functional assay among all tested samples.

Our data outline the major role played by the nanoparticle shape on antigen immunogenicity, with spherical nanoparticles and eliciting the highest protective immune response *in vivo* compared to elongated nanotubes. Our findings extend to the protein-based nanoparticles and the conclusions of recent observations reported on the role of the size and shape of gold and polymeric NPs. Niikura *et al*. demonstrated that spheric gold nanoparticles (AuNPs) coated with West Nile virus envelope protein (WNVE) induced 50% more WNVE-specific IgG antibodies in mice compared to rods [350]. Also, Toraskar *et al.* administered *in vivo* AuNPs coated with tripodal Tn-glycopeptide antigen, showing that the small, spherical-shaped AuNPs induced an effective anti-Tn-glycopeptide IgG response compared with rod-shaped AuNPs [351]. Kumar *et al.* also concluded that among different particle types, spherical polystyrene ovalbumin-conjugated particles generated *in vivo* stronger immune responses by inducing the most potent Th1 and CD8+ T-cells [352]. Several mechanisms have been proposed to explain the superiority of spherical nanoparticles, including more efficient cellular uptake [353, 354], better APC activation, and faster trafficking to lymph nodes [355, 356].

Many comparative studies have demonstrated the influence of particle shape on DC activation, observing that inorganic spherical nanoparticles are more potent in stimulating DCs compared to their non-spherical counterparts, relying on upregulation of CD83 and CD86, a more efficient internalization [353, 354] and cell endocytosis for spherical over rod-shaped nanoparticles [357, 358]. It has been hypothesized that elongated particles may be less efficiently taken up because of the reduced contact area when attached to the cells along their minor axis, whereas spherical

nanoparticles always expose an optimal contact area to the cell membrane, resulting in less energy cost internalization [359-362].

Our data are also in line with evidence on inorganic nanoparticles, indicating that an increase in size can be beneficial for cellular uptake [363, 364]. Indeed, gold nanoparticles of 20–200 nm efficiently enter the lymphatic system and reach the lymphatic organs directly within hours of injection [355, 356]. On the contrary, particles larger than 200 nm do not efficiently enter lymph capillaries in a free form but need DCs transportation requiring 24 h [356, 365]. Furthermore, DC preferentially take up 40 nm nanoparticles over 200 nm [366]. Moreover, smaller particles are most potent in inducing IFN-γ-mediated Th1 immunity compared to particles in the 100 nm range, which induce stronger IL-4 responses and Th2 responses. It was suggested that smaller (<100 nm) particles may enter APCs through one of the mechanisms used by viruses, such as clathrin-coated pit-mediated uptake, which may induce a stronger Th1 immune response [367, 368].
Moreover, it is crucial to highlight that the nanoparticles being compared, although they share a similar molecular weight as the monomeric unit, contain distinct T-cell epitopes. This difference could potentially influence the immune responses they trigger, a topic that warrants further exploration.

In conclusion, our study highlights the potential of self-assembling protein nanoparticles for glycoconjugate vaccine development and remarks that shape over size is a key factor in enhancing the efficiency of the immune response. We present the first example of glycoconjugated *H. Pylori* ferritin as an efficient carrier protein for efficient delivery of bacterial saccharide antigen. We hypothesize that, compared to inorganic nanoparticles, the ferritin scaffold could offer a repertoire of effective peptidic T-cell epitopes to the immune system, thereby enhancing the protective response.

Overall, our findings outline that protein nanoparticles may represent a promising strategy to develop novel glycoconjugate vaccines against bacterial pathogens.

2.4 Materials and Methods

2.4.1 Protein nanoparticles expression in *E.coli*

The mutated Hcp1cc (G90C + R157C) was expressed as His6-tagged protein in *Escherichia coli* BL21(DE3). First, a pre-culture in LB (Tryptone 10 g/L, yeast extract 5 g/L, NaCl 10 g/L) medium supplemented with Ampicillin 100 mg/L from glycerol stock of BL21(DE2) pET303/CT-HIS-HCP1 was incubated at 37 °C, 190 rpm for 16 h. The pre-culture was used to set up batch cultivation of protein in 2YT medium (16 g/L Trypton, 10 g/L Yeast extract, 5 g/L NaCl pH 7.6.) supplemented with Ampicillin 100 mg/L, under shaking at 37 °C for 2 h, until OD value of 0.5, followed by induction with 0.5 mM IPTG for 5 h at 37°C at 180 rpm.

H. Pylori Ferritin was expressed as tag-less protein in *Escherichia coli* BL21(DE3). First, a pre-culture in LB (Tryptone 10 g/L, yeast extract 5 g/L, NaCl 10 g/L) medium supplemented with Kanamycin 50 mg/L from colonies grown on selective plates of BL21(DE2) was incubated at 37 °C, 180 rpm for 7 h. The pre-culture was used to set up batch cultivation of protein in LB medium supplemented with Kanamycin 50 mg/L, under shaking at 32°C for 10 h, followed by induction with 1 mM IPTG for 16 h at 25°C at 160 rpm.

2.4.2 Protein nanoparticles purification

Crude cell lysate obtained after His6-tagged Hcp1cc expression in *E.coli* was purified via Co^{2+} affinity chromatography using His-Trap TALON fast flow crude (Cytiva, Marlborough, MA, USA) column. The column was connected to a peristaltic pump of instrument ÄKTA pure (Cytiva) and washed with distilled water and then equilibrated with buffer 50 mM NaPi 300 mM NaCl pH 8. Crude cell lysate was applied on the column and the flow through was discarded. The column was first washed with 20 CV of buffer 50 mM NaPi, 300 mM NaCl then a gradient of buffer 50 mM NaPi, 300 mM NaCl, 500 mM imidazole in buffer 50 mM NaPi, 300 mM NaCl was applied to elute target protein. Hcp1cc protein was eluted in buffer 50 mM NaPi, 300 mM NaCl, 500 mM imidazole after IMAC purification. The buffer was exchanged into buffer 500 mM NaCl, 50 mM TRIS pH 7.5 via tangential flow filtration using hydrosart membrane with cut-off 30 kDa (Sartoriuos Stedim biotech, Aubagne, France).

Crude cell lysate obtained after tag-less *H. Pylori* Ferritin expression in *E.coli* was purified first in Sephacryl S-300 HR 26/60 column (Cytiva) and eluted in buffer PBS 1x. Then, a second purification was performed in HiLoad Desalting 26/10 (Cytiva) column and the target protein eluted pure in PBS 1x.

2.4.3 Oligomerization process - *In vitro* reassembly for the generation of long Hcp1cc nanotubes

Purified Hcp1cc nanotubes were treated with 5 mM DTT to fully reduce nanotubes into ring form and concentrated at 40 mg/mL in 500 mM NaCl, 50 mM TRIS pH 7.5, 10% glycerol + 5 mM DTT. Protein was dialyzed using dialysis tube with membrane 2K cut-off (MINI Dialysis Unit Thermo Scientific Slide-A-Lyzer, Waltham, MA, USA) against a buffer containing 5% PEG 3350, 50 mM trisodium citrate, 100 mM HEPES pH 7.5, and 2 mM β-mercaptoethanol until a smooth paste formed (after 5 days of dialysis). This paste was diluted to 10 mg/mL of protein in 500 mM NaCl, 50 mM TRIS pH 7.5, 10% glycerol. The Hcp1cc protein solution obtained was analyzed first in TEM and SDS-PAGE to verify the presence of long nanotubes.

2.4.4 MenW oligosaccharide sizing

Oligosaccharides *from Neisseria meningitidis* type W (MenW) capsular polysaccharides have been selected as model antigen to be chemically conjugated to self-assembling nanoparticles. In particular, applying the same conjugation strategy used for the commercial vaccine MenACWY-CRM_{197} (MENVEO™) [336, 337], the MenW capsular polysaccharide has been sized by controlled acid hydrolysis to obtain MenW oligosaccharides with a defined length of 7.8 kDa (average) and subsequently activated via reductive amination and coupling to bis-N-hydroxysuccinimidyl adipate (SIDEA) linkers generating half-ester residues prompt to react with amine groups present on protein nanoparticles in the conditions reported below [336, 340, 341].

2.4.5 Nanoparticles conjugation to MenW oligosaccharide

To produce MenW-Hcp1cc nanorings, Hcp1cc nanotubes at 40 mg/mL in 500 mM NaCl, 50 mM TRIS pH 7.5, 10% glycerol was disassembled in presence of 5 mM DTT. The resulted Hcp1cc nanorings were incubated with 10 equivalents of SIDEA activated MenW oligosaccharide over night at room temperature under gently shaking. The unconjugated oligosaccharide was extensively removed performing serial centrifugal filtration (30 kDa) with reducing buffer to maintain Hcp1cc in ring form. Finally, the purified MenW- Hcp1cc nanorings were recovered in 500 mM NaCl, 50 mM TRIS pH 7.5, 10% glycerol.

Hcp1cc nanotubes and longer ones obtained after oligomerization process were incubated at around 10 mg/mL in 500 mM NaCl, 50 mM TRIS pH 7.5, 10% glycerol with 30 equivalents of MenW oligosaccharide for one night at room temperature under gently shaking. The resulted glycoconjugated nanotubes were purified from unreacted MenW oligosaccharide performing serial centrifugal filtration (30 kDa). The purified MenW- Hcp1cc nanotubes and MenW-Hcp1cc long nanotubes were both recovered in 500 mM NaCl, 50 mM TRIS pH 7.5, 10% glycerol.

H. Pylori Ferritin at 10 mg/mL in PBS 1x was incubated with 10 equivalents of SIDEA activated MenW oligosaccharide over night at room temperature under gently shaking. The glycoconjugates obtained were purified from unreacted oligosaccharide performing serial centrifugal filtration (100 kDa). The purified MenW-Ferritin was recovered in PBS 1x.

2.4.6 TEM

A volume of 5 μl of samples, diluted in PBS 1x at 20 ng/microliter, were loaded for 30 seconds onto a glow discharged copper 200 or 300-square mesh grids. Blotted the excess, the grid was negatively stained using NanoW for 30 seconds and let air dried. The samples were analyzed at UNISI using a Tecnai G2 spirit and the images were acquired using a Tvips TemCam-F216 (EM-Menu 4 software).

2.4.7 SDS-PAGE

Sodium Dodecyl Sulfate- Polyacrylamide gel electrophoresis (SDS-PAGE) was performed on 4-12% pre-casted polyacrylamide gel (NuPAGE Invitrogen, Carlsbad, CA, USA) using MOPS 1x as running buffer (NuPAGE Invitrogen). 5 or 10μg of protein nanoparticles or glycoconjugated nanoparticles were mixed with 3 μL of 4X LDS, 3 μL dithiothreitol (DTT) at 0.5 M when needed, and boiled at 90 °C for 1 min. Samples and prestained protein molecular marker (Pecision Plus Protein Standard Dual color - Biorad) were loaded on precast polyacrylamide gels and run at 200 V, 180 mA for 45 min. Gels were stained with Coomassie ProBlue Safe stain (Giotto, Padua, Italy) for protein visualization.

2.4.8 SE-HPLC

Hcp1cc nanoparticles and corresponding MenW-Hcp1cc nanoparticles were analyzed in Superdex 200 10/300 GL (Cytiva) column in isocratic elution with 50 mM TRIS 500 mM NaCl pH 7.5 + 0.1% SDS as running buffer performing 40 minutes of run at 1 mL/min of flow rate using an Ultimate 3000 HPLC system (Thermo Scientific) equipped with a photodiode array detector and a multiple-wavelength fluorescence detector. While *H. Pylori* Ferritin and MenW-Ferritin were analyzed in TSK4000PW column (7.8 × 300 mm, Tosoh, Tokyo, Japan) in isocratic elution with 100 mM NaPi, 100 mM Na_2SO_4 at pH 7.2 as running buffer performing 50 minutes of run at 0.5 mL/min of flow rate using HPLC system reported above. The resulting chromatographic data were integrated and processed using Chromeleon 7.2 software.

2.4.9 AF4

The asymmetric flow field-flow fractionation (AF4) system (AF2000 – Postnova, Landsberg am Lech, Germany) consisted of an isocratic LC pump (PN1130, Postnova analytics, Salt Lake City, UT, USA), autosampler (PN5300 series, Postnova analytics), column oven (PN4020, Postnova analytics), MALS detector (PN3621, Postnova analytics), UV-Vis detector (SPD-20A prominence, Postnova analytics), and refractive index (RI) instrument (PN3150, Postnova analytics). Microchannel with a 350 μm spacer and a 10 kDa regenerated cellulose membrane was used for all separation.

10 μL of sample are injected in the separation channel at 0.20 mL/min and subjected to a cross flow at 1 mL/min and focus pump at 1.30 mL/min for 3 minutes. Elution step in which focus flow decreases to 0 mL/min and sample is able to elute along the channel for 50 minutes subjected to cross flow that decreases in 40 minutes to 0.1 mL/min in parabolic manner. PBS 1x or 0.9% NaCl filtered 0.1 μm used as mobile phase, 10 μL of sample injected. The UV, MALS signals were integrated to

obtain population distribution analysis using as zim plot method and parameters extinction factor of 1.313 [mL/(mg*cm)] for Hcp1cc and 1.056 [mL/(mg*cm)] for ferritin, calculated from protein sequences, and dn/dc of 0.185 provided by Postnova and literature [369-371].

2.4.10 AF4 Protein conjugates tool for saccharide/ protein molar ratio

For each glycoconjugated nanoparticle, UV signal was integrated to calculate protein contribution in term of MW using as parameters dn/dc: 0.185 mL/g and extinction factor of 1.313 [mL/(mg*cm)] calculated for Hcp1cc and of 1.056 [mL/(mg*cm)] for ferritin; while saccharide contribution in term of MW was calculated from dRI signal using dn/dc: 0.147 mL/g [369-371]. The saccharide and protein MW contributions obtained were divided respectively for saccharide MW of 7.8 kDa and protein MW of 18.3 kDa for Hcp1cc and of 19.3 kDa for Ferritin and compared to get the final molar ratio.

2.4.11 Quantification of protein content by colorimetric assay

Protein concentration was determined by Pierce Micro BCA Protein Assay Kit (mBCA kit, Thermo Fisher Scientific) according to manufacturer's instructions and using the provided Pierce™ Bovine Serum Albumin (BSA, Thermo Fisher Scientific) as standard. Each sample was diluted in duplicate preparing a 5-points calibration curve using a BSA starting solution of 20 μg/mL. Then, the three reagents of mBCA kit are properly mixed following the manufacturer's instructions and added to the sample heated at 60 °C in bath of water for 1 hour. The samples are finally transferred to a plastic disposable cuvette and are read at the spectrophotometer at 562 nm (Evolution 260 Bio Spectrophotometer, Thermo Fisher Scientific, Thermo INSIGHT software 2.1.175). The final protein concentration (μg/mL) is quantified based on the BSA calibration curve.

2.4.12 Quantification of MenW oligosaccharide content by HPAEC-PAD

Glycoconjugated nanoparticles were treated with trifluoroacetic acid (TFA) with a final concentration of 2 M. Samples were heated at 100 ◦C for 2 hours, then refrigerated at 4 ◦C for 15 minutes and finally dried on a Speed Vac at room temperature overnight. Samples to be analyzed were first dissolved in ultrapure water and then filtered (0.45μm). Analysis of the hydrolyzed products was performed using a Dionex ICS5000 (Thermo Fisher Scientific), equipped with a CarboPac PA1 column plus a CarboPac PA1 guard. Separation was performed with a flow rate of 1 mL/min using isocratic elution of NaOH 15 mM of 20 min, following by a regeneration step with NaOAc 50 mM/NaOH 100 mM for 10 min and recondition in the starting condition for 15 min. The effluent was monitored using an electrochemical detector in the pulsed amperometric mode with a gold working electrode and an Ag/AgCl reference electrode. The resulting chromatographic data were integrated and processed using Chromeleon 7.2 software. Galactose concentration was determined using calibration curves set up with commercial standard galactose and then converted in MenW oligosaccharide concentration (μg/mL) by using a conversion factor which takes into account the weight of galactose in the repeating unit structure.

2.4.13 *In vivo* experiment

Animal treatments were performed in compliance with Italian legislation (Dig 26/2014), EU Directive 63/2010, and GSK Animal Welfare Policy and Standards, and approved by the institutional review board (Animal Ethical Committee) of GSK Vaccines Siena, Italy.

Groups of 10 CD-1 female mice, kept in an AAALAC-accredited facility, were immunized intramuscularly (IM) with MenW glycoconjugates nanoparticles produced (1 μg of MenW/dose) adjuvanted with 2.5 μg/dose of AS01, a liposome-based adjuvant which contains two immunostimulants, a TLR4 ligand, 3-*O*-desacyl-4'-monophosphoryl lipid A (MPL), and a saponin, QS-21. MenW-CRM_{197} adjuvanted by AS01 was used as controls. Three different immunizations were performed at days 1, 22 and 43 collecting sera at day 57.

2.4.14 ELISA analysis

The antibody response induced by the glycoconjugates against the polysaccharide has been measured by ELISA. Microtiter plates (96 wells, Thermo Scientific) have been coated with the MenW polysaccharide by adding 100 μl/well of a 5 μg/ml polysaccharide solution in PBS 1x at pH 8.2 followed by incubation overnight (o.n.) at 4°C. After washing three times with PBS 1x with 0.05% of Tween 20 (Sigma) (tPBS). A blocking step has been performed by adding 100 μl of BSA solution at 3% in tPBS and incubating the plates for 1 h at 37°C, then aspirated to remove the solution. Two-fold serial dilutions of test and standard sera in tPBS were added to each well. Plates were then incubated at 37°C for 2 hours, washed with tPBS, and incubated for 1 additional hour at 37°C with either anti-mouse IgG-alkaline phosphatase whole molecule (Sigma-Aldrich, Saint Louis, MO, USA) diluted 1:2000 in tPBS. After washing, the plates were incubated with 100 μL/well of 1 mg/mL p-Nitrophenyl Phosphate (pNPP sodium salt hexahydrate tablet - Sigma Life Science, Darmstadt, Germany) in 0.5 M of di-ethanolammine buffer pH 9.6. The absorbance was measured using a SPECTRAmax340PC plate reader (Molecular Devices, San Jose, CA, USA) with wavelength set at 405 nm. IgG concentrations were expressed as relative ELISA Units/mL (EU/mL) and were calculated as reciprocal of sera dilution corresponding to OD = 1. Each immunization group has been represented as the geometrical mean (GMT) of the single mouse titers. The statistical and graphical analysis has been done by GraphPad 5.0 software.

2.4.15 Human SBA

Functional antibodies were measured by human Serum Bactericidal Activity assay (hSBA) on meningococcal strains 240070 (reference for meningococcal serotype W) using human serum as complement source. The hSBA was performed on sera from mice immunized with 3 doses of AS01 adjuvanted MenW-Hcp1cc nanorings, MenW-Ferritin and MenW-CRM_{197} and collected 2 weeks after the third immunization.

Bacteria were plated on a round agar plate and incubated 16 hours at 37°C with 5% CO_2 in humid atmosphere. The day after, single colonies were inoculated into Mueller-Hilton Broth (MHB) containing 0,25% w/v glucose and incubated at 37°C at 150 rpm until the culture reached OD=0.24-0.26. After that, bacteria were diluted 1:20000 or 1:30000 in SBA buffer (Dulbecco's saline phosphate buffer with 0.1% glucose and 1% BSA (Bovine Serum Albumin) supplemented with heparin solution 5 U/mL and salt solution ($MgCl_2$ 0.01 M, CaCl2 1.5 mM). The assay was assembled in a sterile 96 flat bottom well microplate in a final volume of 40 μL/well where mouse sera were serially diluted (ten

2-fold dilution steps) in SBA buffer and added the serial dilutions to each test sample were incubated with bacteria and human complement at 37 °C with 5% CO_2 for 1 h. Then, 150 μL of agar (TSB 0.7% agar) were added and the plate was incubated overnight at 37°C with 5% CO_2. Bacteria with active human complement (AC) in absence of serum sample is the control used to exclude complement toxicity and to determine 100% bacterial growth. The SBA titer was determined for each test sample as the reciprocal of the sample dilution giving a killing≥ 50% respect to the average number of CFU calculated (using ScanLab software Icarus 1.2.3) on the control.

Chapter 3

Multicomponent glycoconjugate nanoparticle vaccines – toward a single dose vaccine

3.1 Introduction

Vaccines have played a crucial role throughout the last 50 years in improving human health by controlling or eradicating viral diseases like smallpox, measles and polio as well as bacterial diseases such as diphtheria and tetanus. Licensed glycoconjugate vaccines have been particularly successful and cost-effective in preventing illnesses caused by *Haemophilus influenzae* type b (Hib) [16], S*treptococcus pneumoniae* (23 serotypes) [117], *Neisseria meningitidis* (A, C, W135 and Y) [372], and *Salmonella Typhi* [373-375].

Glycoconjugate vaccines originated from the findings of Avery and Goebel in 1929 [376, 377], wherein they demonstrated that non-immunogenic bacterial polysaccharides when covalent linked to carrier proteins become able to generate immunological memory and stimulate long-lasting antibody. The protein epitopes present in glycoconjugates enable carbohydrates, which are per se T-cell independent antigens, to induce a durable and enhanced production of IgG antibodies [55, 125].

However, despite the huge impact that conjugate vaccines have had on global health over the past 30 years, these vaccines have a limited effectiveness in certain populations. Some individuals, such as infants, elderly individuals, or immunocompromised individuals, may not mount a strong immune response to glycoconjugate vaccines. Specifically, the inadequate response to vaccines in certain groups is attributed to the underdeveloped immune system in infants [55, 61, 378], the aging immune system in the elderly [129, 130], and the weakened immune mechanisms in individuals with compromised immunity [379-381]. For instance, these categories of people require multiple doses of the glycoconjugate vaccine to reach sufficient levels of protective antibody [382-386]

To enhance both humoral and cellular immune responses, the addition of immunostimulant adjuvants into the vaccine is a viable strategy [132, 387]. Adjuvants are an essential element of modern vaccines by (i) enhancing the ability of a vaccine to elicit a robust and durable immune responses, especially in individuals with suboptimal or reduced responsiveness [388] (ii) reducing antigen dose and the frequency of immunizations [247, 389]; and (iii) influencing the nature of immune response [390].

The only adjuvants licensed for glycoconjugate vaccines are aluminium salts (aluminium phosphate or aluminium hydroxide) mainly due to their beneficial effect on different vaccine formulations, cost effectiveness, and the outstanding safety in a wide variety of childhood vaccines [391], even if their mechanism is not totally clear hypothesizing a depot effect. However, not all the licensed glycoconjugate vaccines are adjuvanted by aluminium salts (Table 1) and the introduction of new adjuvants and formulations is difficult due to the stringent safety requirements for vaccines, especially targeting healthy infants [392].

TABLE 1 | Carbohydrate-based vaccines approved by the FDA.

Commercial name	Manufacturer	Antigen	Adjuvant
Glycoconjugate vaccines with adjuvants			
Liquid PedvazHIB	Merck Sharp & Dohme	*Haemophilus influenzae* type b; CPS (polyribosyl-ribitol-phosphate)	Amorphous aluminium hydroxyphophate sulfate
Pentacel	Sanofi Pasteur	*Haemophilus influenzae* type b; CPS (polyribosyl-ribitol-phosphate)	Aluminium phosphate
VAXELIS	MCM Vaccine	*Haemophilus influenzae* type b; CPS (polyribosyl-ribitol-phosphate)	Aluminium salts
Prevnar 13	Wyeth Pharmaceuticals	*Streptococcus pneumoniae* serotypes 1, 3, 4, 5, 6A, 6B, 7F, 9V, 14, 18C, 19A, 19F, and 23F; CPS	Aluminium phosphate
Prevnar 20	Wyeth Pharmaceuticals	*Streptococcus pneumoniae* serotypes 1, 3, 4, 5, 6A, 6B, 7F, 8, 9V, 10A, 11A, 12F, 14, 15B, 18C, 19A, 19F, 22F, 23F and 33F; CPS	Aluminium phosphate
VAXNEUVANCE	Merck Sharp & Dohme	*Streptococcus pneumoniae* serotypes 1, 3, 4, 5, 6A, 6B, 7F, 9V, 14, 18C, 19A, 19F, 22F, 23F and 33F; CPS	Aluminium phosphate
Glycoconjugate vaccines without adjuvants			
HIBERIX	GlaxoSmithKline Biologicals	*Haemophilus influenzae* type b; CPS (polyribosyl-ribitol-phosphate)	––
ActHIB	Sanofi Pasteur	*Haemophilus influenzae* type b; CPS (polyribosyl-ribitol-phosphate)	––
Menactra	Sanofi Pasteur	*Neisseria meningitidis serogroups A, C, Y and* W-135; CPS	––
MENVEO	GlaxoSmithKline Biologicals SA	*Neisseria meningitidis* serogroups A, C, Y and W-135; CPS	––
MenQuadfi	Sanofi Pasteur	*Neisseria meningitidis* serogroup W (MenQuadfi); CPS	––
Typhim Vi	Sanofi Pasteur	*Salmonella enterica* serovar Typhi; cell surface Vi polysaccharide	––

Table 1. Glycoconjugate vaccines approved by FDA (https://www.fda.gov/) [47].

The research on novel adjuvant formulations for glycoconjugate vaccines has primary concentrated on pneumococcal vaccines, aiming to increase immune responses in high-risk populations. A significant success emerged in a double-blind placebo controlled clinical trial (NCT00562939) where the addition of 1 mg of CpG 7909, a toll-like receptor 9 (TLR9) agonist, to two doses of 7-valent pneumococcal conjugate vaccine (Prevnar) significantly enhanced vaccine response in HIV-positive patients [287].

In a notable research conducted by Buonsanti and team, they investigated the use of Alum-TLR7 as adjuvant for glycoconjugate vaccine, demonstrating the increased effectiveness of CRM_{197}-MenC vaccine in mice, with a rise in antibody titers and serum bactericidal activity compared to alum-adjuvanted vaccines, even with low antigen doses and after a single immunization [115]. This discovery led to the development of AS37-adjuvanted MenC conjugate vaccine that demonstrated its safety and immunogenicity in phase I randomized, clinical trial in healthy adults (NCT02639351) [393].

Over the past decade the design of new adjuvants improved thanks to the development of systems vaccinology approaches which have simplified the identification of the immunomodulatory mechanisms of action [394]. However, so far, only a small number of adjuvants, such as alum, AS04, MF59, AS03, CpG, and AS01, have received FDA approval for use in humans [212, 218, 395, 396]. The use of some of these adjuvants has played a significant role in improving the immune response and vaccines efficacy in the elderly as demonstrated for MF59-adjuvanted influenza vaccines (Fluad™ [397], seasonal Flu) and AS01-adjuvanted herpes zoster vaccine (Shingrix™) [253, 398]. Furthermore, incorporating adjuvants into new formulations of already licensed products contributes to reducing the vaccination schedule, thereby ensuring protection. For example, the schedule of the HPV vaccine (Cervarix™ from GSK) was reduced to two-dose schedule in 9–25-year-old women when administered in presence of adjuvant AS04, composed of aluminium hydroxide and 3-O-desacyl4 monophosphoryl lipid A (MPL-A). AS04 is believed to handle the high level of vaccine-induced antibody titers that persist for several years even after a single vaccine dose [204, 399-401].

Another recent example is represented by Heplisav-B™, a CpG ODN-adjuvanted vaccine against Hepatitis B virus, which is administered with a two-dose schedule and shows similar safety and immunogenicity profile to three doses of other HBV vaccines not adjuvanted with CpG [402,

403] achieving a rapid, higher and long term seroprotection in HIV-infected adults for up to 5 years [288, 289] and in individuals aged 60-70 years who have diabetes mellitus [286].

Interestingly, the vaccines Cervarix™ and Heplisav-B™ both feature a structure based on nanoparticles. This implies that using a combination of displaying multiple antigens and formulating immune adjuvants could be a crucial strategy in logically designing more effective vaccines that need fewer injections.

As a result, creating a new generation of glycoconjugate formulations which combine nanoparticles and innovative adjuvants, could lead to more effective vaccines. These enhanced vaccines could rapidly produce protective antibody levels, potentially after just one dose, reducing the need for multiple injections. This would offer protection during the most critical and vulnerable stages of life.

One recent and relevant instance exemplifying the development of glycoconjugate vaccines through this approach is represented by the work of Carboni *et al.* [316]. They presented a proof of concept for the development of a single dose Group B Streptococcus (GBS) glycoconjugate for maternal vaccination. They explored the use of bacteriophage coat protein Qβ Virus-like particles (Qβ VLPs) glycoconjugated on their surface to serotype II GBS polysaccharide (GBS PSII) and carrying inside genetic material.

The immunoenhancing effect, which resulted in high anti-PS IgG levels in a murine animal model, was attributed to the single-stranded RNA (ssRNA) contained within Virus-Like Particles (VLPs) [404]. This ssRNA functions as a TLR7/8 agonist and was key to the one-dose effect observed.

In this work, we investigated whether one could provide a more effective immune enhancer inside the VLP, while still maintaining the impact of a single dose, given that the genetic material being delivered is non-uniform and potentially reactogenic. We thought about CpG ssDNA already known for its adjuvant effect in glycoconjugate formulations as discussed above. We decided to encapsulate two types of CpG, class A and class B, which differ on structural characteristics and activity on human peripheral blood mononuclear cells (PBMCs) [274, 279-281]. Moreover, our aim was to explore, using a murine animal model, whether there could be any variations when the adjuvant was presented inside, outside, or simply co-formulated in a physical mixture with the GBS PSII-Qβ antigen.

3.2 Results

3.2.1 Strategy to produce adjuvanted glycoconjugate nanoparticles

To investigate the immunological impact of a different presentation of CpG adjuvant with GBS PSII-Qβ antigen, three distinct glycoconjugate nanoparticles were designed (Fig. 1): PSII-Qβ delivering large ssDNA (CpG A) or small ssDNA (CpG B) inside the nanoparticle cage, and PSII-Qβ delivering CpG B covalently attached to the VLPs surface.

Because CpG A and B had to be encapsulated in nanoparticle cage replacing ssRNA naturally present inside Qβ VLPs, a first step of RNA removal was performed. Moreover, because of diverse 3D structures of CpG A and B, two different strategies were designed to encapsulate the large ssDNA CpG A and the small ssDNA CpG B. To encapsulate CpG A, ssRNA was removed from Qβ after VLPs disassembly and RNA precipitation to obtain RNA-free monomer. Qβ monomer in presence of CpG A spontaneously encapsulated the CpG A molecule, using its 3D conformation as scaffold to restore the VLPs structure. Finally, conjugation of GBS PSII was performed on Qβ(CpG/A) to obtain the final glycoconjugate.

To encapsulate CpG B, a different strategy was designed because of its small dimension unable to guide VLPs reassembly. ssRNA was removed from Qβ VLPs using RNAse enzyme able to enter into VLPs through pores and degrade the genetic material, leaving the VLPs structure intact. The obtained Qβ empty was incubated with a large excess of CpG B able to pass through the VLPs pores and to stack inside through electrostatic interactions. Finally, conjugation of GBS PSII was performed on Qβ(CpG/B).

To covalently conjugate CpG B on GBS PII-Qβ, Qβ empty was first glycoconjugated and then the remained left free lysines on VLPs were conjugated to CpG B with a linker to obtain the desired glycoconjugate.

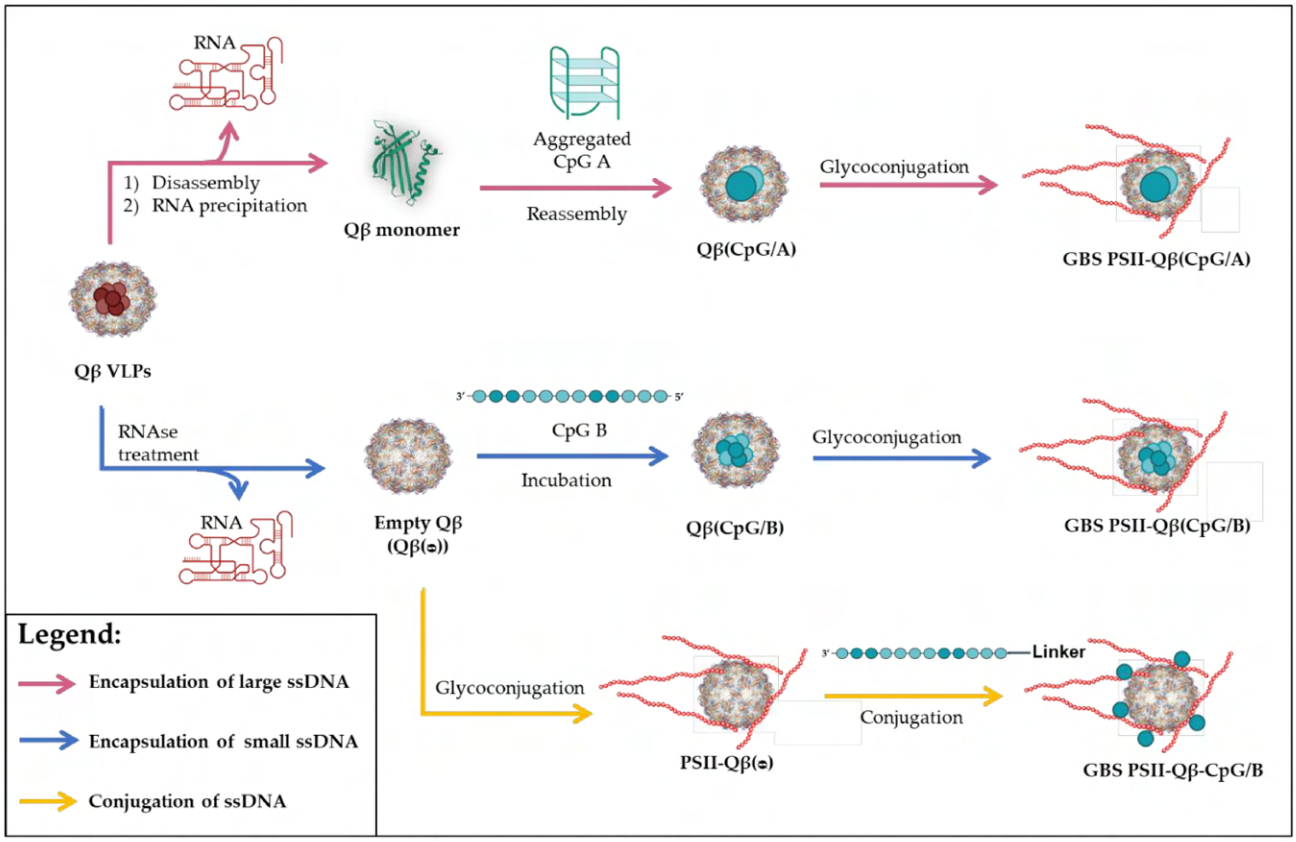

Figure 1. Workflow to produce adjuvanted GBS PSII-Qβ. ssRNA was removed from Qβ VLPs with two different methodologies (through enzyme treatment or disassembly process) and used to produce GBS PSII-Qβ delivering CpG (ssDNA) inside its cage (GBS PSII-Qβ(CpG/A or B)) or outside VLPs through conjugation (GBS PSII-Qβ-CpG/B).

3.2.2 Set up of analytical methodologies on Qβ VLPs

Qβ assembles *in vivo* into a VLP structure entrapping genetic material [405]. More in details, Qβ VLPs packages its single-stranded RNA genome and RNA derived from its host cell by interaction between its positively charged interior VLPs cage and the negatively charged ssRNA [406, 407]. RNA content differs according to Qβ VLPs preparations and ranging from 20 to 30% w/w. Carboni *et al.* produced a Qβ hairpin (Qβ(hp)) [408, 409] that contained a more homogeneous RNA entrapped compared to Qβ wildtype (Qβ wt). Qβ(hp) contained around 20% RNA predominantly composed of genetic material encoding the Qβ coat protein [316].

The RNA contained in Qβ(hp) was here characterized by SE-HPLC and showed that the absorbance intensity at 260 nm was higher than at 280 nm, which is a characteristic feature of nucleic acids (Fig. 2a). The calculated 260/280 peak intensity ratio of 1.7 confirmed the presence of ssRNA entrapped in Qβ VLPs (Fig. 2a). Moreover, the RNA was quantified via RiboGreen assay, a fluorimetric assay assessing a final 23% in terms of w/w ratio between RNA and protein content (Fig. 2b). Qβ(hp) was also analyzed via Asymmetric Flow Field fractionation (AF4) coupled to UV-vis at 280 nm, differential Refractive Index (dRI) [347, 410-412]. RNA content was also evaluated by integrating UV-vis and dRI signals to assess the MW contributions of RNA and protein. As reported in Fig. 2d, 21 % RNA/Protein was calculated in line with the percentage obtained via RiboGreen assay [413]. The RNA was also extracted from VLPs and analyzed in reverse phase-HPLC (RP-HPLC) (Fig. 2c) developing a complementary technique to RNA profiling via Capillary Electrophoresis reported by Carboni *et al* [316].

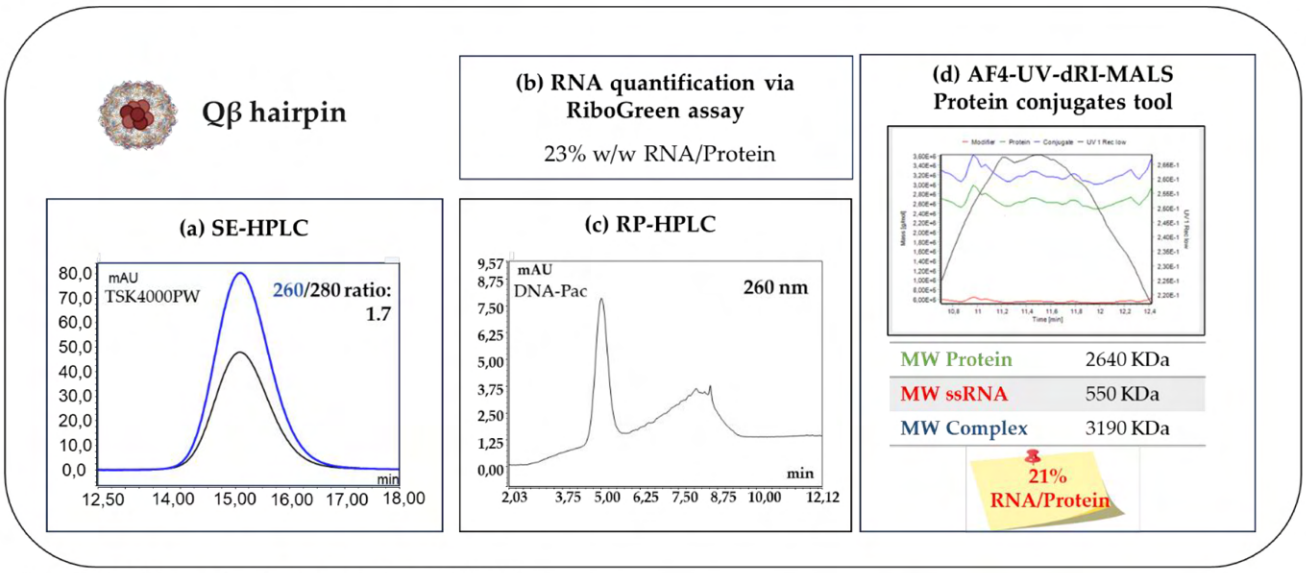

Figure 2. Characterization of Qβ hairpin.
(**a**) SE-HPLC profile and evaluation of 260/280 peak intensity ratio; (**b**) RNA content quantification via RiboGreen; (**c**) profiling of extracted hairpin RNA analyzed in reverse-phase HPLC (RP-HPLC) and (**d**) AF4 analysis using protein conjugates tools.

3.2.3 Removal of *E.coli* RNA

The removal of ssRNA from Qβ(hp) was performed using a patented method based on VLPs disassembly and ssRNA precipitation that results in Qβ in monomeric form without ssRNA [272, 414].
Qβ(hp) was treated with DTT to disrupt the disulfide bonds that are at the basis of VLPs assembly. Then ssRNA was precipitated by adding high a concentration of $MgCl_2$ to form insoluble Mg_2+ complexes. Qβ monomer was recovered from the supernatant and purified by size-exclusion chromatography (Fig. 3b). The RiboGreen analysis indicated that the RNA had been nearly entirely eliminated, leaving only a residual 2% w/w RNA/Protein (Fig. 3a).

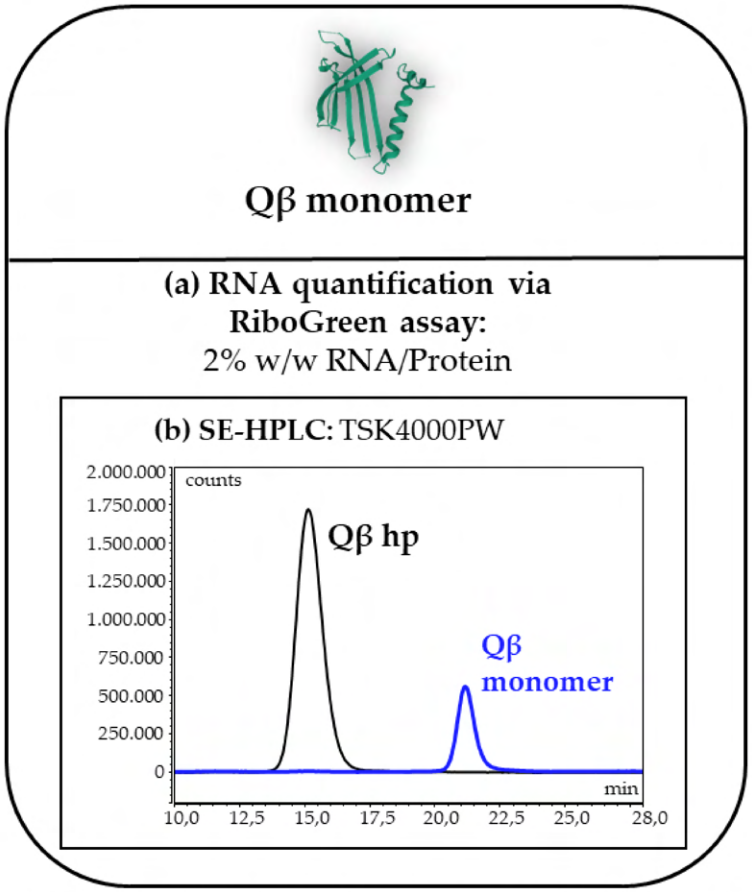

Figure 3. (a) RNA content quantification in Qβ monomer and (b) SE-HPLC profiling of Qβ pre- and post-disassembly.

An alternative approach was employed to eliminate ssRNA from Qβ hp using RNase enzyme treatment. This method was conducted without the need to disassemble the VLPs. [277, 316]. In particular, Qβ(hp) was incubated with an RNAse cocktail of two purified ribonucleases RNase A and T1 at 55 degrees under shaking. RNAse enzymes are able to pass through the VLPs pores and degrade the entrapped ssRNA, leaving its peculiar VLPs structure intact. RNAses and nucleic acids were eliminated by serial centrifugal filtration and dialysis (100 kDa). The resulting empty Qβ (Qβ(Ø)) had an intact VLP structure, with a 260/280 peak intensity ratio of 0.8 (Fig. 4b, right side) and only 1% w/w RNA/Protein left (Fig. 4a, right side).

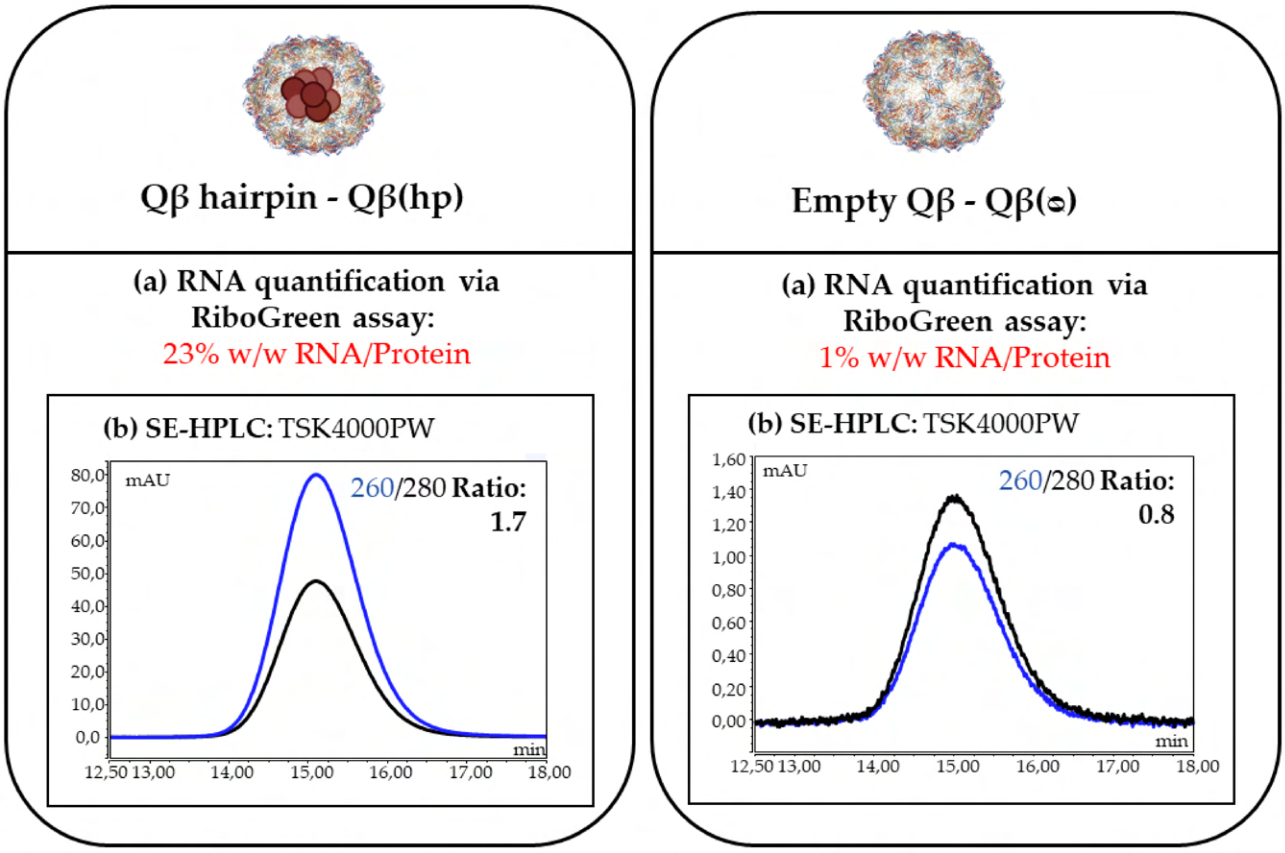

Figure 4. (a) RNA content quantification and (b) SE-HPLC profiling in Qβ pre- (left side) and post RNAse treatment (right side)

We optimized the RNAse reaction conditions (Qβ(hp) treated with RNAse cocktail of RNase A and T1 at a ratio 1:1 w/v VLP/RNAses overnight) to ensure complete RNA removal while utilizing a reduced enzyme concentration. Qβ VLPs were treated with 10:1 w/v VLP/RNAses for 1 day or 4:1 w/v VLP/RNAses for 3 days at 55 degrees under shaking. The resulting Qβ VLPs post RNAse treatment were purified and analyzed to assess the RNA content and VLPs integrity.

SE-HPLC profiles of Qβ VLPs post-treatment confirmed VLPs integrity, eluting at the same retention time of pre-treated Qβ VLPs (Fig. 5b). After 10:1 w/v VLP/RNAses treatment a high 260/280 peak intensity ratio absorbance indicated that RNA was still present. A reduction of RNA content was assessed by RiboGreen assay where only 5% w/w RNA/Protein was left for Qβ VLPs post 10:1 w/v VLP/RNAses. Instead, after 4:1 w/v VLP/RNAses treatment only 1% w/w RNA/Protein for Qβ VLPs remained with a 260/280 peak intensity ratio of 0.8 calculated by SE-HPLC. (Fig. 5a).

Qβ VLPs pre- and post RNAse treatment were also analyzed via AF4-UV-dRI-MALS to evaluate RNA content by integrating UV-vis and dRI signals. The % RNA/Protein calculated were in line with the percentage obtained via RiboGreen assay (Fig. 5c).

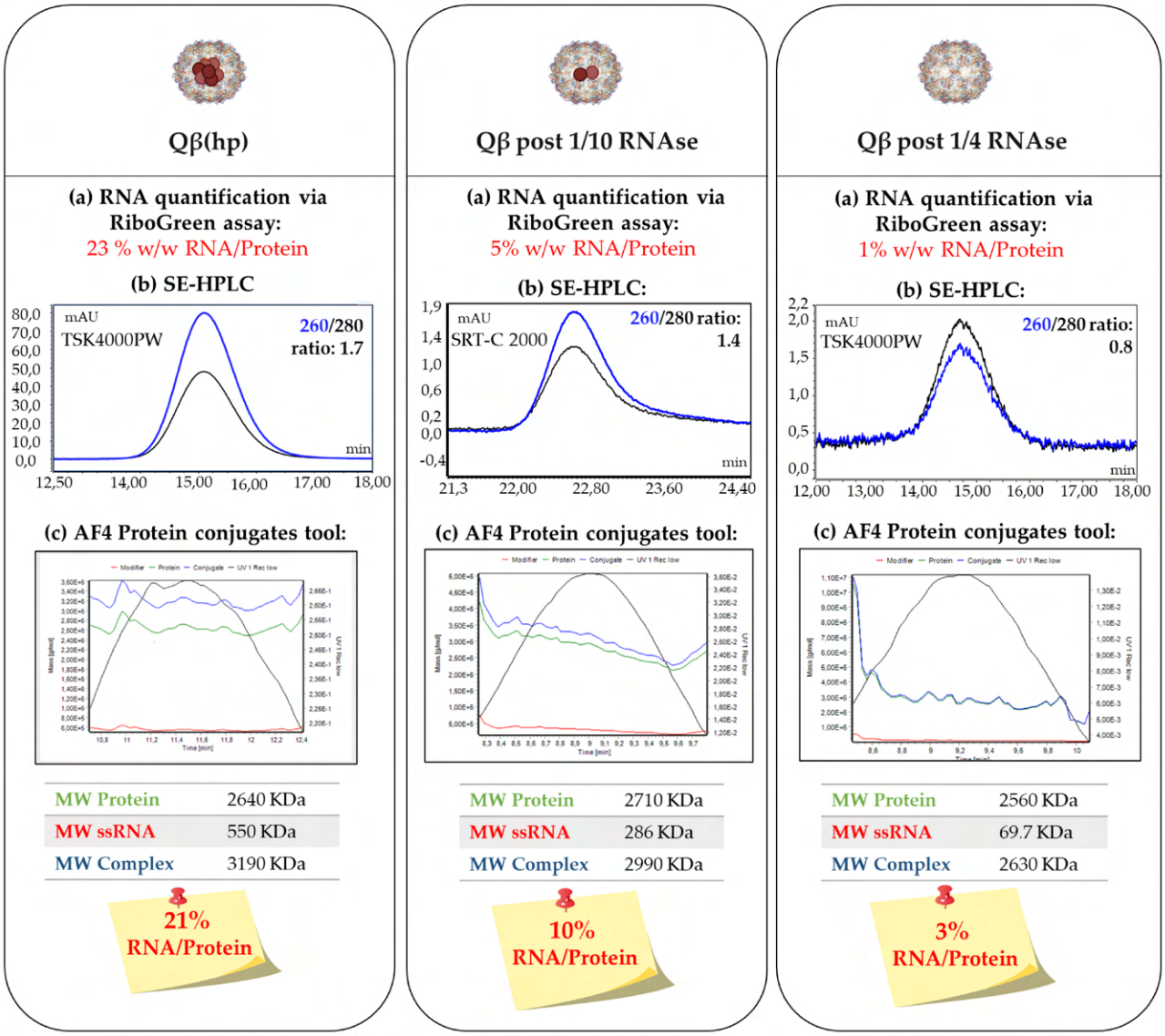

Figure 5. Full characterization of Qβ(hp) before and after RNAse enzyme treatment: (**a**) RNA content quantification, (**b**) SE-HPLC profiles with evaluation of 260/280 peak intensity ratio, (**c**) AF4 analysis for RNA content evaluation using protein conjugates tool.

The dimensions of Qβ VLPs pre- and post RNAse treatment were examined thanks to MALS and DLS analyses (Fig. 6a-b). MALS and DLS can provide respectively information about distribution of mass (Radius of gyration, Rg) and the physical dimension of the VLP (Radius of hydrodynamic, Rh). In a spheric nanoparticle, Rg represents the internal radius of the cage, while Rh represents the external radius. For Qβ VLPs pre- and post RNA removal, the calculated Rh remained quite unvaried indicating that the nanoparticle was intact. Conversely, the Rg increased when RNA content decreased and the VLP gradually became emptier (table in fig. 6).

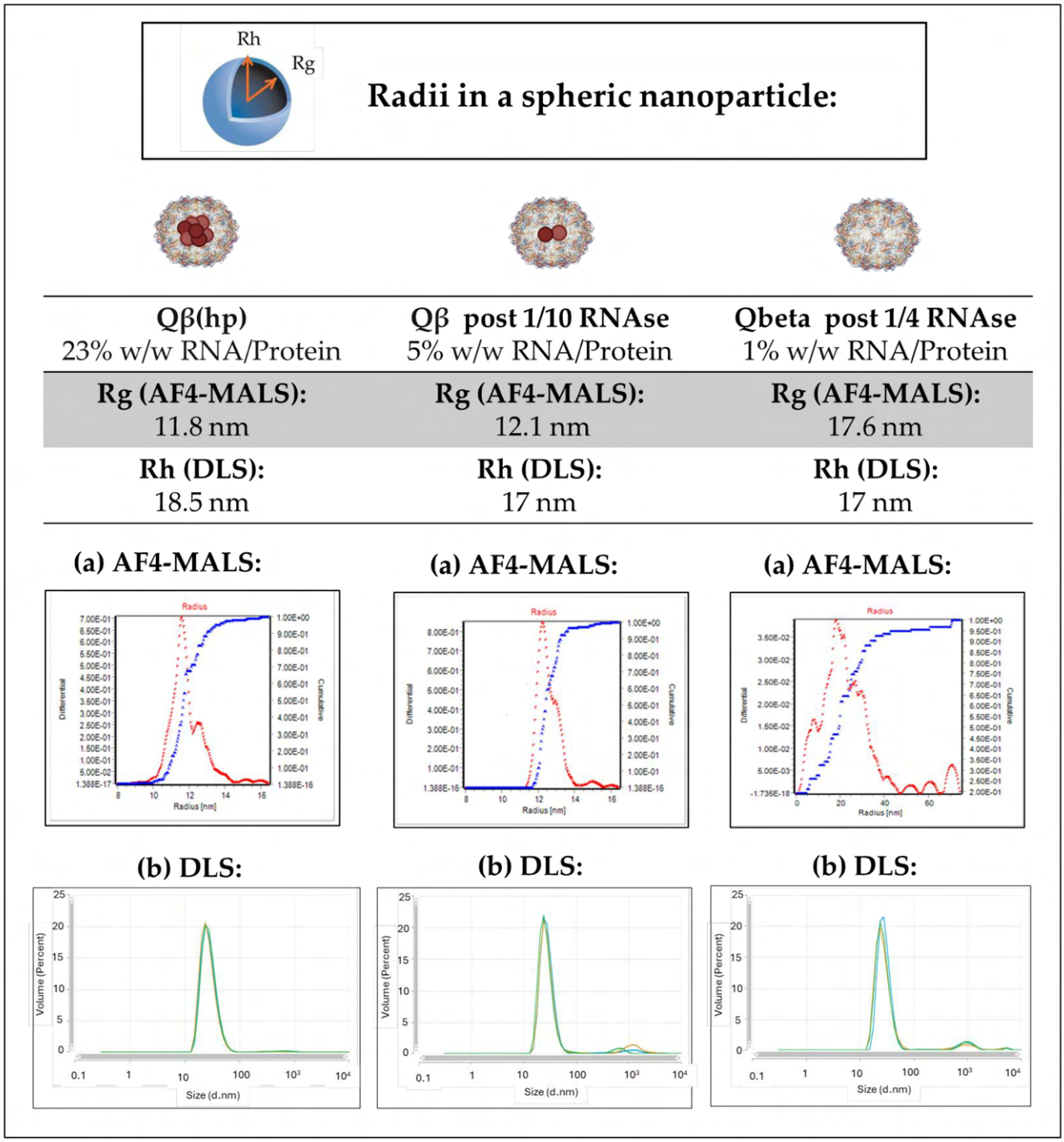

Figure 6. (a) AF4-MALS and (b) DLS analyses to calculate Rg and Rh of Qβ VLPs pre- and post RNAse treatment.

3.2.4 Encapsulation of CpG in GBS PSII- Qβ

To explore the impact of a different presentation of CpG adjuvant, either encapsulated inside glycoconjugate nanoparticles or covalently conjugated to nanoparticle surface, on PSII immunogenicity, different types of CpG were evaluated.

Until now, three classes of CpG ODN have been identified, CpG class A, B and C, each characterized by a different structure and immunological function. We focused on CpG A previously successfully packaged into virus-like particles (VLP) and used as adjuvants in several clinical studies [270-273], and CpG B which is the most extensive studied TLR9 agonist in clinical trials as vaccine adjuvant [265, 274, 278].

CpG class A (CpG A) is characterized by palindromic CpG motifs at the center of its sequence that generate a hairpin structure and two polyG tails. CpG A activates the TLR9 of plasmacytoid dendritic cells (pDC) to mature and secrete IFNα but has no effect on B cells [274, 275, 278]. IFN-α activates the CD8-positive cytotoxic T lymphocyte response [268]. The activated pDCs also promotes the differentiation of Th-0 into Th-1 immune response [415, 416]. It exhibits a propensity to aggregate forming G-quadruplexes structures originated from stacked guanine tetrads [417] essential for a strong IFN-α induction [418, 419] (Fig. 7). CpG A has already proven its immunological value in clinical trials against asthmatic allergies [272].

CpG class B (CpG B) is characterized by straight single stranded DNA sequences that do not form 3D structures as CpG class A. CpG B strong activate B cells to proliferate and secrete cytokines as IL-6 that promotes the multiplication and activation of B cells and, as result, enhanced antibodies production [420, 421] (Fig. 7). CpG B is the most tested TLR9 agonist in clinical studies as vaccine adjuvant [265, 274, 278]. The structural differences between CpG A and B were evaluated via RP-HPLC, where they eluted at distinct times mainly due to the more compact dimension of CpG A determining its early elution respect to CpG B (Fig. 8).

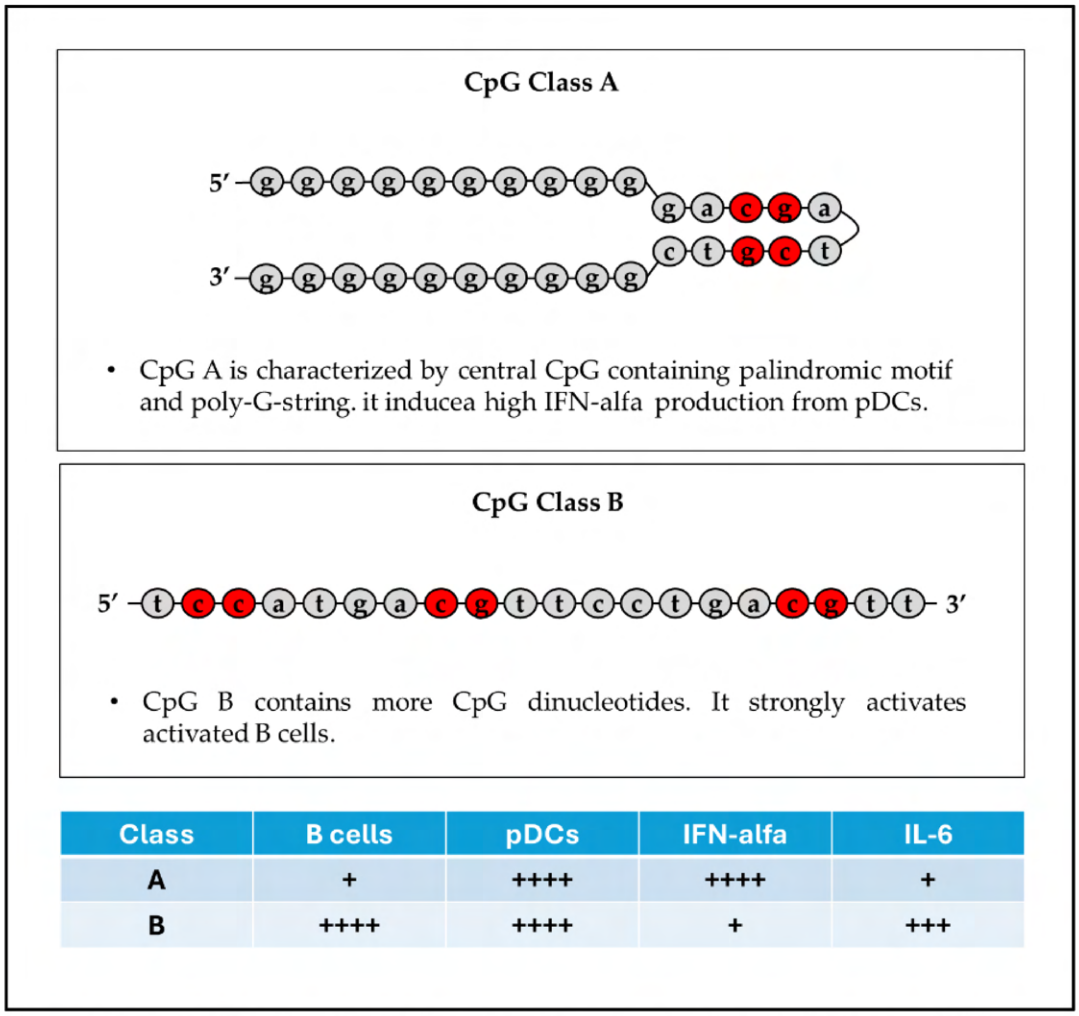

Class	B cells	pDCs	IFN-alfa	IL-6
A	+	++++	++++	+
B	++++	++++	+	+++

Figure 7. Sequences and main characteristics of CpG class A and B

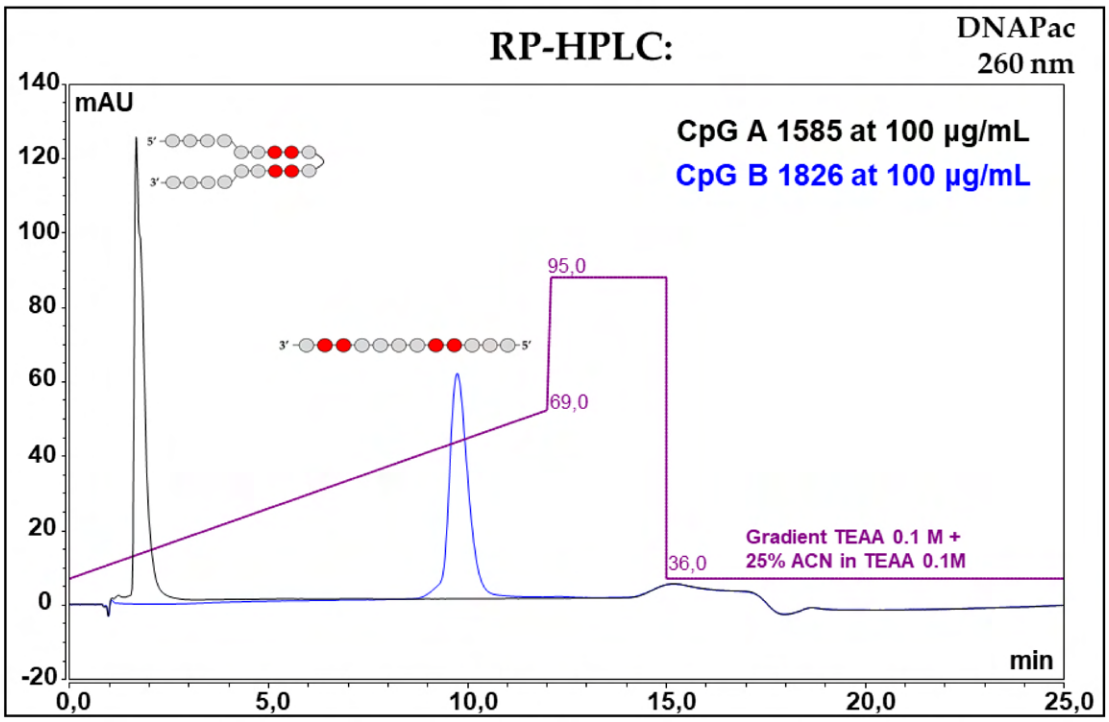

Figure 8. CpG A and B profiling in reverse-phase (RP)-HPLC analysis.

Beeh *et al*. entrapped CpG A into VLPs by incubating Qβ monomer in presence of aggregated CpG A used as scaffold by monomeric protein to restore its VLP structure [272, 414]. Using the same strategy, CpG A was firstly aggregated and then encapsulated by Qβ monomer during *in vitro* VLP formation. In particular, the 3D conformation of CpG A was obtained thanks to a process of disaggregation performed at 50 degrees at alkaline pH and subsequent aggregation at neutral pH performing thermal shock by a rapid change in temperature from 80°C to 0°C. The process of CpG aggregation was monitored using HPLC and DLS analyses. During these analyses, a noticeable increase in size was observed (Fig. 9).

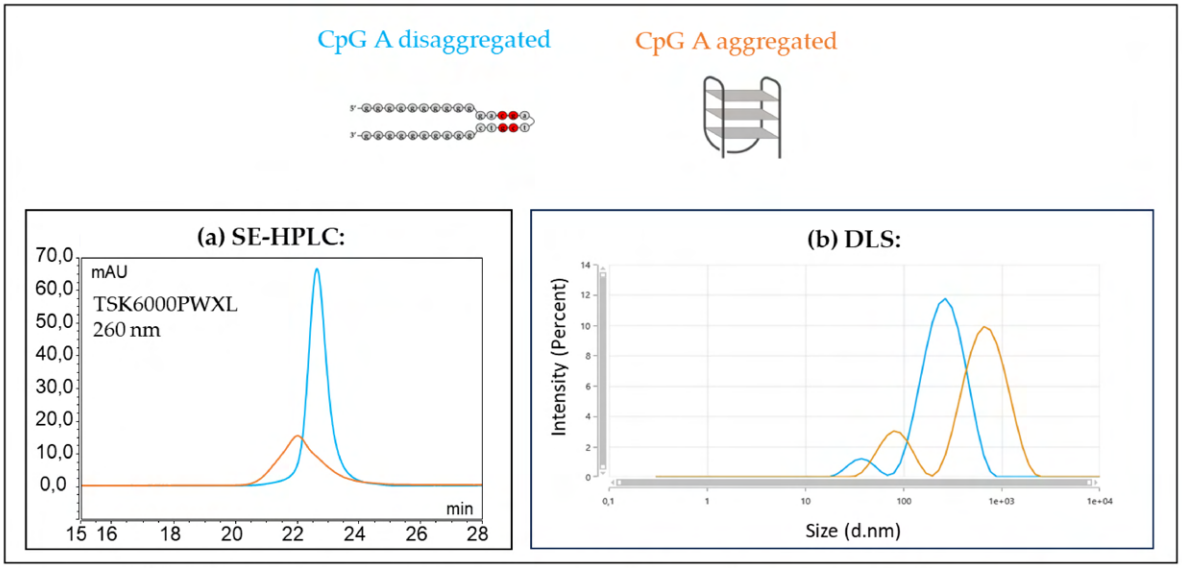

Figure 9. (a) SE-HPLC and (b) DLS analyses of CpG class A pre- and post-aggregation.

Once CpG A was aggregated (Fig. 10a), Qβ monomers were incubated with CpG A and allowed to reassemble into VLPs around ssDNA 3D structure (Fig. 10b). The effective and correct reassembly was checked by HPLC analysis, where the typical peak of Qβ VLPs was reestablished as the original 260/280 peak intensity ratio of 1.7 (Fig. 10c).

Conversely, Qβ monomer is not able to reassemble into VLPs in presence of CpG class B because of tiny dimensions of these ssDNA. But, when Qβ(Ø) empty is incubated with an excess of CpG B (Fig. 10e), CpG B is able to pass through VLPs pores of Qβ(Ø) and stacks inside thanks to electrostatic interactions [277]. The entry of CpG was followed via HPLC analysis monitoring 260/280 peak intensity ratio of Qβ(Ø) that passed from 0.8 (Fig. 10d) to 1.2 after incubation with CpG B and Qβ(CpG/B) purification, confirming its presence in the core of the VLP (Fig. 10f).

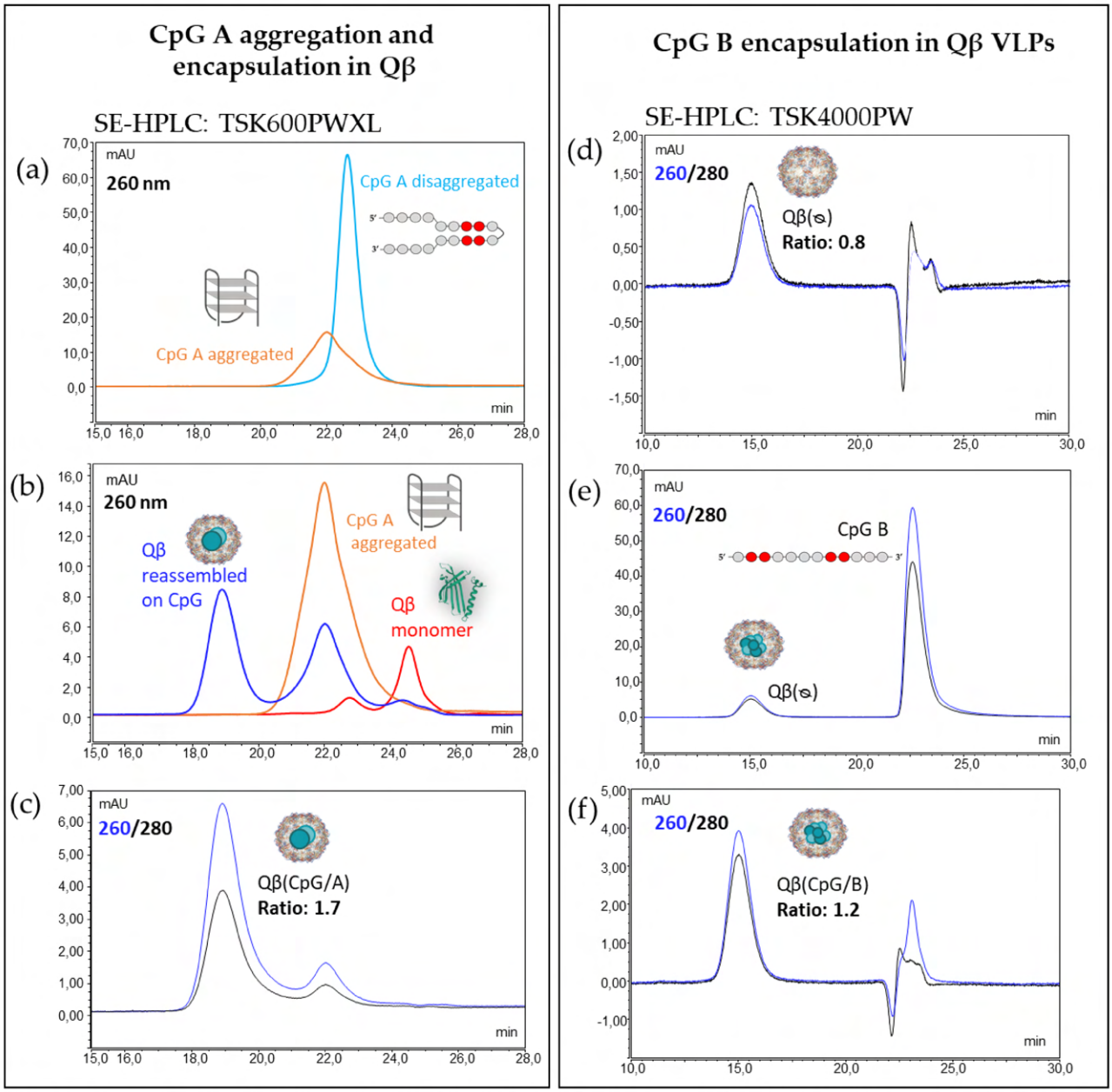

Figure 10. Encapsulation of CpG in Qβ: SE-HPLC analyses of (a-c) CpG class A aggregation and Qβ monomer reassembly around aggregated CpG A; (d-f) encapsulation of CpG class B inside the empty Qβ VLPs.

Qβ with encapsulated CpG in aggregated (Qβ(CpG/A)) and not aggregated form (Qβ(CpG/B)) where conjugated to the serotype II GBS polysaccharide (GBS PSII) using same conjugation method already described by Carboni *et al.* for PSII-Qβ(hp) [316]. Sized GBS polysaccharide after its partial random oxidation with sodium periodate was conjugated to Qβ via reductive amination of ε-amine groups of lysines.

To evaluate the stability of CpG after encapsulation in Qβ performed at room temperature (RT), and after glycoconjugation of Qβ(CpG) performed at 37 °C for 3 days, CpG B was incubated in these conditions and then analyzed via CE comparing the resulting profiles to CpG B starting material (Fig. 11).

After 3 days at RT, the profile obtained (blue profile in Fig. 11) was identical to the starting material profile (red profile in Fig. 11) confirming stability of CpG B. At 37 °C, a similar profile was observed with minimal signs of degradation (green profile in Fig. 11) demonstrating a partial stability of CpG B inside VLPs even after the conjugation process; moreover, we have to consider that the presence of VLPs further stabilizes CpG structure and protects it from degradation.

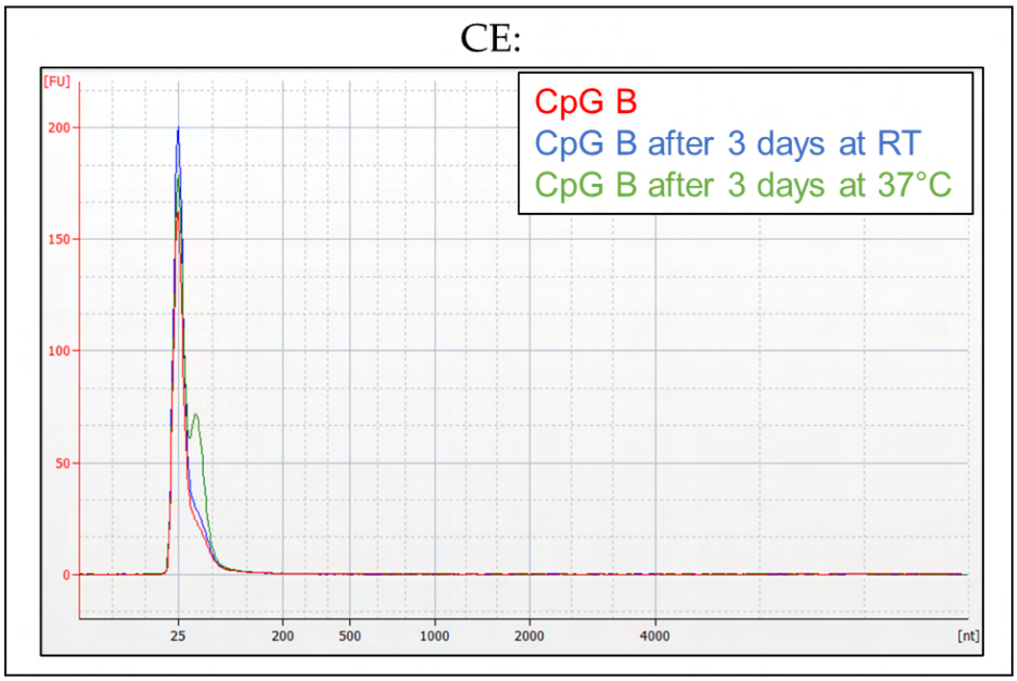

Figure 11. CpG B stability at RT and under glycoconjugation conditions.

3.2.5 Conjugation of CpG B on GBS PSII-Qβ

To investigate the possibility to deliver the CpG outside the glycoconjugates, Qβ(Ø) was first conjugated to GBS PSII and then its residual free lysines were conjugated to CpG B using a method developed by Chatzikleanthous *et al.* based on thiol-maleimide click chemistry [422].

In particular, the remaining free lysines of GBS PSII-Qβ(Ø) were functionalized with a N-ε-malemidocaproyl-oxysuccinimide (EMCS) linker to obtain a terminal maleimide group prompt to react with thiol-CpG (Fig. 12). The correct exposure of CpG outside GBS PSII-Qβ and its integrity were confirmed by dot-blot assay where mAb anti-ssDNA revealed CpG presence in the resulting GBS PSII-Qβ-CpG (Fig. 13a) but did not recognize it when entrapped-in and masked by the VLP core (Fig. 13b) or in its total absence (Fig. 13c).

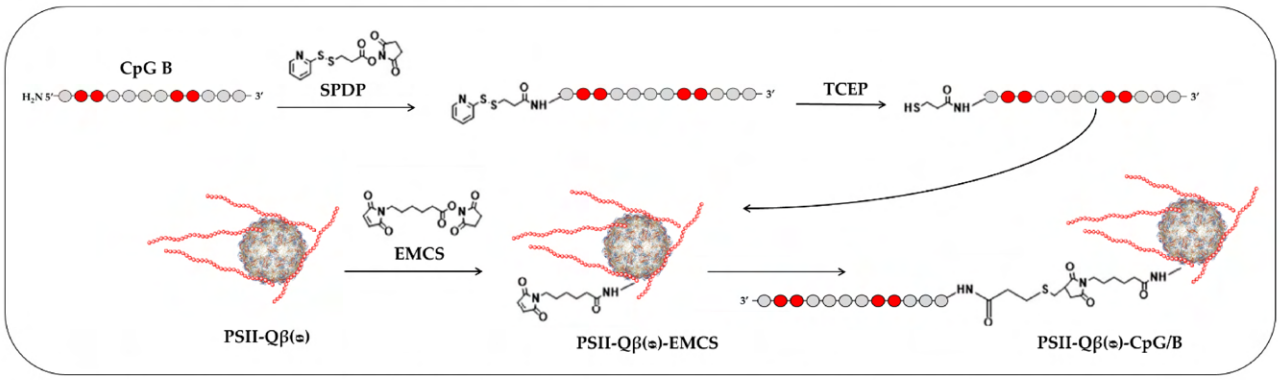

Figure 12. Reaction scheme for the conjugation of CpG B to GBS PSII-Qβ VLPs.

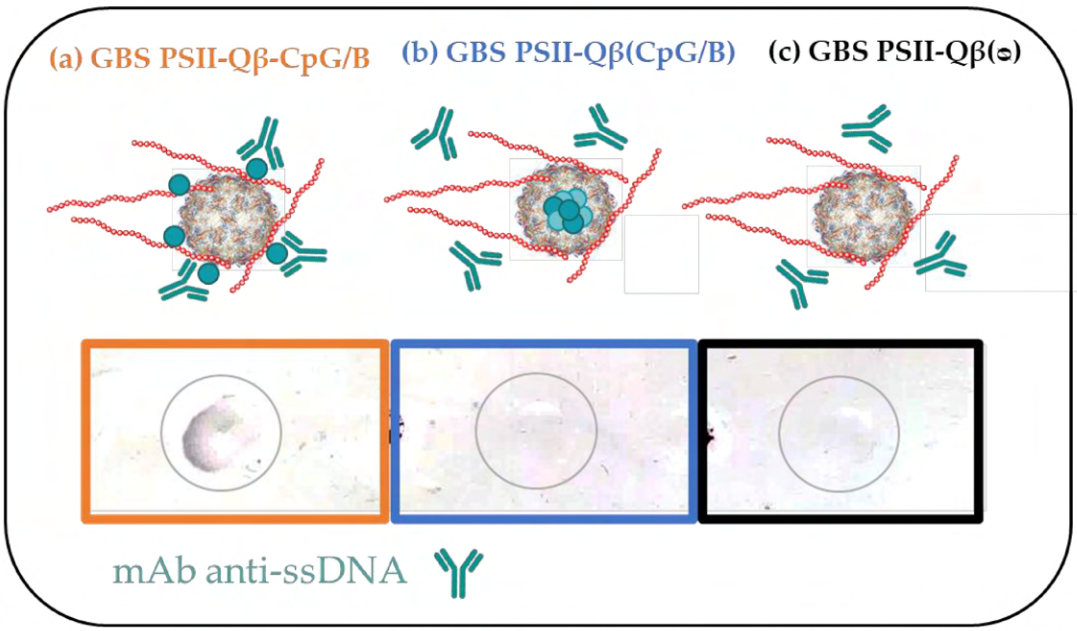

Figure 13. Dot-Blot for the recognition of CpG exposed outside GBS PSII-Qβ VLPs.
Monoclonal antibody against ssDNA structure recognized (**a**) CpG B conjugated on GBS PSII-Qβ VLPs and did not recognize it when encapsulated inside (**b**) GBS PSII-Qβ VLPs or (**c**) in absence of genetic material.

3.2.6 A final comprehensive characterization of prepared glycoconjugate nanoparticles

The different GBS PSII-Qβ prepared as described in the above paragraphs were purified by serial centrifugal filtration (100 kDa) and deeply characterized. In particular, the effective glycoconjugation of Qβ and its integrity were assessed via Size Exclusion High-Performance Liquid Chromatography (SE-HPLC), and the 260/280 peak intensity ratio was monitored to evaluate the absence or presence of genetic material. The nanoparticle integrity was also confirmed by negative-stain Transmission Electron Microscopy (TEM) analysis. Protein, saccharide and CpG contents were quantified respectively by Micro Bicinchoninic Acid (mBCA) colorimetric assay, high-performance anion-exchange chromatography with pulsed amperometric detection (HPAEC-PAD) and RiboGreen assay, a fluorimetric assay. The content of saccharide and CpG was expressed as % w/w per protein for each of the adjuvanted glycoconjugate nanoparticles to be compared.

After glycoconjugation of Qβ(hp), Qβ(CpG/A or B), and Qβ(Ø), a shift of peaks at lower retention times in SE-HPLC described an increase of MW and size, confirming the glycoconjugation of nanoparticles (see overlapped red and black SE-HPLC profiles in Figure 14a, b, c, d). The saccharide/protein ratio of each of the obtained glycoconjugate nanoparticles was calculated, resulting comparable among them. TEM analysis confirmed nanoparticle integrity, showing that glycoconjugation did not impact the VLPs structure.

The presence of CpG or RNA encapsulated in PSII-Qβ, was first confirmed by SE-HPLC monitoring the 260/280 peak intensity ratio, that resulted above 1 for PSII-Qβ(hp), PSII-Qβ(CpG/A) and PSII-Qβ(CpG/B) (see overlapped blue and black SE-HPLC profiles in Fig. 14a, b and c). CpG content was quantified and resulted similar between PSII-Qβ(CpG/A) and PSII-Qβ(CpG/B) while, PSII-Qβ(hp) had a higher RNA content as expected.

Conversely, a lower 260/280 peak intensity ratio was described for PSII-Qβ(Ø), where only 1% w/w of RNA per protein was quantified, confirming complete removal of RNA (see overlapping blue and black SE-HPLC profiles in Fig. 14d).

After CpG conjugation on PSII-Qβ(Ø), a further shift of retention time was described in SE-HPLC analysis, confirming an increase in glycoconjugates dimension after CpG linkages to GBS PSII-Qβ (see red and black SE-HPLC profiles in Fig. 14e). Moreover, an increase of 260/280 peak intensity ratio was observed, indicating the effective presence of CpG (see overlapped blue and black SE-HPLC profiles in Fig. 14e).

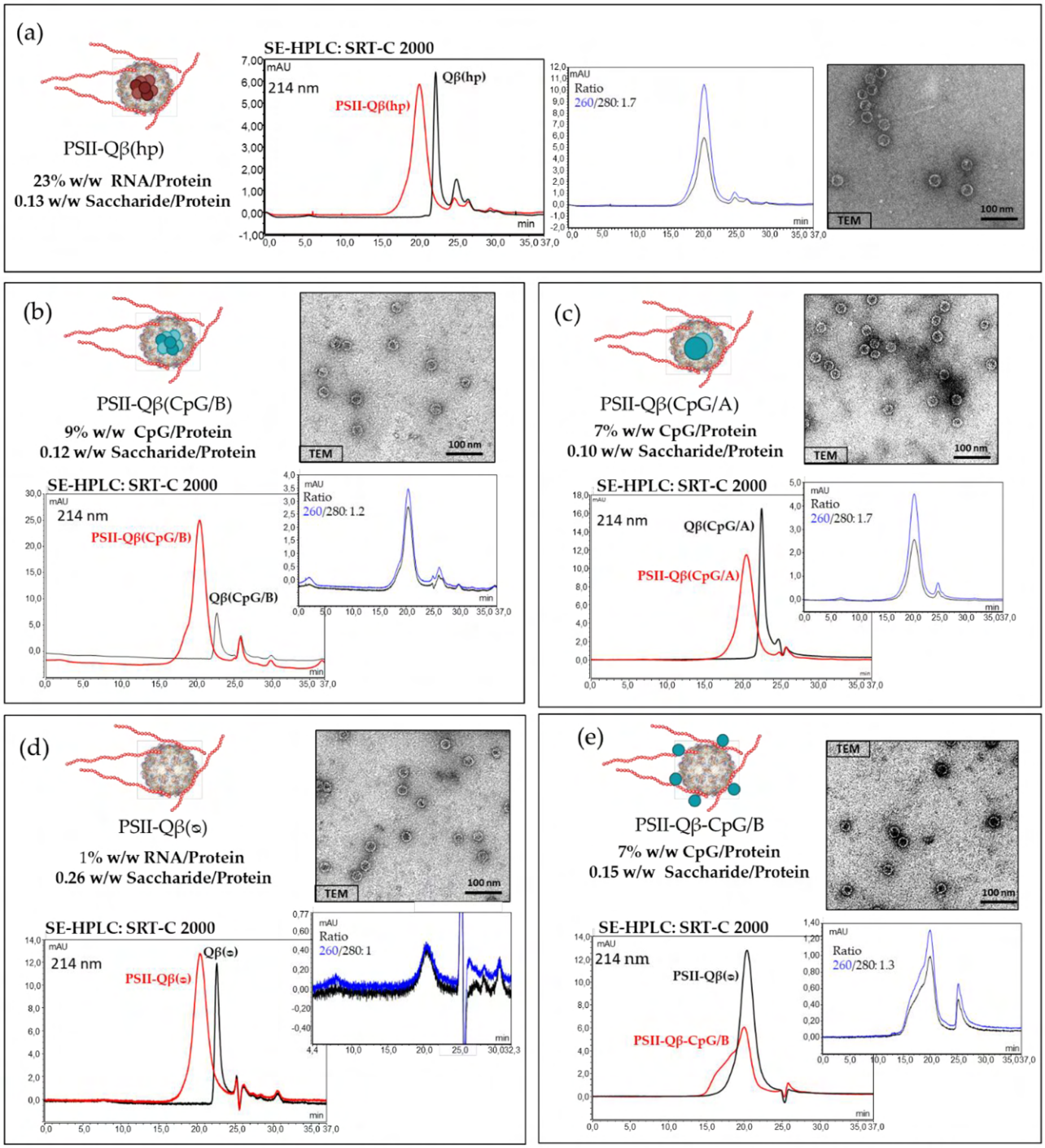

Figure 14. Full characterization of final glycoconjugate nanoparticles to be tested *in vivo*.

For (a) PSII-Qβ(hp), (b) PSII-Qβ(CpG/B), (c) PSII-Qβ(CpG/A), (d) PSII-Qβ(Ø) and (e) PSII-Qβ-CpG/B have been reported CpG or RNA content (% w/w CpG or RNA/Protein), w/w Saccharide/Protein ratio, Size-exclusion High Performance Liquid Chromatography (SE-HPLC) profiling and Transmission electron microscopy (TEM) in negative staining.

3.2.7 Single Dose responses in a Murine Model

Similar to unprimed humans who present a low immune response to GBS PS conjugated to proteins (TT or CRM_{197}), at least two booster doses are required to elicit high IgG responses in mice, rabbits [141, 423], and non-human primates [424]. Optimized self-assembling virus-like particles conjugated to Group B Streptococcus capsular polysaccharides (GBS PSII-Qβ(hp)) induced strong immune responses in mice after one immunization, providing pre-clinical proof of concept for a single-dose vaccine. Here, we performed a head-to-head comparison in mice of adjuvanted GBS PSII-Qβ delivering CpG adjuvant either inside or outside the VLP with similar CpG and saccharide contents (light yellow in table 2). We evaluated whether these vaccines could induce a comparable immune response to GBS PSII-Qβ(hp), equal or superior to two doses of GBS PSII-CRM_{197} (light green row in table 2). Moreover, PSII-Qβ(Ø) was evaluated in absence of any immune enhancers (light red row in table 2) and in physical mixture with high or low dose of CpG (light blue row in table 2).

In table 2, we report all the tested glycoconjugate vaccines in terms of saccharide/protein ration, saccharide and adjuvant content, along with their corresponding administered CpG dose per dose of saccharide antigen.

For each adjuvanted PSII-Qβ, groups of 10 CD-1 mice were immunized with two vaccine doses administered three weeks apart (0.5 μg of GBS PSII/dose) or just one dose (Fig. 15). Two doses of Alum adjuvanted GBS PSII-CRM_{197} were administered as reference vaccine. On day 42, mice sera were collected to measure IgG titers by Luminex assay, using randomly biotinylated GBS PSII as coating reagent (Fig. 16 and 17).

Table 2. Summary of tested glycoconjugates and corresponding CpG or RNA quantity per dose

	Saccharide/protein ratio w/w	**CpG or RNA content % w/w in VLPs**	**Saccharide quantity per dose (μg)**	**CpG or RNA quantity per dose of saccharide (μg)**
PSII-CRM_{197}	1.4	Not present	0.5	Not present
PSII-Qβ(hp)	0.13	20	0.5	0.7
PSII-Qβ(CpG/B) (inside)	0.12	9	0.5	0.4
PSII-Qβ(CpG/A) (inside)	0.10	7	0.5	0.3
PSII-Qβ-CpG/B (outside)	0.15	7	0.5	0.2
PSII-Qβ(Ø)	0.26	1	0.5	0.02
PSII-Qβ(Ø) + high dose CpG (co-formulated)	0.26	1	0.5	30
PSII-Qβ(Ø) + low dose CpG (co-formulated)	0.26	1	0.5	0.4

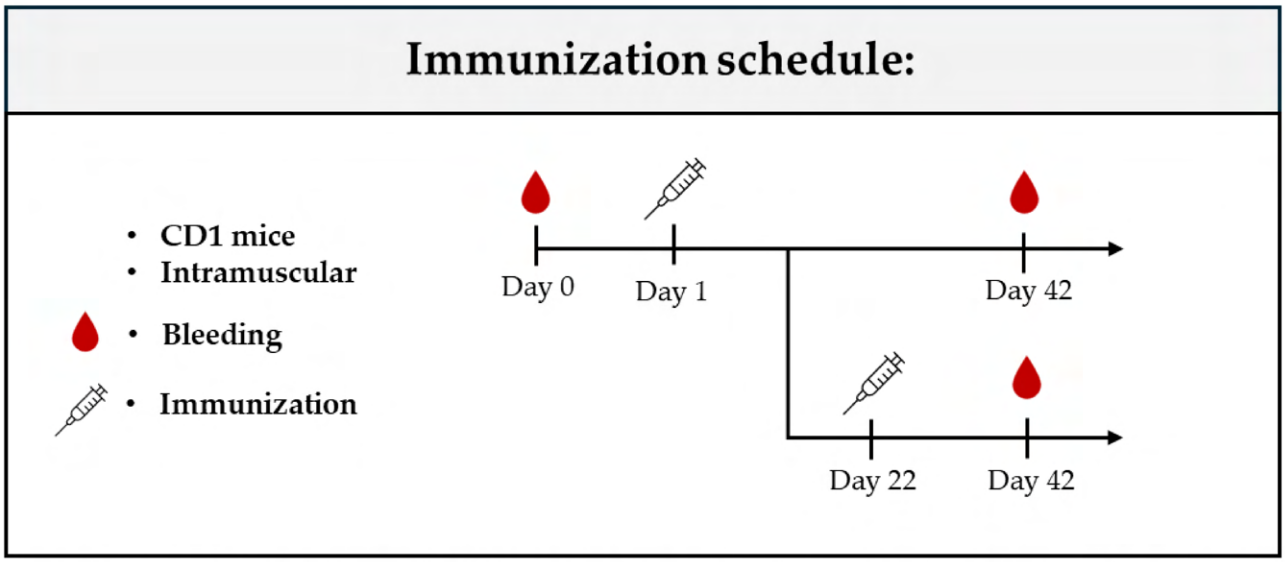

Figure 15. Immunization schedule. Groups of 10 CD-1 female mice were immunized intramuscularly (IM) with one single dose or two doses administered three weeks apart of GBS PSII glycoconjugates nanoparticles (0.5 μg of PSII/dose). Two immunizations were performed at day 1 and day 22 with PSII-CRM$_{197}$ adjuvanted by aluminium hydroxide (2.0 mg/mL) used as controls. The sera were collected at day 42 and analyzed via Luminex and OPKA.

A single dose of PSII-Qβ(hp) generated high levels of IgG antibodies, similar to those produced after two doses of the reference vaccine. The IgG levels elicited by Qβ conjugates decreased when *E.coli* RNA was completely removed, which supports previous findings by Carboni *et al*. [316] about the enhancing effect of RNA on the immune response (Fig. 16). When CpG B was attached to the outside of PSII-Qβ, it resulted in a significantly lower IgG level after one dose. However, when the same quantity of CpG (both types A and B) was entrapped inside PSII-Qβ, it triggered an immune response comparable and not statistically different from two doses of the reference vaccine and one dose of PSII-Qβ(hp) (Fig. 16).

IgG titers elicited after two immunizations at day 42 were also assessed (Fig. 17). PSII-Qβ(CpG/B) was the glycoconjugate that performed better, despite a general increase of IgG titers were observed for PSII-Qβ-CpG/B and PSII-Qβ(Ø) (Fig. 17).

PSII-Qβ(Ø) co-formulated with a low dose of CpG (0.4 μg/dose), the same amount entrapped in PSII-Qβ(CpG/B), was able to induce an immune response comparable to the reference vaccine only when administered two times (Fig. 17) but not when administered in one single dose. The standard mouse dosage of the CpG B adjuvant, which is 100 times higher (30 μg/dose) than the low dose contained in the Qβ, elicited a highly variable immune response among individual mice. This variability was likely due to inconsistent co-delivery and presentation of the antigen alongside the immune enhancer.

Pooled sera after one single immunization were evaluated in an Opsonophagocytic Killing Assay (OPKA) that mimics the *in vivo* killing of GBS by effector cells in presence of complement. Higher functional activity was described for pooled sera of mice immunized with two doses of the reference PSII-CRM$_{197}$ vaccine and one dose of PSII-Qβ(hp) and PSII-Qβ(CpG), confirming IgG data (Fig. 16). Most importantly, one dose of CpG A and B when delivered inside PSII-Qβ were able to

elicit a functional immune response comparable to two doses of PSII-CRM197 and one dose of PSII-Qβ(hp).

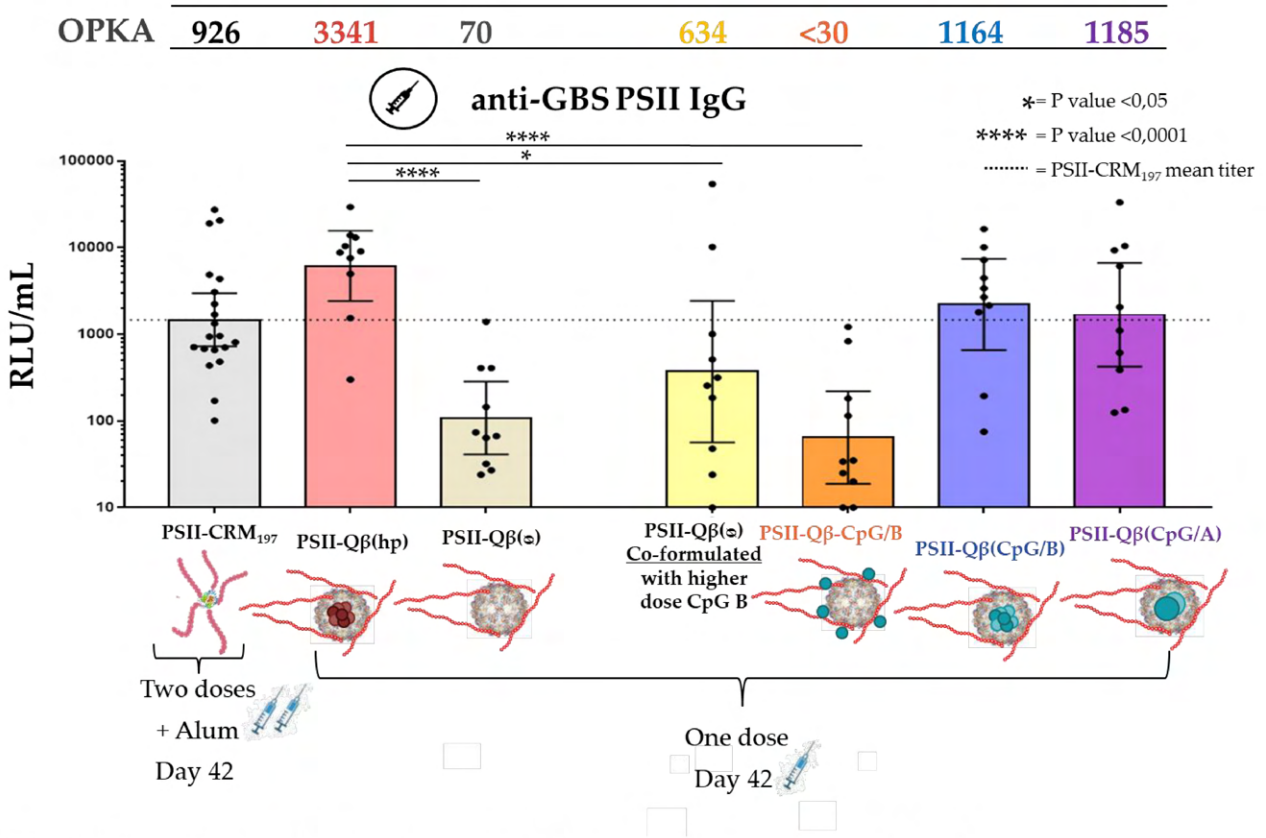

Figure 16. IgG titers and OPKA results after one dose immunization in mice.
Immune response in 10 or 20 mice per group receiving one dose of PSII glycoconjugate nanoparticles compared to two doses of PSII-CRM197 as benchmark vaccine (0.5 µg/dose). The y-axis indicates the geometric mean IgG titer (RLU/mL), individual mice are indicated by the dots, and the 95%, Confidence Interval is indicated by the whiskers. For non-responder sera were assigned GMT titers half of the LLOQ (10 RU/mL). Mann Whitney test was used to compare benchmark titers with the other immunization; *<0.05; ****<0.0001.

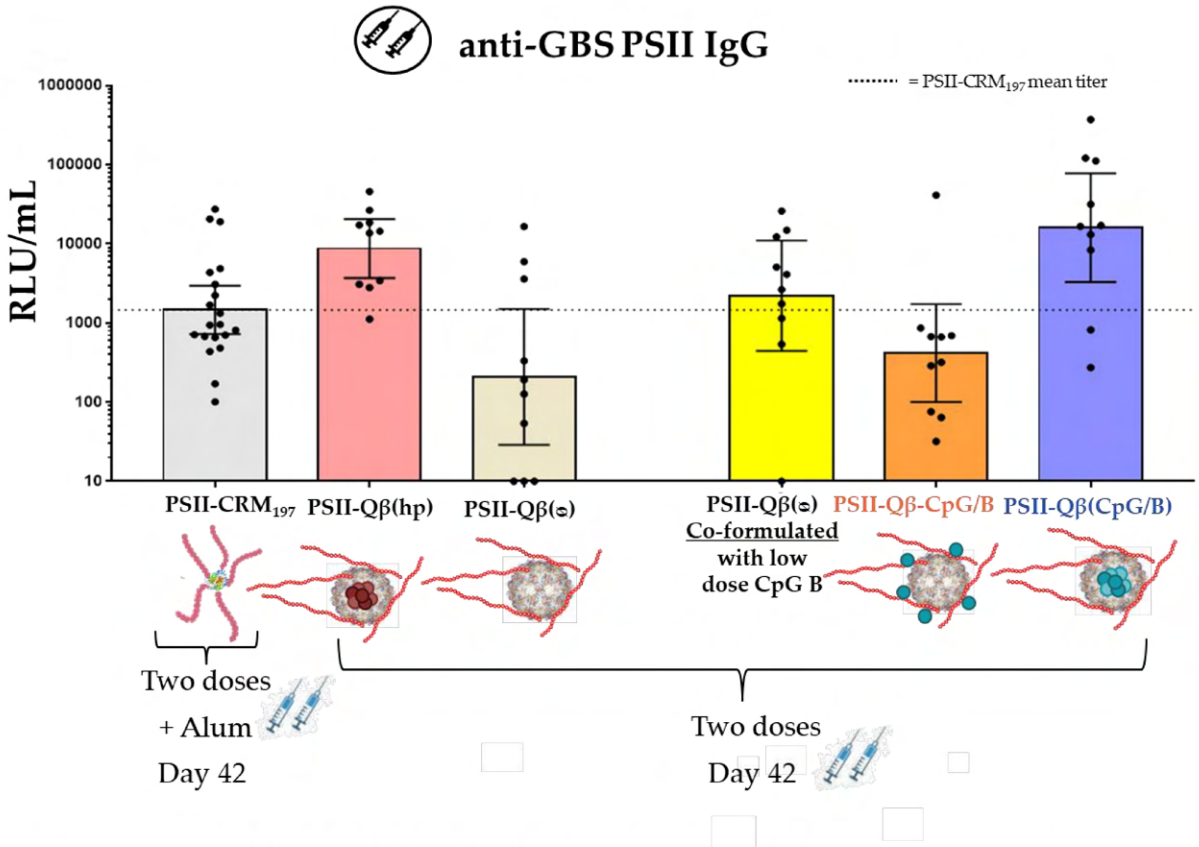

Figure 17. IgG titers after two immunizations in murine model.
Immune response in 10 or 20 mice per group receiving two doses of PSII glycoconjugated nanoparticles compared to two doses of PSII-CRM197 as benchmark vaccine (0.5 μg/dose). The y-axis indicates the geometric mean IgG titer (RLU/mL), individual mice are indicated by the dots, and the 95%, Confidence Interval is indicated by the whiskers. For non-responder sera were assigned GMT titers half of the LLOQ (10 RU/mL).

3.3 Discussion

Improving the efficiency of glycoconjugate vaccines is a challenging goal. This is mainly due to two reasons. Firstly, their mechanism of action is not fully understood. Secondly, immune responses to these vaccines vary among high-risk groups such as infants, the elderly, and people with weakened immune systems. These populations, who need protection the most, often show a lower response to these vaccines [129].

Starting from the first decade of the 21st century, considerable research efforts were directed to advancing the development of novel adjuvants with the aim to increase vaccine immune responses [395]. Technological progress provided valuable mechanistic insights enabling a deeper understanding of how adjuvants work. A pivotal discovery impacting adjuvant research and development was the identification of the Toll like receptor (TLR) system in the signaling pathways of the innate immune system, especially in regulating adaptive responses [207-209]. Toll-like receptors (TLRs), expressed on innate immune cells, such as dendritic cells, recognize the presence of pathogen-associated molecular patterns (PAMPs), which are derived from viruses, bacteria, fungi etc. Most novel adjuvants that led to the license of many new vaccines are PAMPs, including AS01 (Shingrix™, Shingles and Mosquirix™, Malaria), AS03 (Pandemrix™, pandemic Flu), AS04 (Cervarix™, HPV), MF59 (Fluad™, seasonal Flu) and CpG (CpG 1018 in Heplisav-B™, HBV) [395].

In the present work, we investigated a novel approach for co-delivery of glycoconjugates and adjuvants with the final goal of developing more effective multicomponent vaccines. In particular, we explored the combination of a protein component ensuring T-cell engagement against the directly conjugated bacterial saccharide antigen GBS PSII) [125, 303], multivalent display of the saccharide antigen in a VLPs platform (Qβ VLPs) to increase B cell receptor clustering [99] and the effect of the CpG ssDNA TLR9 agonist [277].

Optimal CpG co-delivery to achieve a high immune response was investigated by comparing external delivery on functionalizated VLPs with encapsulation of CpG molecules inside the VLP cage. All formulations were compared with the physical mixture of CpG with a glyco-conjugated VLP as classical antigen-adjuvant delivery. I*n vivo* comparison was performed using a similar CpG quantity per dose of saccharide antigen (around 0.4-0.2 μg of CpG per 0.5 μg of GBS PSII) for each of the prepared glycoconjugated NPs.

In a study conducted in mice, it was observed that a single dose of glycoconjugated VLPs with external covalently linked CpG did not trigger a strong immune response. This response was indeed comparable to that induced by a single dose of glycoconjugated VLP without any adjuvant (PSII-Qβ(Ø)). This result was unexpected, as Chatzikleanthous *et al*. utilized the same approach underling a higher immune response against a protein target antigen when covalent linked to CpG [422]. Because CpG integrity once conjugated to PSII-Qβ was experimentally confirmed prior to immunization, we hypothesize that the conjugated molecule could be partially degraded by DNAses when administered *in vivo*.

Conversely, one dose of glycoconjugated VLPs carrying CpG inside their cage induced IgG titers comparable to two doses of Alum-adjuvanted traditional glycoconjugates based on CRM_{197}, representing our reference vaccine. In this case, CpG is protected by DNases and probably able to

reach the target receptors inside endosomes avoiding possible degradations. Two classes of CpG were investigated (class A and B) that differ for immune cell interactions and form (aggregated and non-aggregated), although no differences in elicited IgG titers between the two vaccines were appreciated. Therefore, preferential stimulation of either pDC or B cells led to similarly enhanced immune responses, probably because of their equal fundamental roles in the generation of humoral responses against the administered antigen.

GBS PSII-Qβ(Ø) co-formulated with CpG elicited highly variable immune responses among animals, resulting in geometric mean titers intermediate between PSII-Qβ(Ø) externally conjugated with CpG and internally delivered CpG VLPs. This result was unexpected on the basis of previous literature data regarding CpG co-formulated vaccines [422, 425, 426], also considering that the co-formulated CpG dose was 2 log higher than internally delivered CpG.

The IgG titers enhancement caused by CpG when encapsulated in glycoconjugated NPs after just one dose is probably determined by the retention of NPs in the endosome leading to a continuous effect by CpG and decreased dosage needed [427, 428].

In conclusion, the devised multicomponent glycoconjugate vaccine strategy was successful to enhance polysaccharide immunogenicity, especially when a TLR agonist was delivered inside and protected by a nanoparticle. *In vitro* experiments to interrogate the mechanism of action of the proposed internally adjuvanted VLP vaccine are ongoing.

Therefore, PSII-Qβ(CpG) resulted a promising vaccine candidate against GBS disease for maternal vaccination (see section I.5 for further information on GBS disease) representing an improved candidate respect to PSII-Qβ(hp) described by Carboni *et al.* [316]. PSII-Qβ(hp) represented a valid initial pre-clinical proof of concept for a single-dose vaccine, although its internal RNA adjuvant component was less well-defined. We propose to replace ssRNA contained in Qβ with a CpG component that has already been tested in vulnerable populations as in HIV- and diabetic patients resulting safe [286, 288, 289]. Moreover, a retrospective analysis evaluating women who were unaware of their pregnancy status during the Hepsaliv™ administration (HBV vaccine co-formulated with CpG) [429] demonstrated a preliminary safety profile of the CpG component in this target population, as despite relatively small cohort, no adverse fetal outcomes were identified. Murine *in vivo* studies confirmed the absence of teratogenic effects of CpG administered [430, 431].

Finally, glycoconjugated NPs carrying inside a well-defined immune enhancer can pave the way for the development of more effective glycoconjugates vaccines and overcome poor immunogenicity of some saccharide antigens.

3.4 Materials and Methods

3.4.1 Expression and purification of Qβ hairpin

The genes encoding for Qβ hp was synthesized as DNA strings by GeneArt (Thermo Fisher Scientific) optimizing the codon usage for expression in the *E. coli*. The gene encoding the Qβ hp coat protein was cloned into plasmid pET24b and purchased by GeneArt (Thermo Fisher Scientific). Protein was expressed in *E. coli* BL21(DE3) (New England Biolabs). First, a pre-culture in HTMC (Glycerol 15 g/L, Yeast Extract 30 g/L, MgSO4 X 7H2O 0.5g/L, K2HPO4 20 g/L, KH2PO4 5 g/L) medium supplemented with Kanamycin 50 mg/L from glycerol stock of BL21(DE3) pET24/ Qβ hp was incubated at 32 °C, 160 rpm for 16 h. The pre-culture was used to set up batch cultivation of protein in HTMC supplemented with Kanamycin 100 mg/L, under shaking at 25 °C, 160 rpm for 8 h, followed by induction with 1 mM IPTG and addition of 150 mg/mL MgCl2, 120 mg/mL CaCl2, 10 g/L glycerol, Kanamycin 50 mg/mL and incubation for 16 h at 25°C, 160 rpm.

Crude cell lysate obtained after sonication was purified via anion exchange chromatography using CaptoQ column (5 mLx2 Cytiva). The column was connected to a peristaltic pump of instrument ÄKTA pure (Cytiva) and equilibrated with buffer 30 mM TRIS pH 8. Crude cell lysate was applied on the column and purified protein was recovered in flow through while impurities remained attached to the column and eluted only after washes with buffer 30 mM TRIS, 1 M NaCl pH 8. A second purification of protein was performed using S500 Sephacryl 26/60 column (318 mL) connected to instrument ÄKTA pure (Cytiva) and equilibrated with buffer PBS 1x. Protein eluted in PBS 1x using flow rate 2.6 mL/min.

3.4.2 Removal of RNA from Qβ hairpin

Qβ hairpin was treated with 10 mM DTT for 15 minutes at room temperature (rt), then 0.7 M MgCl2 was added and left under stirring for 15 minutes at rt. The resulting mixture was centrifuged for 10 min at 4000 rpm at 4 degrees. The supernatant was diluted 1:25 in milliQ and injected in HiTrap SP FF 5 mL column (Cytiva) connected to a peristaltic pump of instrument ÄKTA pure (Cytiva) previously washed with distilled water and then equilibrated with buffer 20 mM NaPi pH 7. Qβ was eluted in monomeric form in buffer 20 mM NaPi, 500 mM NaCl pH 7 and analyzed in TSK4000PW (7.8 mmmx900 mm, Tosoh).

While the removal of ssRNA from Qβ(hp) via enzyme treatment was performed by incubation of NPs at 0.2 mg/mL with an RNase Cocktail (Invitrogen), mixture of two highly purified ribonucleases, RNase A (500 U⁄mL) and RNase T1 (20,000 U⁄mL), at 4:1 w/v VLPs/RNAses in buffer HBS 0.2x pH 7.4. After 3 days at 55 degrees, RNAses and nucleic acids were eliminated by serial centrifugal filtration (100 kDa) and extensive dialysis (100 kDa) over two weeks. The completely removal of ssRNA was assess via RiboGreen quantification and the intact VLP structure assess analysing the purified Qβ(Ø) in TSK4000PW (7.8 mmmx900 mm, Tosoh).

3.4.3 CpG A aggregation

Lyophilized CpG A (5'GGGGGGGGGGGACGATCGTCGGGGGGGGGG 3'- 9612 kDa, Metabion International AG) was dissolved at 2.4 mg/mL in UltraPure DNase/RNase-Free Distilled Water (Invitrogen), treated with 25 mM NaOH and then heated at 50 degrees. After 70 minutes at 50 degrees, the mixture was cooled in ice. The disaggregated CpG was analyzed in TSK6000PWXL (7.8 mm x 30 cm, 13 μm, Tosoh) at flow rate 0.5 mL/min using an Ultimate 3000 HPLC system (Thermo Fisher Scientific) equipped with a photodiode array detector and a multiple-wavelength fluorescence detector. To aggregate the CpG A, 25 mM HCl were added to neutralize the pH and 250 mM NaCl, then heated at 80 degrees. After 30 min at 80 degrees, the resulting mixture was cooled and stored in ice (it should be used within 3 h after the aggregation process). The aggregated CpG A was analyzed in TSK6000PWXL (7.8 mm x 30 cm, 13 μm, Tosoh).

The effective CpG A aggregation was also checked via dynamic light scattering.

3.4.4 Encapsulation of CpG in Qβ

Qβ monomer in 20 mM NaPi, 250 mM NaCl pH 7,2 at 0.74 mg/mL was treated with 10 mM DTT and 1 M urea for 30 min at room temperature (rt) under shaking, then CpG A was incubated with Qβ monomer at ratio 1:100 Qβ mol : CpG A mol for 1 h at rt and then the mixture was dialyzed over night at 4 degrees in dialysis tube with cut off 3.5-5 kDa (MINI Dialysis Unit Thermo Fisher Scientific Slide-A-Lyzer) against buffer 20 mM NaPi, 250 mM NaCl pH 7.2. Qβ reassembled in VLPs with entrapped CpG A was purified from CpG A in excess via dialysis over weekend in dialysis tubes with cut off 300 kDa against buffer 20 mM NaPi, 250 mM NaCl pH 7.2. After purification, the re-assembled Qβ(CpG/A) was analyzed in TSK6000PWXL (7.8 mm x 30 cm, 13 μm, Tosoh) to assess the correct assembly and the increased ratio 260/280 peak intensity ratio compared to Qβ monomer. CpG A content content in VLPs was quantified via RiboGreen Assay.

Qβ(Ø) VLPs was incubated with 100 nmol CpG B per mg of VLPs reaching a protein concentration of 0.6 mg/mL in PBS1x [270]. The mixture was incubated at 4 degrees overnight under shaking. After one night of incubation, CpG B in excess was removed via serial centrifugal filtration (100 kDa) finally analyzed in TSK4000PW (7.8 mmmx900 mm, Tosoh) in 100 mM NaPi, 100 mM Na2SO4 pH 7 at flow rate 0.5 mL/min to assess the increase of 260/280 peak intensity ratio compared to starting Qβ(Ø) VLPs. CpG B content in VLPs was quantified via RiboGreen Assay.

3.4.5 Conjugation of GBS PSII to Qβ

GBS polysaccharide II was oxidized targeting 20% of sialic acid residues [423]. Samples were stirred with 0.1 M sodium periodate in 10 mM sodium phosphate buffer in the dark, for 2 h at room temperature. The mixture was purified by liquid chromatography using G-25 desalting columns. The oxidized polysaccharide was dissolved in 100 mM sodium phosphate buffer at pH 7.2 and mixed to NPs at a final protein concentration of about 10 mg/mL. Sodium cyanoborohydride (1:1 w/w based on the amount of polysaccharide) was added to the solution. The reaction mixture was incubated at 37 °C for 3 days, quenched with sodium borohydride and purified by serial centrifugation filtration (100 kDa filter). The protein content was determined by BCA colorimetric

assay. Finally, the extent of saccharide conjugation was evaluated by HPAEC-PAD and SE-HPLC using a Sepax SRT-C 2000 column.

3.4.6 Preparation of CpG-SH and conjugation to GBS PSII- Qβ

The method used was developed by Chatzikleanthous *et al.* [422] for the conjugation of CpG B to GBS67 protein antigen.
An amount of 5 mg (0.762 μmol) of CpG B 1826 ([5'AmC6]TCCATGACGTTCCTGACGTT – completely phosphorothioated backbone - 6559 g/mol; Custom product Sigma Aldrich) were reacted with 10 equiv. of succinimidyl 3-(2-pyridyldithio)propionate (SPDP, Thermo Scientific) linker (2.38 mg 7.62 μmol) in buffer 9:1 DMSO: 100 mM NaPi pH 7 (230 μL).
The mixture reaction was left for 3 hours at rt under shaking then diluted up to 2 mL of H2O and purified by size exclusion chromatography on G-25 HiTrap Desalting column (10 mL, Cytiva) connected to a peristaltic pump of instrument ÄKTA pure (Cytiva) and eluted with H2O.
To release the free thiol groups, the purified CpG-SPDP (4 mg) were dissolved in 800 uL H2O and treated with large excess of 0.0005 M TCEP solution (20 uL) for 3 hours at rt shield by light. The reaction mixture was purified by G-25 HiTrap Desalting column (10 mL, Cytiva) and eluted with H2O ready to be conjugated.

GBS PSII- Qβ(Ø) at 12 mg/mL in PBS1x was used to set up the reaction with 1 equivalent of N-ε-malemidocaproyl-oxysuccinimide ester (EMCS, Thermo Scientific) linker dissolved in DMSO (final volume 9:1 PBS1x: DMSO) and left at RT for 3 hours shield by light under shaking, then purified by serial centrifugal filtration (100 kDa). GBS PSII- Qβ(Ø)-EMCS was incubated at 0.6 mg/mL with large excess of CpG-SH (1:7 w/w of Qβ:CpG) over night at rt and purified by serial centrifugal filtration (100 kDa) and analyzed via SE-HPLC using a Sepax SRT-C 2000 column. the quantity of CpG conjugated outside glycoconjugates VLPs was quantified by RiboGreen assay and via Dot-Blot to assess the correct conjugation on VLPs outside surface.

3.4.7 RNA profiling via RP-HPLC and CE analysis

30 μg of purified Qβ(hp) were lysed with 600 μL of Trizol at RT for 5 min and 600 μL of absolute ethanol were added to the solution. RNA was extracted by Pure link RNA Mini Kit according to the manufacturer's instructions.

RNA extracted from Qβ(hp), CpG A (1585 – Invivogen) and CpG B (1826-Invivogen) were diluted at 100 μg/mL in buffer 0.1 M TEAA and 5 μL were injected in DNAPac RP Column (2.1x50 mm) and eluted in a gradient of 36% to 69% of buffer 0.1 M TEAA + 25% Acetonitrile in buffer 0.1 M TEAA at flow rate 0.4 mL/min for 25 minutes of run using an Ultimate 3000 HPLC system (Thermo Scientific) equipped with a multiple-wavelength fluorescence detector.

1 μL of CpG B (1826-Invivogen) at 200 μg/mL before and after the incubation at 37 degrees for 3 days were also analyzed in Agilent 2100 Bioanalyzer using Agilent RNA 6000 Nano Kit following manufacturer's instructions for the preparation of the chip and loading of the samples.

3.4.8 ssRNA/ssDNA quantification via RiboGreen

Total RNA or CpG was quantified by Quant-iT RiboGreen RNA Reagent (Thermo Scientific) using rRNA as standard or CpG A or B (ODN 1826 and 1585; Invivogen). Qβ VLPs were denaturated by incubation with 8M urea for 30 min at 95 °C and diluted in TE buffer (10mM Tris-HCl, EDTA, pH 7.5). 100 µL of RiboGreen were added to 100 µL of sample. Fluorescence intensity (Excitation/Emission 485 nm/530 nm) was measured (Infinite 200, Tecan) and RNA total content was expressed as % RNA/Protein w/w.

3.4.9 Quantification of protein content by mBCA colorimetry assay

Protein concentration for each glycoconjugate nanoparticle produced was Protein concentration was determined by Pierce Micro BCA Protein Assay Kit (mBCA kit, Thermo Fisher Scientific) according to manufacturer's instructions and using the provided Pierce Bovine Serum Albumin (BSA, Thermo Fisher Scientific) as standard. Each sample was diluted in duplicate preparing a 5-points calibration curve using a BSA starting solution of 20 µg/mL. Then, the three reagents of mBCA kit are properly mixed following the manufacturer's instructions and added to the sample heated at 60 °C in bath of water for 1 hour. The samples are finally transferred to a plastic disposable cuvette and are read at the spectrophotometer at 562 nm (Evolution 260 Bio Spectrophotometer, Thermo Scientific, Thermo INSIGHT software). The final protein concentration (µg/mL) is quantified based on the BSA calibration curve.

3.4.10 Saccharide quantification via HPAEC-PAD

Saccharide quantification in the conjugates was performed by high-performance anion-exchange chromatography with pulsed amperometric detection (HPAEC-PAD). GBS PSII standard samples at five increasing concentrations ranging between 0.5 and 10 µg/mL, were prepared to build the calibration curve. Test samples were diluted targeting the calibration curve midpoint, while free saccharide samples were analyzed undiluted after separation by solid-phase extraction (SPE) cartridges. The reference and conjugate samples were prepared in 4M trifluoroacetic acid (Supelco), incubated at 100 °C for 3 h, dried under vacuum (SpeedVac Thermo), suspended in water, and filtered with 0.45 µm Phenex-NY (Phenomenex) filters. HPAEC-PAD analysis was performed with a Dionex ICS-6000 equipped with a CarboPac PA1 column (4 × 250 mm; Dionex) coupled with a PA1 guard to column (4 × 50 mm; Dionex). Samples were run at 1 mL/min, using an isocratic elution with 14mM NaOH, followed by a washing step with 500mM NaOH. The effluent was monitored using an electrochemical detector in the pulse amperometric mode, with a gold working electrode and an Ag/AgCl reference electrode. A quadruple-potential waveform for carbohydrates was applied. The resulting chromatographic data were processed using Chromeleon software 7.2 (Thermo Dionex), and sample concentrations were determined based on galactose content.

3.4.11 TEM

A volume of 5 μl of samples, diluted in PBS 1x at 20 ng/microliter, were loaded for 30 seconds onto a glow discharged copper 200 or 300-square mesh grids. Blotted the excess, the grid was negatively stained using NanoW for 30 seconds and let air dried. The samples were analyzed at UNISI using a Tecnai G2 spirit and the images were acquired using a Tvips TemCam-F216 (EM-Menu 4 software).

3.4.12 AF4-UV-dRI-MALS

The asymmetric flow field-flow fractionation (AF4) system (AF2000 – Postnova, Landsberg am Lech, Germany) consisted of an isocratic LC pump (PN1130, Postnova analytics, Salt Lake City, UT, USA), autosampler (PN5300 series, Postnova analytics), column oven (PN4020, Postnova analytics), MALS detector (PN3621, Postnova analytics), UV-Vis detector (SPD-20A prominence, Postnova analytics), and refractive index (RI) instrument (PN3150, Postnova analytics). Microchannel with a 350 μm spacer and a 10 kDa regenerated cellulose membrane was used for all separation. The AF4 method used: Focus step in which 10 μL of sample are injected in the separation channel at 0.20 mL/min and subjected to a cross flow at 1 mL/min and focus pump at 1.30 mL/min for 3 minutes. Elution step in which focus flow decreases to 0 mL/min and sample is able to elute along the channel for 50 minutes subjected to cross flow that descreases in 40 minutes to 0.1 mL/min in parabolic manner. PBS1x filtered 0.1 μm was used as mobile phase, 10 μL of sample injected. UV and dRI signals were integrated to calculate protein and RNA contribution in term of MW. For protein contribution were used an extinction factor of 0.427 [mL/(mg*cm)] calculated from Qβ sequence and dn/dc of 0.185; while for RNA contribution were used an extinction factor of 20 [mL/(mg*cm)] and dn/dc of 0.17. The parameters were provided by Postnova and literature [369-371].

3.4.13 DLS analyses

The effective CpG A aggregation and Qβ post RNAse treatment were analyzed via dynamic light scattering by measuring the time-dependent fluctuations in the intensity of scattered light that determine the diffusion coefficients of the particles converted into a size distribution expressed as hydrodynamic diameter (nm). Measurements were made at 25 °C using a Zetasizer Ultra (Malvern Panalytical Ltd., Malvern, UK) and all measurements were repeated tree times. The instrument settings were optimised automatically by means of the ZS XPLORER software (Malvern Panalytical Ltd., UK).

3.4.14 Dot-Blot

10 μg of glycoconjugate nanoparticles were adsorbed on nitrocellulose thanks to a vacuum pump and the Bio-Dot Micro filtration apparatus. Then, the nitrocellulose quenched with a buffer of tPBS with 3% BSA and left on gently agitation for 1.5 h. Then the buffer was removed, and the layer washed three times with tween PBS 1x (0.05% v/v of Tween 20). Then it was incubated for 1 h with diluted 1:200 primary monoclonal antibody (0.5 μg mAb3868 anti DNA single stranded) in tPBS 1x. After 1 h, the nitrocellulose is washed three times with tPBS pH 7.2 and the secondary antibody added diluted 1:1000 (Anti-Mouse IgG (whole molecule)- alkaline phosphatase antibody produced in goat, SIGMA, A2064). After 30 minutes, the nitrocellulose is washed three times with tPBS and three times with water and developed with the kit "Alkaline Phosphatase Conjugate Substrate Kit" (BIORAD) according to provided instruction by Biorad.

3.4.15 *In vivo* experiment

Animal treatments were performed in compliance with the Italian Italian legislation (Dig 26/2014), EU Directive 63/2010 and GSK Animal Welfare Policy and standards and approved by the institutional review board (Animal Ethical Committee) of GSK Vaccines Siena, Italy. Groups of 10 CD-1 female mice, kept in an AAALAC-accredited facility, were immunized intramuscularly (IM) with one single dose or two doses three weeks apart of GBS PSII glycoconjugates nanoparticles produced (0.5 μg of PSII/dose). Two immunizations were performed at day 1 and day 22 with PSII-CRM_{197} adjuvanted by aluminium hydroxide (2.0 mg/mL) used as controls. The sera were collected at day 42 and analyzed as single sera via Luminex and OPKA analyses as pooled sera.

3.4.16 Biotin-PSII Immunoassay (Luminex analysis)

The immune response to GBS PS conjugates was assessed by Luminex-based monoplex assay [432] using Biotin-PSII (1 μg/mL) conjugated to Radix High capacity (HC) Streptavidin magnetic beads ID 18. Eight steps of threefold dilutions of a standard serum (pool of sera from mice immunized with PSII-CRM_{197} used as reference) and samples were mixed with an equal volume of conjugated Biotin-PS beads (3000 beads/well) in 96-well Greiner (Millipore Corporation, Billerica, MA) and incubated for 60 min at RT in the dark on a plate shaker at 600 rpm. After incubation, the beads were washed three times with 200 μl PBS. Each well was then loaded with 50 μl of a 1/100 dilution of PE-secondary anti-mouse IgG (Jackson Immunoresearch, 115-116-072) and the plates were incubated for 60 min with continued shaking. After washing, beads were suspended in 100 μL of PBS before the analysis with Bioplex 200. Data were acquired in real time by Bioplex Manager Software 6.2 (Bio-Rad Laboratories, Hercules, CA). The median fluorescence intensity (MFI) was converted to RLU/ mL by interpolation to the corresponding 5-PL Standard curve (8 dilution points). IgG concentrations (RLU/mL) were determined from the mean of two sample dilutions for which MFI signals were in the linear range of the standard curve.

3.4.17 Opsonophagocytic killing assay (OPKA)

OPKA was conducted using differentiated HL-60 cells and the GBS strain DK21 (serotype II)65. OPK titers were expressed as the reciprocal serum dilution mediating 50% bacterial killing, estimated through piecewise linear interpolation of the dilution killing OPK data. A fluorescent OPKA was adapted from literature [433, 434] to increase the throughput capacity to 384-wells and to avoid CFU counting by introducing a fluorescent dye (Alamar Blue) that allow to measure the viability endpoint of bacteria through a plate reader. The fluorescent OPKA used the same assay components and titration method. The lower limit of detection was 1:30 dilution and the assay coefficient of variation was ~30% for both assay formats.

GENERAL CONCLUSIONS

Nanoparticles (NPs) represent a powerful platform for the development of more effective vaccines because they promote multiple antigen presentation as well as potent and early responses, thanks to B cell receptor clustering and increased uptake by Antigen Presenting cells and (APC) and T cell engagement. Furthermore, a lot of nanoparticles-based vaccines have been licensed so far (e.g. HPV, HBV, Malaria and HEV vaccines) representing one of the most successful achievements in the vaccine field.

Because of all these advantages we explored the use of protein nanoparticles as carriers for glycoconjugates vaccines to promote more potent immune responses against saccharide antigens.

For the design and development of effective NP glycoconjugates, multiple parameters must be considered beyond those critical for classical glycoconjugates, including size and shape of the NP carrier. Further, advanced analytical techniques are required to better explore all the peculiarities of this system. The ultimate goal is to guide the future design and selection of the best nanoparticles for the development of promising glycoconjugate candidates against the bacterial target mainly investigating: i) if the size and the shape may play a critical role in immunogenicity of saccharide antigens; ii) the set-up of advanced analytical technology to characterize complexity of nanoparticles and glycoconjugate NP; iii) take advantages of the possible co-delivery of immune enhancer to potential develop one dose glycoconjugate vaccine.

To investigate the effect of different size and shapes of carrier NPs, we decided to play with self-assembling NPs that could be manipulated *in vitro* and modelled as desired. The different NPs were conjugated to *Neisseria meningitidis* type W oligosaccharides as model antigen. We identified from literature two self-assembling proteins with equivalent MWs which spontaneously arrange into NPs at different shapes (ring-, rod- like and spherical particles) and sizes (from 9-10 nm to 60 nm) that allow to investigate the effects of different geometry and the impact of carrier size on antigen immunogenicity.

The obtained results highlighted the potential of self-assembling protein nanoparticles for glycoconjugates vaccine development and remarked the shape over size as a key factor for enhancing immune responses. Moreover, we presented the first example of a glycoconjugated *H. Pylori* ferritin as a carrier protein for efficient delivery of a bacterial saccharide antigen inducing a high bactericidal activity.

Further, a panel of complementary techniques was set up to characterize VLPs, NPs and glycoconjugate NPs in terms of size and MW, structural information, saccharide content and particles payload including SDS-PAGE, TEM, HPLC, DLS and AF4 coupled to MALS, UV-vis and dRI detectors.

An immune enhancer effect of *E.coli* RNA (TLR 7/8 agonist) naturally carried in glycoconjugate VLPs had been investigated by Carboni *et al.* [316] establishing the basis for the development of one single dose maternal vaccine against GBS disease. Here, we replaced *E.coli* RNA with CpG ODN, a TLR 9 agonist already known for its excellent adjuvant effect and safety profile. Moreover, we investigated the optimal CpG formulation by testing in mice GBS PSII-Qβ carrying CpG inside or conjugated outside or just co-formulated in a physical mixture. Our data

demonstrated that a single dose effect could be achieved when CpG was delivered within and protected by VLPs. We conclude that the designed multicomponent vaccine is a successful strategy for the development of single dose glycoconjugates vaccines that could improve responses to poorly immunogenic saccharide antigens.

Bibliography

1. WHO, W.H.O. *Child mortality and causes of death*. Available from: https://www.who.int/gho/child_health/mortality/mortality_under_five_text/en/ (2020).
2. Flemming, A., *The origins of vaccination*. 2020: Nature Portfolio.
3. Plotkin, S., *History of vaccination.* Proc Natl Acad Sci U S A, 2014. **111**(34): p. 12283-7.
4. Pollard, A.J. and E.M. Bijker, *A guide to vaccinology: from basic principles to new developments.* Nature Reviews Immunology, 2021. **21**(2): p. 83-100.
5. Glenny, A.T. and B.E. Hopkins, *Diphtheria Toxoid as an Immunising Agent.* Br J Exp Pathol, 1923. **4**(5): p. 283-8.
6. Ramon, G., *"Sur le pouvoir floculant et sur les proprietes immunisantes d'une toxin diphterique rendu anatoxique (anatosine)." CR Acad Sci Paris 177 (1923): 1338-1340*.
7. Thomas, F. and T.P. Magill, *Vaccination of Human Subjects with Virus of Human Influenza.* Proceedings of the Society for Experimental Biology and Medicine, 1936. **33**(4): p. 604-606.
8. *Jonas Salk and ALbert Bruce Sabin*. Science History Institute Museum & Library.
9. Finland, M. and W.D. Sutliff, *SPECIFIC ANTIBODY RESPONSE OF HUMAN SUBJECTS TO INTRACUTANEOUS INJECTION OF PNEUMOCOCCUS PRODUCTS.* J Exp Med, 1932. **55**(6): p. 853-65.
10. Macleod, C.M., et al., *PREVENTION OF PNEUMOCOCCAL PNEUMONIA BY IMMUNIZATION WITH SPECIFIC CAPSULAR POLYSACCHARIDES.* J Exp Med, 1945. **82**(6): p. 445-65.
11. Peltola, H., et al., *Clinical efficacy of meningococcus group A capsular polysaccharide vaccine in children three months to five years of age.* N Engl J Med, 1977. **297**(13): p. 686-91.
12. Mäkelä, P.H., et al., *Polysaccharide vaccines of group A Neisseria meningtitidis and Haemophilus influenzae type b: a field trial in Finland.* J Infect Dis, 1977. **136 Suppl**: p. S43-50.
13. Artenstein, M.S., et al., *Prevention of meningococcal disease by group C polysaccharide vaccine.* N Engl J Med, 1970. **282**(8): p. 417-20.
14. Gold, R. and M.S. Artenstein, *Meningococcal infections. 2. Field trial of group C meningococcal polysaccharide vaccine in 1969-70.* Bull World Health Organ, 1971. **45**(3): p. 279-82.
15. Peltola, H., et al., *Haemophilus influenzae type b capsular polysaccharide vaccine in children: a double-blind field study of 100,000 vaccinees 3 months to 5 years of age in Finland.* Pediatrics, 1977. **60**(5): p. 730-7.
16. Schneerson, R., et al., *Preparation, characterization, and immunogenicity of Haemophilus influenzae type b polysaccharide-protein conjugates.* J Exp Med, 1980. **152**(2): p. 361-76.
17. Eskola, J., et al., *Efficacy of Haemophilus influenzae type b polysaccharide-diphtheria toxoid conjugate vaccine in infancy.* N Engl J Med, 1987. **317**(12): p. 717-22.
18. Black, S.B., et al., *Efficacy in infancy of oligosaccharide conjugate Haemophilus influenzae type b (HbOC) vaccine in a United States population of 61,080 children. The Northern California Kaiser Permanente Vaccine Study Center Pediatrics Group.* Pediatr Infect Dis J, 1991. **10**(2): p. 97-104.
19. Anderson, P.W., et al., *Vaccines consisting of periodate-cleaved oligosaccharides from the capsule of Haemophilus influenzae type b coupled to a protein carrier: structural and temporal requirements for priming in the human infant.* J Immunol, 1986. **137**(4): p. 1181-6.
20. Costantino, P., et al., *Development and phase 1 clinical testing of a conjugate vaccine against meningococcus A and C.* Vaccine, 1992. **10**(10): p. 691-8.
21. Eby, R., *Pneumococcal conjugate vaccines.* Pharm Biotechnol, 1995. **6**: p. 695-718.
22. Lakshman, R. and A. Finn, *Meningococcal serogroup C conjugate vaccine.* Expert Opin Biol Ther, 2002. **2**(1): p. 87-96.
23. Snape, M.D., et al., *Immunogenicity of a tetravalent meningococcal glycoconjugate vaccine in infants: a randomized controlled trial.* Jama, 2008. **299**(2): p. 173-84.
24. Black, S., et al., *Immunogenicity and tolerability of a quadrivalent meningococcal glycoconjugate vaccine in children 2-10 years of age.* Vaccine, 2010. **28**(3): p. 657-63.
25. Nooraei, S., et al., *Virus-like particles: preparation, immunogenicity and their roles as nanovaccines and drug nanocarriers.* J Nanobiotechnology, 2021. **19**(1): p. 59.

26. Romano, L. and A.R. Zanetti, *Hepatitis B Vaccination: A Historical Overview with a Focus on the Italian Achievements.* Viruses, 2022. **14**(7).
27. Pattyn, J., et al., *Hepatitis B Vaccines.* J Infect Dis, 2021. **224**(12 Suppl 2): p. S343-s351.
28. Mohsen, M.O., et al., *Major findings and recent advances in virus–like particle (VLP)-based vaccines.* Seminars in Immunology, 2017. **34**: p. 123-132.
29. Zuckerman, A.J., *The development of novel hepatitis B vaccines.* Bull World Health Organ, 1987. **65**(3): p. 265-75.
30. Deinhardt, F. and A.J. Zuckerman, *Immunization against hepatitis B: report on a WHO meeting on viral hepatitis in Europe.* J Med Virol, 1985. **17**(3): p. 209-17.
31. Cheng, L., Y. Wang, and J. Du, *Human Papillomavirus Vaccines: An Updated Review.* Vaccines (Basel), 2020. **8**(3).
32. Mazalovska, M. and J.C. Kouokam, *Progress in the Production of Virus-Like Particles for Vaccination against Hepatitis E Virus.* Viruses, 2020. **12**(8).
33. Mora, M., et al., *Reverse vaccinology.* Drug Discov Today, 2003. **8**(10): p. 459-64.
34. Pizza, M., et al., *Identification of vaccine candidates against serogroup B meningococcus by whole-genome sequencing.* Science, 2000. **287**(5459): p. 1816-20.
35. Zhang, C., et al., *Advances in mRNA Vaccines for Infectious Diseases.* Front Immunol, 2019. **10**: p. 594.
36. Ross, J. and T.D. Sullivan, *Half-lives of beta and gamma globin messenger RNAs and of protein synthetic capacity in cultured human reticulocytes.* Blood, 1985. **66**(5): p. 1149-54.
37. Gallie, D.R., *The cap and poly(A) tail function synergistically to regulate mRNA translational efficiency.* Genes Dev, 1991. **5**(11): p. 2108-16.
38. Gustafsson, C., S. Govindarajan, and J. Minshull, *Codon bias and heterologous protein expression.* Trends Biotechnol, 2004. **22**(7): p. 346-53.
39. Pardi, N., et al., *mRNA vaccines - a new era in vaccinology.* Nat Rev Drug Discov, 2018. **17**(4): p. 261-279.
40. Karikó, K., et al., *Incorporation of pseudouridine into mRNA yields superior nonimmunogenic vector with increased translational capacity and biological stability.* Mol Ther, 2008. **16**(11): p. 1833-40.
41. Karikó, K., et al., *Suppression of RNA recognition by Toll-like receptors: the impact of nucleoside modification and the evolutionary origin of RNA.* Immunity, 2005. **23**(2): p. 165-75.
42. Hood, J.L., *Post isolation modification of exosomes for nanomedicine applications.* Nanomedicine (Lond), 2016. **11**(13): p. 1745-56.
43. Brisse, M., et al., *Emerging Concepts and Technologies in Vaccine Development.* Front Immunol, 2020. **11**: p. 583077.
44. van den Boorn, J.G. and G. Hartmann, *Turning tumors into vaccines: co-opting the innate immune system.* Immunity, 2013. **39**(1): p. 27-37.
45. Elion, D.L. and R.S. Cook, *Harnessing RIG-I and intrinsic immunity in the tumor microenvironment for therapeutic cancer treatment.* Oncotarget, 2018. **9**(48): p. 29007-29017.
46. Rappuoli, R., *Timeline: Vaccines.* Cell, 2020. **183**(2): p. 552.
47. Stefanetti, G., et al., *Immunobiology of Carbohydrates: Implications for Novel Vaccine and Adjuvant Design Against Infectious Diseases.* Front Cell Infect Microbiol, 2022. **11**.
48. Luong, P. and D.H. Dube, *Dismantling the bacterial glycocalyx: Chemical tools to probe, perturb, and image bacterial glycans.* Bioorg Med Chem, 2021. **42**: p. 116268.
49. Jha, V. and E.N. Janoff, *Complementary Role of CD4+ T Cells in Response to Pneumococcal Polysaccharide Vaccines in Humans.* Vaccines (Basel), 2019. **7**(1).
50. Vos, Q., et al., *B-cell activation by T-cell-independent type 2 antigens as an integral part of the humoral immune response to pathogenic microorganisms.* Immunol Rev, 2000. **176**: p. 154-70.
51. Craxton, A., et al., *Macrophage- and dendritic cell--dependent regulation of human B-cell proliferation requires the TNF family ligand BAFF.* Blood, 2003. **101**(11): p. 4464-71.
52. Khatun, F., I. Toth, and R.J. Stephenson, *Immunology of carbohydrate-based vaccines.* Adv Drug Deliv Rev, 2020. **165-166**: p. 117-126.
53. Snapper, C.M. and J.J. Mond, *A model for induction of T cell-independent humoral immunity in response to polysaccharide antigens.* J Immunol, 1996. **157 6**: p. 2229-33.
54. Pace, D., *Glycoconjugate vaccines.* Expert Opin Biol Ther, 2013. **13**(1): p. 11-33.

55. Rappuoli, R., *Glycoconjugate vaccines: Principles and mechanisms.* Sci Transl Med, 2018. **10**(456).
56. Pishesha, N., T.J. Harmand, and H.L. Ploegh, *A guide to antigen processing and presentation.* Nat Rev Immunol, 2022. **22**(12): p. 751-764.
57. Richmond, P., et al., *Meningococcal C polysaccharide vaccine induces immunologic hyporesponsiveness in adults that is overcome by meningococcal C conjugate vaccine.* J Infect Dis, 2000. **181**(2): p. 761-4.
58. Brynjolfsson, S.F., et al., *Hyporesponsiveness Following Booster Immunization With Bacterial Polysaccharides Is Caused by Apoptosis of Memory B Cells.* J Infect Dis, 2011. **205**(3): p. 422-430.
59. Bjarnarson, S.P., et al., *Pneumococcal polysaccharide abrogates conjugate-induced germinal center reaction and depletes antibody secreting cell pool, causing hyporesponsiveness.* PLoS One, 2013. **8**(9): p. e72588.
60. Zandvoort, A. and W. Timens, *The dual function of the splenic marginal zone: essential for initiation of anti-TI-2 responses but also vital in the general first-line defense against blood-borne antigens.* Clin Exp Immunol, 2002. **130**(1): p. 4-11.
61. Siegrist, C.A. and R. Aspinall, *B-cell responses to vaccination at the extremes of age.* Nat Rev Immunol, 2009. **9**(3): p. 185-94.
62. Sun, L., et al., *Carbohydrates as T-cell antigens with implications in health and disease.* Glycobiology, 2016. **26**(10): p. 1029-1040.
63. Avci, F.Y., et al., *A mechanism for glycoconjugate vaccine activation of the adaptive immune system and its implications for vaccine design.* Nat Med, 2011. **17**(12): p. 1602-9.
64. Koj, S., C. Lugowski, and T. Niedziela, *In-cell depolymerization of polysaccharide antigens. Exploring the processing pathways of glycans and why some glycoconjugate vaccines are less effective than expected: A review.* Carbohydr Polym, 2023. **315**: p. 120969.
65. Micoli, F., G. Stefanetti, and C.A. MacLennan, *Exploring the variables influencing the immune response of traditional and innovative glycoconjugate vaccines.* Front Mol Biosci, 2023. **10**.
66. Middleton, D.R., et al., *T Cell-Mediated Humoral Immune Responses to Type 3 Capsular Polysaccharide of Streptococcus pneumoniae.* J Immunol, 2017. **199**(2): p. 598-603.
67. Sun, X., et al., *Polysaccharide structure dictates mechanism of adaptive immune response to glycoconjugate vaccines.* Proc Natl Acad Sci USA, 2019. **116**(1): p. 193-198.
68. Agency, U.H.S., *Haemophilus influenzae type b (Hib)*, in *the Green Book*. 2013, GOV.UK.
69. Murphy, T.V., et al., *Declining incidence of Haemophilus influenzae type b disease since introduction of vaccination.* Jama, 1993. **269**(2): p. 246-8.
70. Smith, D.H., et al., *Responses of children immunized with the capsular polysaccharide of Hemophilus influenzae, type b.* Pediatrics, 1973. **52**(5): p. 637-44.
71. Miller, E., D. Salisbury, and M. Ramsay, *Planning, registration, and implementation of an immunisation campaign against meningococcal serogroup C disease in the UK: a success story.* Vaccine, 2001. **20 Suppl 1**: p. S58-67.
72. Agency, U.H.S., *Meningococcal*. Vol. Chapter 22. 2022, The Green Book: GOV.UK.
73. Trotter, C.L., et al., *Epidemiology of invasive pneumococcal disease in the pre-conjugate vaccine era: England and Wales, 1996-2006.* J Infect, 2010. **60**(3): p. 200-8.
74. Waight, P.A., et al., *Effect of the 13-valent pneumococcal conjugate vaccine on invasive pneumococcal disease in England and Wales 4 years after its introduction: an observational cohort study.* Lancet Infect Dis, 2015. **15**(5): p. 535-43.
75. Ryan Gierke, M., et al., *Manual for the Surveillance of Vaccine-Preventable Diseases*. Center for Disease Control and Prevention (CDC).
76. Micoli, F., P. Costantino, and R. Adamo, *Potential targets for next generation antimicrobial glycoconjugate vaccines.* FEMS Microbiol Rev, 2018. **42**(3): p. 388-423.
77. Romano, M.R., F. Berti, and R. Rappuoli, *Classical- and bioconjugate vaccines: comparison of the structural properties and immunological response.* Curr Opin Immunol, 2022. **78**: p. 102235.
78. Del Bino, L., et al., *Synthetic Glycans to Improve Current Glycoconjugate Vaccines and Fight Antimicrobial Resistance.* Chem Rev, 2022. **122**(20): p. 15672-15716.
79. Micoli, F., et al., *Glycoconjugate vaccines: current approaches towards faster vaccine design.* Expert Rev Vaccines, 2019. **18**(9): p. 881-895.

80. Verez-Bencomo, V., et al., *A synthetic conjugate polysaccharide vaccine against Haemophilus influenzae type b.* Science, 2004. **305**(5683): p. 522-5.
81. Cohen, D., et al., *Safety and immunogenicity of a synthetic carbohydrate conjugate vaccine against Shigella flexneri 2a in healthy adult volunteers: a phase 1, dose-escalating, single-blind, randomised, placebo-controlled study.* Lancet Infect Dis, 2021. **21**(4): p. 546-558.
82. Seeberger, P.H., *Discovery of Semi- and Fully-Synthetic Carbohydrate Vaccines Against Bacterial Infections Using a Medicinal Chemistry Approach.* Chem Rev, 2021. **121**(7): p. 3598-3626.
83. Fiebig, T., et al., *Molecular cloning and functional characterization of components of the capsule biosynthesis complex of Neisseria meningitidis serogroup A: toward in vitro vaccine production.* J Biol Chem, 2014. **289**(28): p. 19395-19407.
84. Fiebig, T., et al., *An efficient cell free enzyme-based total synthesis of a meningococcal vaccine candidate.* NPJ Vaccines, 2016. **1**(1): p. 16017.
85. Oldrini, D., et al., *Combined Chemical Synthesis and Tailored Enzymatic Elongation Provide Fully Synthetic and Conjugation-Ready Neisseria meningitidis Serogroup X Vaccine Antigens.* ACS Chem Biol, 2018. **13**(4): p. 984-994.
86. Micoli, F., R. Adamo, and P. Costantino, *Protein Carriers for Glycoconjugate Vaccines: History, Selection Criteria, Characterization and New Trends.* Molecules, 2018. **23**(6).
87. Donnelly, J.J., R.R. Deck, and M.A. Liu, *Immunogenicity of a Haemophilus influenzae polysaccharide-Neisseria meningitidis outer membrane protein complex conjugate vaccine.* J Immunol, 1990. **145**(9): p. 3071-9.
88. Kilpi, T., et al., *Protective efficacy of a second pneumococcal conjugate vaccine against pneumococcal acute otitis media in infants and children: randomized, controlled trial of a 7-valent pneumococcal polysaccharide-meningococcal outer membrane protein complex conjugate vaccine in 1666 children.* Clin Infect Dis, 2003. **37**(9): p. 1155-64.
89. Forsgren, A., K. Riesbeck, and H. Janson, *Protein D of Haemophilus influenzae: a protective nontypeable H. influenzae antigen and a carrier for pneumococcal conjugate vaccines.* Clin Infect Dis, 2008. **46**(5): p. 726-31.
90. Prymula, R., et al., *Pneumococcal capsular polysaccharides conjugated to protein D for prevention of acute otitis media caused by both Streptococcus pneumoniae and non-typable Haemophilus influenzae: a randomised double-blind efficacy study.* Lancet, 2006. **367**(9512): p. 740-8.
91. Giannini, G., R. Rappuoli, and G. Ratti, *The amino-acid sequence of two non-toxic mutants of diphtheria toxin: CRM45 and CRM197.* Nucleic Acids Res, 1984. **12**(10): p. 4063-9.
92. Malito, E., et al., *Structural basis for lack of toxicity of the diphtheria toxin mutant CRM197.* Proc Natl Acad Sci U S A, 2012. **109**(14): p. 5229-34.
93. Bröker, M., et al., *Biochemical and biological characteristics of cross-reacting material 197 CRM197, a non-toxic mutant of diphtheria toxin: use as a conjugation protein in vaccines and other potential clinical applications.* Biologicals, 2011. **39**(4): p. 195-204.
94. Shinefield, H.R., *Overview of the development and current use of CRM(197) conjugate vaccines for pediatric use.* Vaccine, 2010. **28**(27): p. 4335-9.
95. Cohen, D., et al., *Double-blind vaccine-controlled randomised efficacy trial of an investigational Shigella sonnei conjugate vaccine in young adults.* Lancet, 1997. **349**(9046): p. 155-9.
96. Fattom, A.I., et al., *Development of StaphVAX, a polysaccharide conjugate vaccine against S. aureus infection: from the lab bench to phase III clinical trials.* Vaccine, 2004. **22**(7): p. 880-7.
97. Kossaczka, Z., et al., *Safety and immunogenicity of Vi conjugate vaccines for typhoid fever in adults, teenagers, and 2- to 4-year-old children in Vietnam.* Infect Immun, 1999. **67**(11): p. 5806-10.
98. Szu, S.C., et al., *Vi capsular polysaccharide-protein conjugates for prevention of typhoid fever. Preparation, characterization, and immunogenicity in laboratory animals.* J Exp Med, 1987. **166**(5): p. 1510-24.
99. López-Sagaseta, J., et al., *Self-assembling protein nanoparticles in the design of vaccines.* Comput Struct Biotechnol J, 2016. **14**: p. 58-68.
100. Berti, F. and R. Adamo, *Antimicrobial glycoconjugate vaccines: an overview of classic and modern approaches for protein modification.* Chem Soc Rev, 2018. **47**(24): p. 9015-9025.

101. Kapoor, N., et al., *Malaria Derived Glycosylphosphatidylinositol Anchor Enhances Anti-Pfs25 Functional Antibodies That Block Malaria Transmission.* Biochem, 2018. **57**(5): p. 516-519.
102. Kapoor, N., et al., *Non-Native Amino Acid Click Chemistry-Based Technology for Site-Specific Polysaccharide Conjugation to a Bacterial Protein Serving as Both Carrier and Vaccine Antigen.* ACS Omega, 2022. **7**(28): p. 24111-24120.
103. Fairman, J., et al., *Non-clinical immunological comparison of a Next-Generation 24-valent pneumococcal conjugate vaccine (VAX-24) using site-specific carrier protein conjugation to the current standard of care (PCV13 and PPV23).* Vaccine, 2021. **39**(23): p. 3197-3206.
104. Dow, J.M., et al., *Improving protein glycan coupling technology (PGCT) for glycoconjugate vaccine production.* Expert Rev Vaccines, 2020. **19**(6): p. 507-527.
105. Wacker, M., et al., *N-linked glycosylation in Campylobacter jejuni and its functional transfer into E. coli.* Science, 2002. **298**(5599): p. 1790-3.
106. Kay, E., J. Cuccui, and B.W. Wren, *Recent advances in the production of recombinant glycoconjugate vaccines.* NPJ Vaccines, 2019. **4**(1): p. 16.
107. Kowarik, M., et al., *Definition of the bacterial N-glycosylation site consensus sequence.* EMBO J, 2006. **25**(9): p. 1957-66.
108. Kowarik, M., et al., *The development and characterization of an E. coli O25B bioconjugate vaccine.* Glycoconj J, 2021. **38**(4): p. 421-435.
109. Herbert, J.A., et al., *Production and efficacy of a low-cost recombinant pneumococcal protein polysaccharide conjugate vaccine.* Vaccine, 2018. **36**(26): p. 3809-3819.
110. Harding, C.M. and M.F. Feldman, *Glycoengineering bioconjugate vaccines, therapeutics, and diagnostics in E. coli.* Glycobiology, 2019. **29**(7): p. 519-529.
111. Riddle, M.S., et al., *Safety and Immunogenicity of a Candidate Bioconjugate Vaccine against Shigella flexneri 2a Administered to Healthy Adults: a Single-Blind, Randomized Phase I Study.* Clin Vaccine Immunol, 2016. **23**(12): p. 908-917.
112. Talaat, K.R., et al., *Human challenge study with a Shigella bioconjugate vaccine: Analyses of clinical efficacy and correlate of protection.* eBioMedicine, 2021. **66**.
113. Saade, E., et al., *Characterization of Escherichia coli isolates potentially covered by ExPEC4V and ExPEC10V, that were collected from post-transrectal ultrasound-guided prostate needle biopsy invasive urinary tract and bloodstream infections.* Vaccine, 2020. **38**(33): p. 5100-5104.
114. Avci, F.Y. and D.L. Kasper, *How bacterial carbohydrates influence the adaptive immune system.* Annu Rev Immunol, 2010. **28**: p. 107-30.
115. Buonsanti, C., et al., *Novel adjuvant Alum-TLR7 significantly potentiates immune response to glycoconjugate vaccines.* Sci Rep, 2016. **6**: p. 29063.
116. Herva, E., et al., *The effect of polyvalent pneumococcal polysaccharide vaccine on nasopharyngeal and nasal carriage of Streptococcus pneumoniae.* Scand J Infect Dis, 1980. **12**(2): p. 97-100.
117. Geno, K.A., et al., *Pneumococcal Capsules and Their Types: Past, Present, and Future.* Clin Microbiol Rev, 2015. **28**(3): p. 871-99.
118. Ji, X., et al., *Capsule switching of Neisseria meningitidis sequence type 7 serogroup A to serogroup X.* J Infect, 2017. **75**(6): p. 521-531.
119. Micoli, F., et al., *Strengths and weaknesses of pneumococcal conjugate vaccines.* Glycoconj J, 2023. **40**(2): p. 135-148.
120. Stacey, H.L., et al., *Safety and immunogenicity of 15-valent pneumococcal conjugate vaccine (PCV-15) compared to PCV-13 in healthy older adults.* Hum Vaccin Immunother, 2019. **15**(3): p. 530-539.
121. Hurley, D., et al., *Safety, Tolerability, and Immunogenicity of a 20-Valent Pneumococcal Conjugate Vaccine (PCV20) in Adults 60 to 64 Years of Age.* Clin Infect Dis, 2021. **73**(7): p. e1489-e1497.
122. Bröker, M., et al., *Polysaccharide conjugate vaccine protein carriers as a "neglected valency" - Potential and limitations.* Vaccine, 2017. **35**(25): p. 3286-3294.
123. Dagan, R., et al., *Reduced response to multiple vaccines sharing common protein epitopes that are administered simultaneously to infants.* Infect Immun, 1998. **66**(5): p. 2093-8.
124. Barington, T., et al., *Influence of prevaccination immunity on the human B-lymphocyte response to a Haemophilus influenzae type b conjugate vaccine.* Infect Immun, 1991. **59**(3): p. 1057-64.

125. Costantino, P., R. Rappuoli, and F. Berti, *The design of semi-synthetic and synthetic glycoconjugate vaccines.* Expert Opin Drug Discov, 2011. **6**(10): p. 1045-66.
126. Richichi, B., et al., *2.23 - Conjugation Techniques and Linker Strategies for Carbohydrate-Based Vaccines*, in *Comprehensive Glycoscience (Second Edition)*, J.J. Barchi, Editor. 2021, Elsevier: Oxford. p. 676-705.
127. Stefanetti, G., et al., *Sugar-Protein Connectivity Impacts on the Immunogenicity of Site-Selective Salmonella O-Antigen Glycoconjugate Vaccines.* Angew Chem Int Ed Engl, 2015. **54**(45): p. 13198-203.
128. Khatun, F., R.J. Stephenson, and I. Toth, *An Overview of Structural Features of Antibacterial Glycoconjugate Vaccines That Influence Their Immunogenicity.* Chemistry, 2017. **23**(18): p. 4233-4254.
129. Simon, A.K., G.A. Hollander, and A. McMichael, *Evolution of the immune system in humans from infancy to old age.* Proc Biol Sci, 2015. **282**(1821): p. 20143085.
130. Gustafson, C.E., et al., *Influence of immune aging on vaccine responses.* J Allergy Clin Immunol, 2020. **145**(5): p. 1309-1321.
131. Crooke, S.N., et al., *Immunosenescence and human vaccine immune responses.* Immun Ageing, 2019. **16**: p. 25.
132. Sakala, I.G., K.M. Eichinger, and N. Petrovsky, *Neonatal vaccine effectiveness and the role of adjuvants.* Expert Rev Clin Immunol, 2019. **15**(8): p. 869-878.
133. Hadjipanayis, A., *Compliance with vaccination schedules.* Hum Vaccin Immunother, 2019. **15**(4): p. 1003-1004.
134. Kurosky, S.K., K.L. Davis, and G. Krishnarajah, *Completion and compliance of childhood vaccinations in the United States.* Vaccine, 2016. **34**(3): p. 387-94.
135. Prevention, C.f.D.C.a., *Recommended immunization schedules for persons aged 0–18 years — United States.* 2011, *Morb. Mortal. Wkly Rep* **60** (5), 1–4.
136. Etti, M., et al., *Maternal vaccination: a review of current evidence and recommendations.* Am J Obstet Gynecol, 2022. **226**(4): p. 459-474.
137. Russell, N.J., et al., *Risk of Early-Onset Neonatal Group B Streptococcal Disease With Maternal Colonization Worldwide: Systematic Review and Meta-analyses.* Clin Infect Dis, 2017. **65**(suppl_2): p. S152-s159.
138. Lawn, J.E., et al., *Group B Streptococcal Disease Worldwide for Pregnant Women, Stillbirths, and Children: Why, What, and How to Undertake Estimates?* Clin Infect Dis, 2017. **65**(suppl_2): p. S89-s99.
139. Madrid, L., et al., *Infant Group B Streptococcal Disease Incidence and Serotypes Worldwide: Systematic Review and Meta-analyses.* Clin Infect Dis, 2017. **65**(suppl_2): p. S160-s172.
140. Schrag, S.J. and J.R. Verani, *Intrapartum antibiotic prophylaxis for the prevention of perinatal group B streptococcal disease: experience in the United States and implications for a potential group B streptococcal vaccine.* Vaccine, 2013. **31 Suppl 4**: p. D20-6.
141. Paoletti, L.C., et al., *Neonatal mouse protection against infection with multiple group B streptococcal (GBS) serotypes by maternal immunization with a tetravalent GBS polysaccharide-tetanus toxoid conjugate vaccine.* Infect Immun, 1994. **62**(8): p. 3236-43.
142. Baker, C.J. and D.L. Kasper, *Correlation of maternal antibody deficiency with susceptibility to neonatal group B streptococcal infection.* N Engl J Med, 1976. **294**(14): p. 753-6.
143. Baker, C.J. and M.S. Edwards, *Group B streptococcal conjugate vaccines.* Arch Dis Child, 2003. **88**(5): p. 375-8.
144. Fabbrini, M., et al., *Functional activity of maternal and cord antibodies elicited by an investigational group B Streptococcus trivalent glycoconjugate vaccine in pregnant women.* J Infect, 2018. **76**(5): p. 449-456.
145. Paoletti, L.C., et al., *Effects of alum adjuvant or a booster dose on immunogenicity during clinical trials of group B streptococcal type III conjugate vaccines.* Infect Immun, 2001. **69**(11): p. 6696-701.
146. Madhi, S.A., et al., *Safety and immunogenicity of an investigational maternal trivalent group B streptococcus vaccine in healthy women and their infants: a randomised phase 1b/2 trial.* Lancet Infect Dis, 2016. **16**(8): p. 923-34.

147. Madhi, S.A., et al., *Antibody Kinetics and Response to Routine Vaccinations in Infants Born to Women Who Received an Investigational Trivalent Group B Streptococcus Polysaccharide CRM197-Conjugate Vaccine During Pregnancy.* Clin Infect Dis, 2017. **65**(11): p. 1897-1904.
148. Beran, J., et al., *Safety and immunogenicity of fully liquid and lyophilized formulations of an investigational trivalent group B streptococcus vaccine in healthy non-pregnant women: Results from a randomized comparative phase II trial.* Vaccine, 2020. **38**(16): p. 3227-3234.
149. Absalon, J., et al., *Safety and immunogenicity of a novel hexavalent group B streptococcus conjugate vaccine in healthy, non-pregnant adults: a phase 1/2, randomised, placebo-controlled, observer-blinded, dose-escalation trial.* Lancet Infect Dis, 2021. **21**(2): p. 263-274.
150. Leroux-Roels, G., et al., *A randomized, observer-blind Phase Ib study to identify formulations and vaccine schedules of a trivalent Group B Streptococcus vaccine for use in non-pregnant and pregnant women.* Vaccine, 2016. **34**(15): p. 1786-91.
151. Leroux-Roels, G., et al., *Safety and Immunogenicity of a Second Dose of an Investigational Maternal Trivalent Group B Streptococcus Vaccine in Nonpregnant Women 4-6 Years After a First Dose: Results From a Phase 2 Trial.* Clin Infect Dis, 2020. **70**(12): p. 2570-2579.
152. van Werkhoven, C.H., et al., *The Impact of Age on the Efficacy of 13-valent Pneumococcal Conjugate Vaccine in Elderly.* Clin Infect Dis, 2015. **61**(12): p. 1835-8.
153. O'Hagan, D.T., et al., *MF59 adjuvant: the best insurance against influenza strain diversity.* Expert Rev Vaccines, 2011. **10**(4): p. 447-62.
154. Coleman, B.L., et al., *Effectiveness of the MF59-adjuvanted trivalent or quadrivalent seasonal influenza vaccine among adults 65 years of age or older, a systematic review and meta-analysis.* Influenza Other Respir Viruses, 2021. **15**(6): p. 813-823.
155. Lal, H., et al., *Efficacy of an adjuvanted herpes zoster subunit vaccine in older adults.* N Engl J Med, 2015. **372**(22): p. 2087-96.
156. Rappuoli, R., et al., *Vaccines for the twenty-first century society*, in *Nat Rev Immunol*. 2011: England. p. 865-72.
157. Crum-Cianflone, N.F. and M.R. Wallace, *Vaccination in HIV-infected adults.* AIDS Patient Care STDS, 2014. **28**(8): p. 397-410.
158. Nomah, D.K., et al., *Comparative Analysis of Primary and Monovalent Booster SARS-CoV-2 Vaccination Coverage in Adults with and without HIV in Catalonia, Spain.* Vaccines (Basel), 2023. **12**(1).
159. Bernadac, A., et al., *Escherichia coli tol-pal mutants form outer membrane vesicles.* J Bacteriol, 1998. **180**(18): p. 4872-8.
160. Turner, L., et al., *Increased Outer Membrane Vesicle Formation in a Helicobacter pylori tolB Mutant.* Helicobacter, 2015. **20**(4): p. 269-83.
161. Mancini, F., et al., *GMMA-Based Vaccines: The Known and The Unknown.* Front Immunol, 2021. **12**: p. 715393.
162. Micoli, F., et al., *Antibodies Elicited by the Shigella sonnei GMMA Vaccine in Adults Trigger Complement-Mediated Serum Bactericidal Activity: Results From a Phase 1 Dose Escalation Trial Followed by a Booster Extension.* Front Immunol, 2021. **12**: p. 671325.
163. Di Benedetto, R., et al., *Novel Simple Conjugation Chemistries for Decoration of GMMA with Heterologous Antigens.* Int J Mol Sci, 2021. **22**(19).
164. Palmieri, E., et al., *GMMA as an Alternative Carrier for a Glycoconjugate Vaccine against Group A Streptococcus.* Vaccines (Basel), 2022. **10**(7).
165. Gasperini, G., et al., *Salmonella Paratyphi A Outer Membrane Vesicles Displaying Vi Polysaccharide as a Multivalent Vaccine against Enteric Fever.* Infect Immun, 2021. **89**(4).
166. Micoli, F., et al., *Generalized Modules for Membrane Antigens as Carrier for Polysaccharides: Impact of Sugar Length, Density, and Attachment Site on the Immune Response Elicited in Animal Models.* Front Immunol, 2021. **12**: p. 719315.
167. Raso, M.M., et al., *GMMA and Glycoconjugate Approaches Compared in Mice for the Development of a Vaccine against Shigella flexneri Serotype 6.* Vaccines (Basel), 2020. **8**(2).
168. Valguarnera, E. and M.F. Feldman, *Glycoengineered Outer Membrane Vesicles as a Platform for Vaccine Development.* Methods Enzymol, 2017. **597**: p. 285-310.

169. Gnopo, Y.M.D., et al., *Designer outer membrane vesicles as immunomodulatory systems - Reprogramming bacteria for vaccine delivery.* Adv Drug Deliv Rev, 2017. **114**: p. 132-142.
170. Chen, L., et al., *Outer membrane vesicles displaying engineered glycotopes elicit protective antibodies.* Proc Natl Acad Sci USA, 2016. **113**(26): p. E3609-18.
171. Price, N.L., et al., *Glycoengineered Outer Membrane Vesicles: A Novel Platform for Bacterial Vaccines.* Sci Rep, 2016. **6**(1): p. 24931.
172. Stevenson, T.C., et al., *Immunization with outer membrane vesicles displaying conserved surface polysaccharide antigen elicits broadly antimicrobial antibodies.* Proc Natl Acad Sci USA, 2018. **115**(14): p. E3106-E3115.
173. Zhang, F., Y.J. Lu, and R. Malley, *Multiple antigen-presenting system (MAPS) to induce comprehensive B- and T-cell immunity.* Proc Natl Acad Sci USA, 2013. **110**(33): p. 13564-9.
174. Zhang, F., et al., *Carrier Proteins Facilitate the Generation of Antipolysaccharide Immunity via Multiple Mechanisms.* mBio, 2022. **13**(3): p. e0379021.
175. Zhang, F., et al., *Protection against Staphylococcus aureus Colonization and Infection by B- and T-Cell-Mediated Mechanisms.* mBio, 2018. **9**(5).
176. Chichili, G.R., et al., *Phase 1/2 study of a novel 24-valent pneumococcal vaccine in healthy adults aged 18 to 64 years and in older adults aged 65 to 85 years.* Vaccine, 2022. **40**(31): p. 4190-4198.
177. Choi, M., et al., *Progress towards the development of Klebsiella vaccines.* Expert Rev Vaccines, 2019. **18**(7): p. 681-691.
178. Doan, T.A., T. Forward, and B.A.J. Tamburini, *Trafficking and retention of protein antigens across systems and immune cell types.* Cell Mol Life Sci, 2022. **79**(5): p. 275.
179. van der Put, R.M.F., B. Metz, and R.J. Pieters, *Carriers and Antigens: New Developments in Glycoconjugate Vaccines.* Vaccines, 2023. **11**(2): p. 219.
180. Zottig, X., et al., *Protein Supramolecular Structures: From Self-Assembly to Nanovaccine Design.* Nanomaterials, 2020. **10**(5): p. 1008.
181. Olshefsky, A., et al., *Engineering Self-Assembling Protein Nanoparticles for Therapeutic Delivery.* Bioconjug Chem, 2022. **33**(11): p. 2018-2034.
182. Fuenmayor, J., F. Gòdia, and L. Cervera, *Production of virus-like particles for vaccines.* N Biotechnol, 2017. **39**(Pt B): p. 174-180.
183. Venters, C., W. Graham, and W. Cassidy, *Recombivax-HB: perspectives past, present and future.* Expert Rev Vaccines, 2004. **3**(2): p. 119-129.
184. Kheirollahpour, M., et al., *Nanoparticles and Vaccine Development.* Pharm Nanotechnol, 2020. **8**(1): p. 6-21.
185. Polonskaya, Z., et al., *T cells control the generation of nanomolar-affinity anti-glycan antibodies.* J Clin Invest, 2017. **127**(4): p. 1491-1504.
186. Xu, L., et al., *Development of meningococcal polysaccharide conjugate vaccine that can elicit long-lasting and strong cellular immune response with hepatitis B core antigen virus-like particles as a novel carrier protein.* Vaccine, 2019. **37**(7): p. 956-964.
187. Rashidijahanabad, Z., et al., *Virus-like Particle Display of Vibrio choleraeO-Specific Polysaccharide as a Potential Vaccine against Cholera.* ACS Infect Dis, 2022. **8**(3): p. 574-583.
188. King, N.P., et al., *Computational design of self-assembling protein nanomaterials with atomic level accuracy.* Science, 2012. **336**(6085): p. 1171-4.
189. Correnti, C.E., et al., *Engineering and functionalization of large circular tandem repeat protein nanoparticles.* Nat Struct Mol Biol, 2020. **27**(4): p. 342-350.
190. Pan, C., et al., *Biosynthesis of Self-Assembled Proteinaceous Nanoparticles for Vaccination.* Adv Mater, 2020. **32**(42): p. e2002940.
191. Peng, Z., et al., *Production of a Promising Biosynthetic Self-Assembled Nanoconjugate Vaccine against Klebsiella Pneumoniae Serotype O2 in a General Escherichia Coli Host.* Adv Sci (Weinh), 2021. **8**(14): p. e2100549.
192. Marcandalli, J., et al., *Induction of Potent Neutralizing Antibody Responses by a Designed Protein Nanoparticle Vaccine for Respiratory Syncytial Virus.* Cell, 2019. **176**(6): p. 1420-1431.e17.
193. Walls, A.C., et al., *Elicitation of Potent Neutralizing Antibody Responses by Designed Protein Nanoparticle Vaccines for SARS-CoV-2.* Cell, 2020. **183**(5): p. 1367-1382.e17.

194. Arunachalam, P.S., et al., *Adjuvanting a subunit COVID-19 vaccine to induce protective immunity.* Nature, 2021. **594**(7862): p. 253-258.
195. Boyoglu-Barnum, S., et al., *Quadrivalent influenza nanoparticle vaccines induce broad protection.* Nature, 2021. **592**(7855): p. 623-628.
196. Schijns, V.E. and E.C. Lavelle, *Trends in vaccine adjuvants.* Expert Rev Vaccines, 2011. **10**(4): p. 539-50.
197. Champion, C.R., *Heplisav-B: A Hepatitis B Vaccine With a Novel Adjuvant.* Ann Pharmacother, 2021. **55**(6): p. 783-791.
198. Wiley, S.R., et al., *Targeting TLRs expands the antibody repertoire in response to a malaria vaccine.* Sci Transl Med, 2011. **3**(93): p. 93ra69.
199. Draper, E., et al., *A randomized, observer-blinded immunogenicity trial of Cervarix(®) and Gardasil(®) Human Papillomavirus vaccines in 12-15 year old girls.* PLoS One, 2013. **8**(5): p. e61825.
200. Galli, G., et al., *Fast rise of broadly cross-reactive antibodies after boosting long-lived human memory B cells primed by an MF59 adjuvanted prepandemic vaccine.* Proc Natl Acad Sci U S A, 2009. **106**(19): p. 7962-7.
201. Girard, M.P., et al., *Report of the 7th meeting on Evaluation of Pandemic Influenza Vaccines in Clinical Trials, World Health Organization, Geneva, 17-18 February 2011*, in *Vaccine*. 2011, Copyright © 2011. Published by Elsevier Ltd.. All rights reserved.: Netherlands. p. 7579-86.
202. O'Hagan, D.T. and C.B. Fox, *New generation adjuvants--from empiricism to rational design.* Vaccine, 2015. **33 Suppl 2**: p. B14-20.
203. Kasturi, S.P., et al., *Programming the magnitude and persistence of antibody responses with innate immunity.* Nature, 2011. **470**(7335): p. 543-7.
204. Romanowski, B., et al., *Immune response to the HPV-16/18 AS04-adjuvanted vaccine administered as a 2-dose or 3-dose schedule up to 4 years after vaccination: results from a randomized study.* Hum Vaccin Immunother, 2014. **10**(5): p. 1155-65.
205. Lofano, G., et al., *Technological approaches to streamline vaccination schedules, progressing towards single-dose vaccines.* NPJ Vaccines, 2020. **5**: p. 88.
206. Zhao, T., et al., *Vaccine adjuvants: mechanisms and platforms.* Signal Transduct Target Ther, 2023. **8**(1): p. 283.
207. Kaur, A., et al., *Toll-like receptor (TLR) agonists as a driving force behind next-generation vaccine adjuvants and cancer therapeutics.* Curr Opin Chem Biol, 2022. **70**: p. 102172.
208. Yang, J.X., et al., *Recent Advances in the Development of Toll-like Receptor Agonist-Based Vaccine Adjuvants for Infectious Diseases.* Pharmaceutics, 2022. **14**(2).
209. Steinhagen, F., et al., *TLR-based immune adjuvants.* Vaccine, 2011. **29**(17): p. 3341-55.
210. Kool, M., K. Fierens, and B.N. Lambrecht, *Alum adjuvant: some of the tricks of the oldest adjuvant.* J Med Microbiol, 2012. **61**(Pt 7): p. 927-934.
211. Clapp, T., et al., *Vaccines with aluminum-containing adjuvants: optimizing vaccine efficacy and thermal stability.* J Pharm Sci, 2011. **100**(2): p. 388-401.
212. Shi, S., et al., *Vaccine adjuvants: Understanding the structure and mechanism of adjuvanticity.* Vaccine, 2019. **37**(24): p. 3167-3178.
213. Principi, N. and S. Esposito, *Aluminum in vaccines: Does it create a safety problem?* Vaccine, 2018. **36**(39): p. 5825-5831.
214. Zhang, T., et al., *Research Progress of Aluminum Phosphate Adjuvants and Their Action Mechanisms.* Pharmaceutics, 2023. **15**(6).
215. Oleszycka, E. and E.C. Lavelle, *Immunomodulatory properties of the vaccine adjuvant alum.* Curr Opin Immunol, 2014. **28**: p. 1-5.
216. Senders, S., et al., *Safety and Immunogenicity of a 20-valent Pneumococcal Conjugate Vaccine in Healthy Infants in the United States.* Pediatr Infect Dis J, 2021. **40**(10): p. 944-951.
217. Coffman, R.L., A. Sher, and R.A. Seder, *Vaccine adjuvants: putting innate immunity to work.* Immunity, 2010. **33**(4): p. 492-503.
218. Di Pasquale, A., et al., *Vaccine Adjuvants: from 1920 to 2015 and Beyond.* Vaccines (Basel), 2015. **3**(2): p. 320-43.

219. Glenny, A.T., G.A.H. Buttle, and M.F. Stevens, *Rate of disappearance of diphtheria toxoid injected into rabbits and guinea-pigs: toxoid precipitated with alum.* Journal of Pathology and Bacteriology, 1931. **34**: p. 267-75.
220. De Gregorio, E., E. Tritto, and R. Rappuoli, *Alum adjuvanticity: unraveling a century old mystery.* Eur J Immunol, 2008. **38**(8): p. 2068-71.
221. Shah, H.B., et al., *Type II NKT cells facilitate Alum-sensing and humoral immunity.* J Leukoc Biol, 2012. **92**(4): p. 883-93.
222. Garçon, N., P. Chomez, and M. Van Mechelen, *GlaxoSmithKline Adjuvant Systems in vaccines: concepts, achievements and perspectives.* Expert Rev Vaccines, 2007. **6**(5): p. 723-39.
223. Casella, C.R. and T.C. Mitchell, *Putting endotoxin to work for us: monophosphoryl lipid A as a safe and effective vaccine adjuvant.* Cell Mol Life Sci, 2008. **65**(20): p. 3231-40.
224. Didierlaurent, A.M., et al., *AS04, an aluminum salt- and TLR4 agonist-based adjuvant system, induces a transient localized innate immune response leading to enhanced adaptive immunity.* J Immunol, 2009. **183**(10): p. 6186-97.
225. Leroux-Roels, G., et al., *Impact of adjuvants on CD4+ T cell and B cell responses to a protein antigen vaccine: Results from a phase II, randomized, multicenter trial.* Clinical Immunology, 2016. **169**: p. 16-27.
226. Giannini, S.L., et al., *Enhanced humoral and memory B cellular immunity using HPV16/18 L1 VLP vaccine formulated with the MPL/aluminium salt combination (AS04) compared to aluminium salt only.* Vaccine, 2006. **24**(33): p. 5937-5949.
227. Kundi, M., *New hepatitis B vaccine formulated with an improved adjuvant system.* Expert Rev Vaccines, 2007. **6**(2): p. 133-40.
228. Naud, P.S., et al., *Sustained efficacy, immunogenicity, and safety of the HPV-16/18 AS04-adjuvanted vaccine.* Human Vaccines & Immunotherapeutics, 2014. **10**(8): p. 2147-2162.
229. Shing, J.Z., et al., *Precancerous cervical lesions caused by non-vaccine-preventable HPV types after vaccination with the bivalent AS04-adjuvanted HPV vaccine: an analysis of the long-term follow-up study from the randomised Costa Rica HPV Vaccine Trial.* Lancet Oncol, 2022. **23**(7): p. 940-949.
230. Wheeler, C.M., et al., *Cross-protective efficacy of HPV-16/18 AS04-adjuvanted vaccine against cervical infection and precancer caused by non-vaccine oncogenic HPV types: 4-year end-of-study analysis of the randomised, double-blind PATRICIA trial.* The Lancet Oncology, 2012. **13**(1): p. 100-110.
231. Garçon, N., D.W. Vaughn, and A.M. Didierlaurent, *Development and evaluation of AS03, an Adjuvant System containing α-tocopherol and squalene in an oil-in-water emulsion.* Expert Rev Vaccines, 2012. **11**(3): p. 349-66.
232. O'Hagan, D.T., et al., *The history of MF59(®) adjuvant: a phoenix that arose from the ashes.* Expert Rev Vaccines, 2013. **12**(1): p. 13-30.
233. Morel, S., et al., *Adjuvant System AS03 containing α-tocopherol modulates innate immune response and leads to improved adaptive immunity.* Vaccine, 2011. **29**(13): p. 2461-73.
234. Seubert, A., et al., *Adjuvanticity of the oil-in-water emulsion MF59 is independent of Nlrp3 inflammasome but requires the adaptor protein MyD88.* Proc Natl Acad Sci U S A, 2011. **108**(27): p. 11169-74.
235. O'Hagan, D.T., A. Wack, and A. Podda, *MF59 is a safe and potent vaccine adjuvant for flu vaccines in humans: what did we learn during its development?* Clin Pharmacol Ther, 2007. **82**(6): p. 740-4.
236. Vesikari, T., et al., *Enhanced immunogenicity of seasonal influenza vaccines in young children using MF59 adjuvant.* Pediatr Infect Dis J, 2009. **28**(7): p. 563-71.
237. Vesikari, T., et al., *Efficacy, immunogenicity, and safety evaluation of an MF59-adjuvanted quadrivalent influenza virus vaccine compared with non-adjuvanted influenza vaccine in children: a multicentre, randomised controlled, observer-blinded, phase 3 trial.* Lancet Respir Med, 2018. **6**(5): p. 345-356.
238. Reisinger, K.S., et al., *A dose-ranging study of MF59(®)-adjuvanted and non-adjuvanted A/H1N1 pandemic influenza vaccine in young to middle-aged and older adult populations to assess safety, immunogenicity, and antibody persistence one year after vaccination.* Hum Vaccin Immunother, 2014. **10**(8): p. 2395-407.

239. Nakaya, H.I., et al., *Systems biology of immunity to MF59-adjuvanted versus nonadjuvanted trivalent seasonal influenza vaccines in early childhood.* Proc Natl Acad Sci U S A, 2016. **113**(7): p. 1853-8.
240. Knuf, M., et al., *Immunogenicity and safety of cell-derived MF59®-adjuvanted A/H1N1 influenza vaccine for children.* Hum Vaccin Immunother, 2015. **11**(2): p. 358-76.
241. Iob, A., et al., *Evidence of increased clinical protection of an MF59-adjuvant influenza vaccine compared to a non-adjuvant vaccine among elderly residents of long-term care facilities in Italy.* Epidemiol Infect, 2005. **133**(4): p. 687-93.
242. Mannino, S., et al., *Effectiveness of adjuvanted influenza vaccination in elderly subjects in northern Italy.* Am J Epidemiol, 2012. **176**(6): p. 527-33.
243. Palma, P., et al., *Safety and immunogenicity of a monovalent MF59®-adjuvanted A/H1N1 vaccine in HIV-infected children and young adults.* Biologicals, 2012. **40**(2): p. 134-9.
244. Fabbiani, M., et al., *Immune response to influenza A (H1N1)v monovalent MF59-adjuvanted vaccine in HIV-infected patients.* Vaccine, 2011. **29**(16): p. 2836-9.
245. Noh, J.Y., et al., *Immunogenicity of trivalent influenza vaccines in patients with chronic kidney disease undergoing hemodialysis: MF59-adjuvanted versus non-adjuvanted vaccines.* Hum Vaccin Immunother, 2016. **12**(11): p. 2902-2908.
246. Tregoning, J.S., R.F. Russell, and E. Kinnear, *Adjuvanted influenza vaccines.* Hum Vaccin Immunother, 2018. **14**(3): p. 550-564.
247. Langley, J.M., et al., *Dose-sparing H5N1 A/Indonesia/05/2005 pre-pandemic influenza vaccine in adults and elderly adults: a phase III, placebo-controlled, randomized study.* J Infect Dis, 2011. **203**(12): p. 1729-38.
248. van der Most Robbert, G., et al., *Long-Term Persistence of Cell-Mediated and Humoral Responses to A(H1N1)pdm09 Influenza Virus Vaccines and the Role of the AS03 Adjuvant System in Adults during Two Randomized Controlled Trials.* Clinical and Vaccine Immunology, 2017. **24**(6): p. e00553-16.
249. Lansbury, L.E., et al., *Effectiveness of 2009 pandemic influenza A(H1N1) vaccines: A systematic review and meta-analysis.* Vaccine, 2017. **35**(16): p. 1996-2006.
250. Garçon, N. and M. Van Mechelen, *Recent clinical experience with vaccines using MPL- and QS-21-containing Adjuvant Systems.* Expert Review of Vaccines, 2011. **10**(4): p. 471-486.
251. Didierlaurent, A.M., et al., *Adjuvant system AS01: helping to overcome the challenges of modern vaccines.* Expert Rev Vaccines, 2017. **16**(1): p. 55-63.
252. Laupèze, B., et al., *Adjuvant Systems for vaccines: 13 years of post-licensure experience in diverse populations have progressed the way adjuvanted vaccine safety is investigated and understood.* Vaccine, 2019. **37**(38): p. 5670-5680.
253. Food and Drug Administration, *Shingrix . https://www.fda.gov/ BiologicsBloodVaccines/Vaccines/ApprovedProducts/ucm581491.htm*
254. Agency, E.M., *Mosquirix - opinion on medicine for use outside EU. https://www.ema.europa.eu/en/opinion-medicine-use-outside-EU/human/mosquirix*.
255. *Efficacy and safety of RTS,S/AS01 malaria vaccine with or without a booster dose in infants and children in Africa: final results of a phase 3, individually randomised, controlled trial.* Lancet, 2015. **386**(9988): p. 31-45.
256. Keating, G.M., *Shingles (Herpes Zoster) Vaccine (Zostavax(®)): A Review in the Prevention of Herpes Zoster and Postherpetic Neuralgia.* BioDrugs, 2016. **30**(3): p. 243-54.
257. Levin, M.J., et al., *Varicella-zoster virus-specific immune responses in elderly recipients of a herpes zoster vaccine.* J Infect Dis, 2008. **197**(6): p. 825-35.
258. Coccia, M., et al. *Cellular and molecular synergy in AS01-adjuvanted vaccines results in an early IFNγ response promoting vaccine immunogenicity*. NPJ vaccines, 2017. **2**, 25 DOI: 10.1038/s41541-017-0027-3.
259. Cunningham, A.L., et al., *Immune Responses to a Recombinant Glycoprotein E Herpes Zoster Vaccine in Adults Aged 50 Years or Older.* J Infect Dis, 2018. **217**(11): p. 1750-1760.
260. Underhill, D.M. and A. Ozinsky, *Toll-like receptors: key mediators of microbe detection.* Curr Opin Immunol, 2002. **14**(1): p. 103-10.
261. Wagner, H., *Bacterial CpG DNA activates immune cells to signal infectious danger.* Adv Immunol, 1999. **73**: p. 329-68.

262. Takeshita, F., et al., *Cutting edge: Role of Toll-like receptor 9 in CpG DNA-induced activation of human cells.* J Immunol, 2001. **167**(7): p. 3555-8.
263. Razin, A. and J. Friedman, *DNA methylation and its possible biological roles.* Prog Nucleic Acid Res Mol Biol, 1981. **25**: p. 33-52.
264. Cardon, L.R., et al., *Pervasive CpG suppression in animal mitochondrial genomes.* Proc Natl Acad Sci U S A, 1994. **91**(9): p. 3799-803.
265. Kayraklioglu, N., B. Horuluoglu, and D.M. Klinman, *CpG Oligonucleotides as Vaccine Adjuvants.* Methods Mol Biol, 2021. **2197**: p. 51-85.
266. Klinman, D.M., *Immunotherapeutic uses of CpG oligodeoxynucleotides.* Nat Rev Immunol, 2004. **4**(4): p. 249-58.
267. Hemmi, H., et al., *A Toll-like receptor recognizes bacterial DNA.* Nature, 2000. **408**(6813): p. 740-5.
268. Steinhagen, F., et al., *Activation of type I interferon-dependent genes characterizes the "core response" induced by CpG DNA.* J Leukoc Biol, 2012. **92**(4): p. 775-85.
269. Aderem, A. and R.J. Ulevitch, *Toll-like receptors in the induction of the innate immune response.* Nature, 2000. **406**(6797): p. 782-7.
270. Storni, T., et al., *Nonmethylated CG motifs packaged into virus-like particles induce protective cytotoxic T cell responses in the absence of systemic side effects.* J Immunol, 2004. **172**(3): p. 1777-85.
271. Speiser, D.E., et al., *Memory and effector CD8 T-cell responses after nanoparticle vaccination of melanoma patients.* J Immunother, 2010. **33**(8): p. 848-58.
272. Beeh, K.M., et al., *The novel TLR-9 agonist QbG10 shows clinical efficacy in persistent allergic asthma.* J Allergy Clin Immunol, 2013. **131**(3): p. 866-74.
273. Goldinger, S.M., et al., *Nano-particle vaccination combined with TLR-7 and -9 ligands triggers memory and effector CD8$^+$ T-cell responses in melanoma patients.* Eur J Immunol, 2012. **42**(11): p. 3049-61.
274. Verthelyi, D., et al., *Human peripheral blood cells differentially recognize and respond to two distinct CPG motifs.* J Immunol, 2001. **166**(4): p. 2372-7.
275. Krug, A., et al., *Toll-like receptor expression reveals CpG DNA as a unique microbial stimulus for plasmacytoid dendritic cells which synergizes with CD40 ligand to induce high amounts of IL-12.* Eur J Immunol, 2001. **31**(10): p. 3026-37.
276. Mutwiri, G.K., et al., *Strategies for enhancing the immunostimulatory effects of CpG oligodeoxynucleotides.* J Control Release, 2004. **97**(1): p. 1-17.
277. Jegerlehner, A., et al., *TLR9 signaling in B cells determines class switch recombination to IgG2a.* J Immunol, 2007. **178**(4): p. 2415-20.
278. Hartmann, G., et al., *Rational design of new CpG oligonucleotides that combine B cell activation with high IFN-alpha induction in plasmacytoid dendritic cells.* Eur J Immunol, 2003. **33**(6): p. 1633-41.
279. Marshall, J.D., et al., *Identification of a novel CpG DNA class and motif that optimally stimulate B cell and plasmacytoid dendritic cell functions.* J Leukoc Biol, 2003. **73**(6): p. 781-92.
280. Vollmer, J., et al., *Characterization of three CpG oligodeoxynucleotide classes with distinct immunostimulatory activities.* Eur J Immunol, 2004. **34**(1): p. 251-62.
281. Bode, C., et al., *CpG DNA as a vaccine adjuvant.* Expert Rev Vaccines, 2011. **10**(4): p. 499-511.
282. Cooper, C.L., et al., *CPG 7909, an immunostimulatory TLR9 agonist oligodeoxynucleotide, as adjuvant to Engerix-B HBV vaccine in healthy adults: a double-blind phase I/II study.* J Clin Immunol, 2004. **24**(6): p. 693-701.
283. Halperin, S.A., et al., *A phase I study of the safety and immunogenicity of recombinant hepatitis B surface antigen co-administered with an immunostimulatory phosphorothioate oligonucleotide adjuvant.* Vaccine, 2003. **21**(19-20): p. 2461-7.
284. Eng, N.F., et al., *The potential of 1018 ISS adjuvant in hepatitis B vaccines: HEPLISAV™ review.* Hum Vaccin Immunother, 2013. **9**(8): p. 1661-72.
285. Cooper, C. and D. Mackie, *Hepatitis B surface antigen-1018 ISS adjuvant-containing vaccine: a review of HEPLISAV™ safety and efficacy.* Expert Rev Vaccines, 2011. **10**(4): p. 417-27.
286. Hyer, R.N. and R.S. Janssen, *Immunogenicity and safety of a 2-dose hepatitis B vaccine, HBsAg/CpG 1018, in persons with diabetes mellitus aged 60-70 years.* Vaccine, 2019. **37**(39): p. 5854-5861.

287. Søgaard, O.S., et al., *Improving the immunogenicity of pneumococcal conjugate vaccine in HIV-infected adults with a toll-like receptor 9 agonist adjuvant: a randomized, controlled trial.* Clin Infect Dis, 2010. **51**(1): p. 42-50.
288. Cooper, C.L., et al., *CPG 7909 adjuvant improves hepatitis B virus vaccine seroprotection in antiretroviral-treated HIV-infected adults.* Aids, 2005. **19**(14): p. 1473-9.
289. Cooper, C.L., et al., *CPG 7909 adjuvant plus hepatitis B virus vaccination in HIV-infected adults achieves long-term seroprotection for up to 5 years.* Clin Infect Dis, 2008. **46**(8): p. 1310-4.
290. Angel, J.B., et al., *CpG increases vaccine antigen-specific cell-mediated immunity when administered with hepatitis B vaccine in HIV infection.* J Immune Based Ther Vaccines, 2008. **6**: p. 4.
291. Ellis, R.D., et al., *Phase 1 trial of the Plasmodium falciparum blood stage vaccine MSP1(42)-C1/Alhydrogel with and without CPG 7909 in malaria naïve adults.* PLoS One, 2010. **5**(1): p. e8787.
292. Ezoe, S., et al., *First-in-human randomised trial and follow-up study of Plasmodium falciparum blood-stage malaria vaccine BK-SE36 with CpG-ODN(K3).* Vaccine, 2020. **38**(46): p. 7246-7257.
293. Ouédraogo, A., et al., *Safety and immunogenicity of BK-SE36/CpG malaria vaccine in healthy Burkinabe adults and children: a phase 1b randomised, controlled, double-blinded, age de-escalation trial.* Front Immunol, 2023. **14**: p. 1267372.
294. Rynkiewicz, D., et al., *Marked enhancement of the immune response to BioThrax® (Anthrax Vaccine Adsorbed) by the TLR9 agonist CPG 7909 in healthy volunteers.* Vaccine, 2011. **29**(37): p. 6313-20.
295. Hopkins, R.J., et al., *Randomized, double-blind, active-controlled study evaluating the safety and immunogenicity of three vaccination schedules and two dose levels of AV7909 vaccine for anthrax post-exposure prophylaxis in healthy adults.* Vaccine, 2016. **34**(18): p. 2096-105.
296. Wolfe, D.N., et al., *Evaluation of BioThrax® and AV7909 anthrax vaccines in adults 66 years of age or older.* Vaccine, 2020. **38**(50): p. 7970-7976.
297. Cooper, C.L., et al., *Safety and immunogenicity of CPG 7909 injection as an adjuvant to Fluarix influenza vaccine.* Vaccine, 2004. **22**(23-24): p. 3136-43.
298. Varki, A., et al., *Essentials of Glycobiology [internet].* 2022.
299. Varki, A., *Biological roles of glycans.* Glycobiology, 2017. **27**(1): p. 3-49.
300. Hulbert, S.W., et al., *Glycovaccinology: The design and engineering of carbohydrate-based vaccine components.* Biotechnol Adv, 2023. **68**: p. 108234.
301. Anderluh, M., et al., *Recent advances on smart glycoconjugate vaccines in infections and cancer.* Febs j, 2022. **289**(14): p. 4251-4303.
302. Rappuoli, R., E. De Gregorio, and P. Costantino, *On the mechanisms of conjugate vaccines.* Proceedings of the National Academy of Sciences, 2019. **116**(1): p. 14-16.
303. Avci, F.Y., et al., *A mechanism for glycoconjugate vaccine activation of the adaptive immune system and its implications for vaccine design.* Nature Medicine, 2011. **17**(12): p. 1602-1609.
304. van der Put, R.M.F., et al., *The First-in-Human Synthetic Glycan-Based Conjugate Vaccine Candidate against Shigella.* ACS Cent Sci, 2022. **8**(4): p. 449-460.
305. Guazzelli, L., et al., *A synthetic strategy to xylose-containing thioglycoside tri- and tetrasaccharide building blocks corresponding to Cryptococcus neoformans capsular polysaccharide structures.* Org Biomol Chem, 2015. **13**(23): p. 6598-610.
306. Baschong, W., et al., *Repetitive versus monomeric antigen presentation: direct visualization of antibody affinity and specificity.* J Struct Biol, 2003. **143**(3): p. 258-62.
307. Nascimento, I.P. and L.C. Leite, *Recombinant vaccines and the development of new vaccine strategies.* Braz J Med Biol Res, 2012. **45**(12): p. 1102-11.
308. Ahire, E.D. and S.J. Kshirsagar, *Immune responses induced by different vaccine platforms against coronavirus disease-19.* 2021: p. 243-257.
309. Park, J., T. Pho, and J.A. Champion, *Chemical and biological conjugation strategies for the development of multivalent protein vaccine nanoparticles.* Biopolymers, 2023. **114**(8): p. e23563.
310. Nguyen, B. and N.H. Tolia, *Protein-based antigen presentation platforms for nanoparticle vaccines.* NPJ Vaccines, 2021. **6**(1): p. 70.
311. Irvine, D.J. and B.J. Read, *Shaping humoral immunity to vaccines through antigen-displaying nanoparticles.* Curr Opin Immunol, 2020. **65**: p. 1-6.

312. Curley, S.M. and D. Putnam, *Biological Nanoparticles in Vaccine Development.* Front Bioeng Biotechnol, 2022. **10**: p. 867119.
313. Cabral, G.A., et al., *Cellular and humoral immunity in guinea pigs to two major polypeptides derived from hepatitis B surface antigen.* J Gen Virol, 1978. **38**(2): p. 339-50.
314. Facciolà, A., et al., *The new era of vaccines: the "nanovaccinology".* Eur Rev Med Pharmacol Sci, 2019. **23**(16): p. 7163-7182.
315. Li, X., et al., *Orthogonal modular biosynthesis of nanoscale conjugate vaccines for vaccination against infection.* Nano Res, 2022. **15**(2): p. 1645-1653.
316. Carboni, F., et al., *Proof of concept for a single-dose Group B Streptococcus vaccine based on capsular polysaccharide conjugated to Qβ virus-like particles.* NPJ Vaccines, 2023. **8**(1): p. 152.
317. Kang, S.M., M.C. Kim, and R.W. Compans, *Virus-like particles as universal influenza vaccines.* Expert Rev Vaccines, 2012. **11**(8): p. 995-1007.
318. Kanekiyo, M., et al., *Self-assembling influenza nanoparticle vaccines elicit broadly neutralizing H1N1 antibodies.* Nature, 2013. **499**(7456): p. 102-6.
319. He, L., et al., *Presenting native-like trimeric HIV-1 antigens with self-assembling nanoparticles.* Nat Commun, 2016. **7**: p. 12041.
320. Wang, L., et al., *Structure-based design of ferritin nanoparticle immunogens displaying antigenic loops of Neisseria gonorrhoeae.* FEBS Open Bio, 2017. **7**(8): p. 1196-1207.
321. Aston-Deaville, S., et al., *An assessment of the use of Hepatitis B Virus core protein virus-like particles to display heterologous antigens from Neisseria meningitidis.* Vaccine, 2020. **38**(16): p. 3201-3209.
322. Cappelli, L., et al., *Self-assembling protein nanoparticles and virus like particles correctly display β-barrel from meningococcal factor H-binding protein through genetic fusion.* PLoS One, 2022. **17**(9): p. e0273322.
323. Veggi, D., et al., *Effective Multivalent Oriented Presentation of Meningococcal NadA Antigen Trimers by Self-Assembling Ferritin Nanoparticles.* Int J Mol Sci, 2023. **24**(7).
324. Wilby, K.J., et al., *Mosquirix (RTS,S): a novel vaccine for the prevention of Plasmodium falciparum malaria.* Ann Pharmacother, 2012. **46**(3): p. 384-93.
325. Storni, F., et al., *Vaccine against peanut allergy based on engineered virus-like particles displaying single major peanut allergens.* J Allergy Clin Immunol, 2020. **145**(4): p. 1240-1253.e3.
326. Jennings, G.T. and M.F. Bachmann, *Immunodrugs: therapeutic VLP-based vaccines for chronic diseases.* Annu Rev Pharmacol Toxicol, 2009. **49**: p. 303-26.
327. Wu, X., et al., *Synthesis and Immunological Evaluation of Disaccharide Bearing MUC-1 Glycopeptide Conjugates with Virus-like Particles.* ACS Chem Biol, 2019. **14**(10): p. 2176-2184.
328. Shafieichaharberoud, F., et al., *Enhancing Protective Antibodies against Opioids through Antigen Display on Virus-like Particles.* Bioconjug Chem, 2023.
329. Sungsuwan, S., X. Wu, and X. Huang, *Evaluation of Virus-Like Particle-Based Tumor-Associated Carbohydrate Immunogen in a Mouse Tumor Model.* Methods Enzymol, 2017. **597**: p. 359-376.
330. Chiba, S., et al., *Multivalent nanoparticle-based vaccines protect hamsters against SARS-CoV-2 after a single immunization.* Commun Biol, 2021. **4**(1): p. 597.
331. Arunachalam, P.S., et al., *Adjuvanting a subunit COVID-19 vaccine to induce protective immunity.* Nature, 2021. **594**(7862): p. 253-258.
332. Martinez-Cano, D., et al., *Process development of a SARS-CoV-2 nanoparticle vaccine.* Process Biochem, 2023. **129**: p. 241-256.
333. Azharuddin, M., et al., *Nano toolbox in immune modulation and nanovaccines.* Trends Biotechnol, 2022. **40**(10): p. 1195-1212.
334. Ballister, E.R., et al., *In vitro self-assembly of tailorable nanotubes from a simple protein building block.* Proc Natl Acad Sci U S A, 2008. **105**(10): p. 3733-8.
335. Mougous, J.D., et al., *A virulence locus of Pseudomonas aeruginosa encodes a protein secretion apparatus.* Science, 2006. **312**(5779): p. 1526-30.
336. Bröker, M., et al., *Chemistry of a new investigational quadrivalent meningococcal conjugate vaccine that is immunogenic at all ages.* Vaccine, 2009. **27**(41): p. 5574-80.

337. Bardotti, A., et al., *Size determination of bacterial capsular oligosaccharides used to prepare conjugate vaccines against Neisseria meningitidis groups Y and W135.* Vaccine, 2005. **23**(16): p. 1887-99.
338. Bian, J., et al., *The Power of Field-Flow Fractionation in Characterization of Nanoparticles in Drug Delivery.* Molecules, 2023. **28**(10).
339. Hu, Y., R.M. Crist, and J.D. Clogston, *The utility of asymmetric flow field-flow fractionation for preclinical characterization of nanomedicines.* Anal Bioanal Chem, 2020. **412**(2): p. 425-438.
340. Berti, F., et al., *Carbohydrate based meningococcal vaccines: past and present overview.* Glycoconj J, 2021. **38**(4): p. 401-409.
341. Bröker, M., F. Berti, and P. Costantino, *Factors contributing to the immunogenicity of meningococcal conjugate vaccines.* Hum Vaccin Immunother, 2016. **12**(7): p. 1808-24.
342. Rodrigues, M.Q., P.M. Alves, and A. Roldão, *Functionalizing Ferritin Nanoparticles for Vaccine Development.* Pharmaceutics, 2021. **13**(10).
343. Zhang, B., et al., *A platform incorporating trimeric antigens into self-assembling nanoparticles reveals SARS-CoV-2-spike nanoparticles to elicit substantially higher neutralizing responses than spike alone.* Sci Rep, 2020. **10**(1): p. 18149.
344. Swanson, K.A., et al., *A respiratory syncytial virus (RSV) F protein nanoparticle vaccine focuses antibody responses to a conserved neutralization domain.* Sci Immunol, 2020. **5**(47).
345. Weidenbacher, P.A.B., et al., *A ferritin-based COVID-19 nanoparticle vaccine that elicits robust, durable, broad-spectrum neutralizing antisera in non-human primates.* Nature Communications, 2023. **14**(1): p. 2149.
346. Caputo, F., et al., *Asymmetric-flow field-flow fractionation for measuring particle size, drug loading and (in)stability of nanopharmaceuticals. The joint view of European Union Nanomedicine Characterization Laboratory and National Cancer Institute - Nanotechnology Characterization Laboratory.* J Chromatogr A, 2021. **1635**: p. 461767.
347. Citkowicz, A., et al., *Characterization of virus-like particle assembly for DNA delivery using asymmetrical flow field-flow fractionation and light scattering.* Anal Biochem, 2008. **376**(2): p. 163-72.
348. Ansar, S.M. and T. Mudalige, *Characterization of doxorubicin liposomal formulations for size-based distribution of drug and excipients using asymmetric-flow field-flow fractionation (AF4) and liquid chromatography-mass spectrometry (LC-MS).* Int J Pharm, 2020. **574**: p. 118906.
349. Shakiba, S., et al., *Asymmetric flow field-flow fractionation (AF4) with fluorescence and multi-detector analysis for direct, real-time, size-resolved measurements of drug release from polymeric nanoparticles.* J Control Release, 2021. **338**: p. 410-421.
350. Niikura, K., et al., *Gold nanoparticles as a vaccine platform: influence of size and shape on immunological responses in vitro and in vivo.* ACS Nano, 2013. **7**(5): p. 3926-38.
351. Toraskar, S., P. Madhukar Chaudhary, and R. Kikkeri, *The Shape of Nanostructures Encodes Immunomodulation of Carbohydrate Antigen and Vaccine Development.* ACS Chem Biol, 2022. **17**(5): p. 1122-1130.
352. Kumar, S., et al., *Shape and size-dependent immune response to antigen-carrying nanoparticles.* J Control Release, 2015. **220**(Pt A): p. 141-148.
353. Mathaes, R., et al., *Influence of particle geometry and PEGylation on phagocytosis of particulate carriers.* Int J Pharm, 2014. **465**(1-2): p. 159-64.
354. Mathaes, R., et al., *Influence of particle size, an elongated particle geometry, and adjuvants on dendritic cell activation.* Eur J Pharm Biopharm, 2015. **94**: p. 542-9.
355. Swartz, M.A., *The physiology of the lymphatic system.* Adv Drug Deliv Rev, 2001. **50**(1-2): p. 3-20.
356. Reddy, S.T., et al., *Exploiting lymphatic transport and complement activation in nanoparticle vaccines.* Nat Biotechnol, 2007. **25**(10): p. 1159-64.
357. Chithrani, B.D., A.A. Ghazani, and W.C. Chan, *Determining the size and shape dependence of gold nanoparticle uptake into mammalian cells.* Nano Lett, 2006. **6**(4): p. 662-8.
358. Li, Y., M. Kröger, and W.K. Liu, *Shape effect in cellular uptake of PEGylated nanoparticles: comparison between sphere, rod, cube and disk.* Nanoscale, 2015. **7**(40): p. 16631-46.

359. Chen, L., et al., *Shape-dependent internalization kinetics of nanoparticles by membranes.* Soft Matter, 2016. **12**(9): p. 2632-41.
360. Dasgupta, S., T. Auth, and G. Gompper, *Wrapping of ellipsoidal nano-particles by fluid membranes.* Soft Matter, 2013. **2013**: p. 5473.
361. Baranov, M.V., et al., *Modulation of Immune Responses by Particle Size and Shape.* Front Immunol, 2020. **11**: p. 607945.
362. Sadhu, R.K., et al., *A theoretical model of efficient phagocytosis driven by curved membrane proteins and active cytoskeleton forces.* Soft Matter, 2022. **19**(1): p. 31-43.
363. Paul, D., et al., *Phagocytosis dynamics depends on target shape.* Biophys J, 2013. **105**(5): p. 1143-50.
364. Champion, J.A. and S. Mitragotri, *Role of target geometry in phagocytosis.* Proc Natl Acad Sci U S A, 2006. **103**(13): p. 4930-4.
365. Manolova, V., et al., *Nanoparticles target distinct dendritic cell populations according to their size.* Eur J Immunol, 2008. **38**(5): p. 1404-13.
366. Shima, F., et al., *Size effect of amphiphilic poly(γ-glutamic acid) nanoparticles on cellular uptake and maturation of dendritic cells in vivo.* Acta Biomater, 2013. **9**(11): p. 8894-901.
367. Fifis, T., et al., *Size-dependent immunogenicity: therapeutic and protective properties of nano-vaccines against tumors.* J Immunol, 2004. **173**(5): p. 3148-54.
368. Mottram, P.L., et al., *Type 1 and 2 immunity following vaccination is influenced by nanoparticle size: formulation of a model vaccine for respiratory syncytial virus.* Mol Pharm, 2007. **4**(1): p. 73-84.
369. Tumolo, T., L. Angnes, and M.S. Baptista, *Determination of the refractive index increment (dn/dc) of molecule and macromolecule solutions by surface plasmon resonance.* Anal Biochem, 2004. **333**(2): p. 273-9.
370. Theisen, A., et al., *"Refractive Increment Data-Book for Polymer and Biomolecular Scientists"* ISBN: 1-897676-29-8 ed. N. Nottingham University Press, UK. 2000.
371. Postnova. *Characterization of Macromolecules in Beer Using Asymmetrical Flow Field-FLow Fractionation*. Available from: https://www.postnova.com/knowledge/application-notes/application-note/348-id0076-macromolecules-in-beer-af4-mals.html.
372. Pace, D. and A.J. Pollard, *Meningococcal A, C, Y and W-135 polysaccharide-protein conjugate vaccines.* Arch Dis Child, 2007. **92**(10): p. 909-15.
373. Acharya, I.L., et al., *Prevention of typhoid fever in Nepal with the Vi capsular polysaccharide of Salmonella typhi. A preliminary report.* N Engl J Med, 1987. **317**(18): p. 1101-4.
374. Klugman, K.P., et al., *Protective activity of Vi capsular polysaccharide vaccine against typhoid fever.* Lancet, 1987. **2**(8569): p. 1165-9.
375. Tacket, C.O., M.M. Levine, and J.B. Robbins, *Persistence of antibody titres three years after vaccination with Vi polysaccharide vaccine against typhoid fever.* Vaccine, 1988. **6**(4): p. 307-8.
376. Avery, O.T. and W.F. Goebel, *CHEMO-IMMUNOLOGICAL STUDIES ON CONJUGATED CARBOHYDRATE-PROTEINS : II. IMMUNOLOGICAL SPECIFICITY OF SYNTHETIC SUGAR-PROTEIN ANTIGENS.* J Exp Med, 1929. **50**(4): p. 533-50.
377. Avery, O.T. and W.F. Goebel, *CHEMO-IMMUNOLOGICAL STUDIES ON CONJUGATED CARBOHYDRATE-PROTEINS : V. THE IMMUNOLOGICAL SPECIFITY OF AN ANTIGEN PREPARED BY COMBINING THE CAPSULAR POLYSACCHARIDE OF TYPE III PNEUMOCOCCUS WITH FOREIGN PROTEIN.* J Exp Med, 1931. **54**(3): p. 437-47.
378. Siegrist, C.A., *Neonatal and early life vaccinology.* Vaccine, 2001. **19**(25-26): p. 3331-46.
379. El Chaer, F. and H.M. El Sahly, *Vaccination in the Adult Patient Infected with HIV: A Review of Vaccine Efficacy and Immunogenicity.* The American Journal of Medicine, 2019. **132**(4): p. 437-446.
380. Lane, H.C., et al., *Abnormalities of B-cell activation and immunoregulation in patients with the acquired immunodeficiency syndrome.* N Engl J Med, 1983. **309**(8): p. 453-8.
381. Hanson, D.L., et al., *Distribution of CD4+ T lymphocytes at diagnosis of acquired immunodeficiency syndrome-defining and other human immunodeficiency virus-related illnesses. The Adult and Adolescent Spectrum of HIV Disease Project Group.* Arch Intern Med, 1995. **155**(14): p. 1537-42.
382. Karlsson, J., et al., *Pneumococcal vaccine responses in elderly patients with multiple myeloma, Waldenstrom's macroglobulinemia, and monoclonal gammopathy of undetermined significance.* Trials in Vaccinology, 2013. **2**: p. 31-38.

383. Jackson, L.A. and E.N. Janoff, *Pneumococcal vaccination of elderly adults: new paradigms for protection.* Clin Infect Dis, 2008. **47**(10): p. 1328-38.
384. *Use of 13-valent pneumococcal conjugate vaccine and 23-valent pneumococcal polysaccharide vaccine for adults with immunocompromising conditions: recommendations of the Advisory Committee on Immunization Practices (ACIP).* MMWR Morb Mortal Wkly Rep, 2012. **61**(40): p. 816-9.
385. Tomczyk, S., et al., *Use of 13-valent pneumococcal conjugate vaccine and 23-valent pneumococcal polysaccharide vaccine among adults aged ≥65 years: recommendations of the Advisory Committee on Immunization Practices (ACIP).* MMWR Morb Mortal Wkly Rep, 2014. **63**(37): p. 822-5.
386. French, N., et al., *A trial of a 7-valent pneumococcal conjugate vaccine in HIV-infected adults.* N Engl J Med, 2010. **362**(9): p. 812-22.
387. Leroux-Roels, I., et al., *Adjuvant system AS02V enhances humoral and cellular immune responses to pneumococcal protein PhtD vaccine in healthy young and older adults: randomised, controlled trials.* Vaccine, 2015. **33**(4): p. 577-84.
388. Reed, S.G., M.T. Orr, and C.B. Fox, *Key roles of adjuvants in modern vaccines.* Nat Med, 2013. **19**(12): p. 1597-608.
389. Vanni, T., et al., *Dose-sparing effect of two adjuvant formulations with a pandemic influenza A/H7N9 vaccine: A randomized, double-blind, placebo-controlled, phase 1 clinical trial.* PLoS One, 2022. **17**(10): p. e0274943.
390. Bonam, S.R., et al., *An Overview of Novel Adjuvants Designed for Improving Vaccine Efficacy.* Trends Pharmacol Sci, 2017. **38**(9): p. 771-793.
391. Moni, S.S., et al., *Advancements in Vaccine Adjuvants: The Journey from Alum to Nano Formulations.* Vaccines (Basel), 2023. **11**(11).
392. Stefanetti, G., et al., *Immunobiology of Carbohydrates: Implications for Novel Vaccine and Adjuvant Design Against Infectious Diseases.* Front Cell Infect Microbiol, 2021. **11**: p. 808005.
393. Gonzalez-Lopez, A., et al., *Adjuvant effect of TLR7 agonist adsorbed on aluminum hydroxide (AS37): A phase I randomized, dose escalation study of an AS37-adjuvanted meningococcal C conjugated vaccine.* Clin Immunol, 2019. **209**: p. 108275.
394. Pulendran, B., S.A. P, and D.T. O'Hagan, *Emerging concepts in the science of vaccine adjuvants.* Nat Rev Drug Discov, 2021. **20**(6): p. 454-475.
395. O'Hagan, D.T., R.N. Lodaya, and G. Lofano, *The continued advance of vaccine adjuvants - 'we can work it out'.* Semin Immunol, 2020. **50**: p. 101426.
396. Del Giudice, G., R. Rappuoli, and A.M. Didierlaurent, *Correlates of adjuvanticity: A review on adjuvants in licensed vaccines.* Semin Immunol, 2018. **39**: p. 14-21.
397. U.S. Food and Drug Administration. *Fluad, https://www.fda.gov/vaccines-blood-biologics/vaccines/fluad*. 2021 (Accessed on 28 March 2024).
398. European Medicines Agency. *Shingrix, https://www.ema.europa.eu/en/medicines/human/EPAR/shingrix*. Accessed 28 March 2024.
399. Romanowski, B., et al., *Immunogenicity and safety of the HPV-16/18 AS04-adjuvanted vaccine administered as a 2-dose schedule compared with the licensed 3-dose schedule: results from a randomized study.* Hum Vaccin, 2011. **7**(12): p. 1374-86.
400. Markowitz, L.E., et al., *Human papillomavirus vaccine effectiveness by number of doses: Systematic review of data from national immunization programs.* Vaccine, 2018. **36**(32 Pt A): p. 4806-4815.
401. Kreimer, A.R., et al., *Proof-of-principle evaluation of the efficacy of fewer than three doses of a bivalent HPV16/18 vaccine.* J Natl Cancer Inst, 2011. **103**(19): p. 1444-51.
402. Hyer, R., et al., *Safety of a two-dose investigational hepatitis B vaccine, HBsAg-1018, using a toll-like receptor 9 agonist adjuvant in adults.* Vaccine, 2018. **36**(19): p. 2604-2611.
403. Lee, G.H. and S.G. Lim, *CpG-Adjuvanted Hepatitis B Vaccine (HEPLISAV-B®) Update.* Expert Rev Vaccines, 2021. **20**(5): p. 487-495.
404. Akache, B., et al., *Anti-IgE Qb-VLP Conjugate Vaccine Self-Adjuvants through Activation of TLR7.* Vaccines (Basel), 2016. **4**(1).
405. Chang, J.Y., et al., *Structural Assembly of Qβ Virion and Its Diverse Forms of Virus-like Particles.* Viruses, 2022. **14**(2).

406. Fiedler, J.D., et al., *RNA-directed packaging of enzymes within virus-like particles.* Angew Chem Int Ed Engl, 2010. **49**(50): p. 9648-51.
407. Tariq, H., et al., *Virus-Like Particles: Revolutionary Platforms for Developing Vaccines Against Emerging Infectious Diseases.* Front Microbiol, 2021. **12**: p. 790121.
408. Fang, P.Y., et al., *RNA: packaged and protected by VLPs.* RSC Adv, 2018. **8**(38): p. 21399-21406.
409. Carboni, F., Cozzi, R., Margarit, I., Romagnoli, G. & Romano, M. R., *Bacterial immunization using qbeta hairpin nanoparticle constructs.* WO/2023/111826 (2023).
410. Pease, L.F., 3rd, et al., *Quantitative characterization of virus-like particles by asymmetrical flow field flow fractionation, electrospray differential mobility analysis, and transmission electron microscopy.* Biotechnol Bioeng, 2009. **102**(3): p. 845-55.
411. Chuan, Y.P., et al., *Quantitative analysis of virus-like particle size and distribution by field-flow fractionation.* Biotechnol Bioeng, 2008. **99**(6): p. 1425-33.
412. Eskelin, K., M.M. Poranen, and H.M. Oksanen, *Asymmetrical Flow Field-Flow Fractionation on Virus and Virus-Like Particle Applications.* Microorganisms, 2019. **7**(11).
413. Golmohammadi, R., et al., *The crystal structure of bacteriophage Q beta at 3.5 A resolution.* Structure, 1996. **4**(5): p. 543-54.
414. Kinzler M., P.K., *Processes for packaging oligonucleotides into virus-like particles of RNA Bacteriophages*. US 2018/0171358 A1, 2018.
415. Napolitani, G., et al., *Selected Toll-like receptor agonist combinations synergistically trigger a T helper type 1-polarizing program in dendritic cells.* Nat Immunol, 2005. **6**(8): p. 769-76.
416. Roman, M., et al., *Immunostimulatory DNA sequences function as T helper-1-promoting adjuvants.* Nat Med, 1997. **3**(8): p. 849-54.
417. Kolesnikova, S. and E.A. Curtis, *Structure and Function of Multimeric G-Quadruplexes.* Molecules, 2019. **24**(17).
418. Wu, C.C., et al., *Necessity of oligonucleotide aggregation for toll-like receptor 9 activation.* J Biol Chem, 2004. **279**(32): p. 33071-8.
419. Kerkmann, M., et al., *Spontaneous formation of nucleic acid-based nanoparticles is responsible for high interferon-alpha induction by CpG-A in plasmacytoid dendritic cells.* J Biol Chem, 2005. **280**(9): p. 8086-93.
420. Jung, J., et al., *Distinct response of human B cell subpopulations in recognition of an innate immune signal, CpG DNA.* J Immunol, 2002. **169**(5): p. 2368-73.
421. Bernasconi, N.L., E. Traggiai, and A. Lanzavecchia, *Maintenance of serological memory by polyclonal activation of human memory B cells.* Science, 2002. **298**(5601): p. 2199-202.
422. Chatzikleanthous, D., et al., *Design of a novel vaccine nanotechnology-based delivery system comprising CpGODN-protein conjugate anchored to liposomes.* J Control Release, 2020. **323**: p. 125-137.
423. Wessels, M.R., et al., *Immunogenicity in Animals of a Polysaccharide-Protein Conjugate Vaccine against Type III Group B Streptococcus.* J. Clin. Invest., 1990. **86**: p. 1428-1433.
424. Paoletti, L.C., et al., *Immunogenicity of Group B Streptococcus Type III Polysaccharide-Tetanus Toxoid Vaccine in Baboons.* Infect. Immun., 1996. **64**(2): p. 677–679.
425. Molino, N.M., et al., *Biomimetic protein nanoparticles facilitate enhanced dendritic cell activation and cross-presentation.* ACS Nano, 2013. **7**(11): p. 9743-52.
426. Mo, M., et al., *Enhancement of Immune Response of Bioconjugate Nanovaccine by Loading of CpG through Click Chemistry.* J Pers Med, 2023. **13**(3).
427. Sokolova, V., et al., *The use of calcium phosphate nanoparticles encapsulating Toll-like receptor ligands and the antigen hemagglutinin to induce dendritic cell maturation and T cell activation.* Biomaterials, 2010. **31**(21): p. 5627-33.
428. Zhu, Y., et al., *Hollow Mesoporous Silica/Poly(l-lysine) Particles for Codelivery of Drug and Gene with Enzyme-Triggered Release Property.* The Journal of Physical Chemistry C, 2011. **115**(28): p. 13630-13636.
429. Kushner, T., V. Huang, and R. Janssen, *Safety and immunogenicity of HepB-CpG in women with documented pregnancies post-vaccination: A retrospective chart review.* Vaccine, 2022. **40**(21): p. 2899-2903.

430. Delannois, F., et al., *Signal management in pharmacovigilance and human risk assessment of CpG 7909, integrating embryo-fetal and post-natal developmental toxicity studies in rats and rabbits.* Reprod Toxicol, 2018. **75**: p. 110-120.
431. Ito, S., et al., *CpG oligodeoxynucleotides improve the survival of pregnant and fetal mice following Listeria monocytogenes infection.* Infect Immun, 2004. **72**(6): p. 3543-8.
432. Buffi, G., et al., *Novel Multiplex Immunoassays for Quantification of IgG against Group B Streptococcus Capsular Polysaccharides in Human Sera.* mSphere, 2019. **4**(4).
433. Mountzouros, K.T. and A.P. Howell, *Detection of complement-mediated antibody-dependent bactericidal activity in a fluorescence-based serum bactericidal assay for group B Neisseria meningitidis.* J Clin Microbiol, 2000. **38**(8): p. 2878-84.
434. Bieging, K.T., et al., *Fluorescent multivalent opsonophagocytic assay for measurement of functional antibodies to Streptococcus pneumoniae.* Clin Diagn Lab Immunol, 2005. **12**(10): p. 1238-42.

DISCLAIMER

TRANSPARENCY STATEMENT

This work was sponsored by GlaxoSmithKline Biologicals SA. Marta Dolce is a PhD student at the University of Siena and partecipates in a post graduate studentship program at GSK, Siena, Italy.

ANIMAL SAMPLES

All animal sera used in this study derived from mouse immunization experiments performed at the GSK Animal Facility in Siena, Italy, in compliance with the ARRIVE guidelines, the current Italian legislation on the care and use of animals in experimentation (Italian Legislative Decree 116/92) and consecutive ministerial newsletter (Circolare Ministeriale n.8 del 22 Aprile 1994), and with the GSK Animal Welfare Policy and Standards. The animal protocol was approved by the Animal Welfare Body of GSK Vaccines, Siena, Italy, and by the Italian Ministry of Health.